Impact of feed addition on UPR-related gene expression in CHO

A thesis submitted to The University of Manchester for the degree of Master of Philosophy of Bioprocess and Bioengineering in the Faculty of Science and Engineering.

2023

Ana M Wheeler

School of Engineering, Department of Chemical Engineering

Table of Contents

Word count: 35300

List of Figures

List of Tables

Abbreviations

ANOVA	Analysis of variance
APS	Ammonium Persulfate
ATF4	Activating Transcription Factor 4
ATF6	Activating Transcription Factor 6
ATP	Adenosine Triphosphate
BC	Batch culture
BCL-2	B-cell leukemia/lymphoma 2 protein
BIM	Bcl-2 Interacting Mediator of cell death
BiP/ GRP78/ HSPA5	Binding Immunoglobulin Protein
BSC	Biological Safety Cabinet
bZIP	Basic leucine zipper
cDNA	Complementary Deoxyribose Nucleic Acid
CHO	Chinese Hamster Ovary
CHOP/ DDIT3/ GADD153	C/EBP homologous protein
COVID-19	Coronavirus Disease 2019
ddH_2O	MilliQ water
DHFR	Dihydrofolate reductase
DNA	Deoxyribose Nucleic Acid
eIF2α	Eukaryotic translation initiation factor 2 subunit-α
ELISA	Enzyme-linked immunoassay
EMA	European Medicines Agency
ER	Endoplasmic Reticulum
ERAD	Endoplasmic Reticulum-associated degradation
ERAF	Endoplasmic Reticulum-Assisted Folding
ERK1	Extracellular signal-regulated kinase 1
ERK2	Extracellular signal-regulated kinase 2
ERSE	Endoplasmic Reticulum Stress Response Element
ERSE-II	Endoplasmic Reticulum Stress Response Element - II
FACS	Fluorescence-Activated Cell Sorting
FBC	Fed-batch culture
FDA	Food and Drug Administration
GC-MS	Gas Chromatography-Mass Spectrometry
GOI	Gene Of Interest
GRP94	Glucose regulated protein 94
GS	Glutamine synthetase
HCl	Hydrogen Chloride
IGF-I	Insulin-like Growth Factor I
IGF-II	Insulin-like Growth Factor II
IgG	Immunoglobulin G
IRE1	Inositol-requiring enzyme 1
ITPR1	Inositol 1,4,5-trisphosphate receptor type 1
KLF9	Kruppel-like factor 9
LD	Acidic Linker Domain
LDH	Lactate dehydrogenase
mAb	Monoclonal Antibody
MD	Middle Domain
MOX	Methoxyamine hydrochloride
mRNA	Messenger Ribose Nucleic Acid
MSTFA	N-methyl-N-(trimethylsilyl) trifluoroacetamide

NAD	Nicotinamide adenine dinucleotide
NADH	Nicotinamide adenine dinucleotide hydrogen
NaOH	Sodium hydroxide
NBD	Nucleotide-Binding Domain
NFW	Nuclease Free Water
pac	Puromycin N-acetyl transferase
PBS	Phosphate Buffered Saline
PDIs	Protein Disulfide Isomerases
PERK	Protein Endoplasmic Reticulum Kinase
PP1	Protein phosphatase 1
PTM	Post-Translational Modification
qRT-PCR	Quantitative Reverse Transcription-Polymerase Chain Reaction
rAB	Recombinant Antibody
RIP1	Receptor Interacting Protein Kinase 1
RMP	Reference Medicinal Product
RNA	Ribose Nucleic Acid
RT	Reverse Transcription
RTL	Retention Time Locked
RTP	Room Temperature Pressure
RT-PCR	Reverse Transcription-Polymerase Chain Reaction
S1P	Sphingosine-1-phosphate
S2P	Sphingosine-2-phosphate
SBD	Substrate-Binding Domain
SDS-PAGE	Sodium Dodecyl Sulfate-Polyacrylamide Gel Electrophoresis
SERCA	Sarcoplasmic-endoplasmic-reticulum Ca^{2+}-ATPase
TAE	Tris-acetate-EDTA
TCA cycle	Tricarboxylic acid cycle
TCMS	Trichloromethylsilane
TEMED	Tetramethylethylenediamine
TMB	3,3′,5,5′-Tetramethylbenzidine
TMEM38B	Transmembrane protein 38B
tPA	Tissue Plasminogen Activator
TRB3	Tribbles Pseudokinase 3
tRNA	Transfer Ribose Nucleic Acid
UPR	Unfolded Protein Response
UPRE	Unfolded Protein Response Element
UPS	Ubiquitin-Proteasome System
VCD	Viable Cell Density
Xbp1	X-box-binding protein 1
Xbp1s	X-box-binding protein 1 spliced

Abstract

Biopharmaceuticals are used therapeutically in a variety of human and animal conditions. Expression systems, such as Chinese Hamster Ovary (CHO) cell lines, are used in the production of recombinant proteins. Since the approval of the first FDA-approved therapeutic recombinant protein, tissue plasminogen activator (tPA), CHO cell lines have been the predominant expression systems used in the biopharmaceutical industry. There is a continual endeavour to optimise CHO expression systems to increase product yield and quality, through molecular and bioprocess engineering strategies.

The aim of this report was to contribute to a better understanding of the molecular biology of the recombinant IgG1 CHO-S cell line for the improvement of manufacture capacity. To achieve this, the first objective was to study growth and productivity of the CHO-S cell line in batch and fed-batch culture, to assess the impact of feed addition on those parameters. Feed addition resulted in a 48hr extension in culture duration, an almost two-fold increase in peak cell density and an over three-fold increase in IgG1 titre. The specific productivity was not altered between the two culture methods. The second objective was to develop methods to assess the expression of proteins involved in the unfolded protein response (UPR). The UPR has been implicated in secretory bottlenecks in CHO expression systems. This resulted in the development of primers specific to BiP, GRP94, Xbp1s and CHOP. The third objective was to examine the mRNA expression of these UPR-relevant proteins in batch and fed-batch culture, which was done using RT-PCR, qRT-PCR techniques. This confirmed that the proteins were expressed in the IgG1 CHO-S line. In batch culture there was no significant difference in gene expression but in fed-batch culture CHOP was significantly up-regulated later in culture. Between days 4, 6 and 8 of batch and fed-batch the expression of Xbp1 was significantly different between the culture method. BiP and Xbp1 expression was investigated using western blot analysis. The relationship between the expression of the UPR-relevant proteins, the specific productivity of the cell line and the overall IgG1 yield in response to BC and FBC conditions was assessed in the final objective of the report, but proved in conclusive due to the lack of change in specific productivity between the two cultures.

Further work to assess the impact of feed on CHO expression systems, factors that influence the extent of UPR activation, as well as factors that influence the specific productivity of cell lines is proposed.

Declaration

No portion of the work referred to in the thesis has been submitted in support of an application for another degree or qualification of this or any other university or other institute of learning.

Copyright Statement

Dedication

To Victoria, Peter and Pops.

Acknowledgements

I'd like to thank my supervisor, Professor Alan Dickson for guiding me in this project and for his enthusiasm for his field that has helped me find confidence in my capacity for research. I'd also like to thank Mauro, Andre, Ellie, Will and Matthew for their patience in the lab and for sharing their expertise! I'd also like to thank my family and friends who I will forever be grateful for and have supported me throughout this degree.

Chapter 1: Introduction

1.1 Biopharmaceuticals

1.1.1 Defining Biopharmaceuticals

The biopharmaceutical industry is a subsection of the pharmaceutical industry that is mostly agreed to have materialised in the 1980s with the advent of transfection methods that were able to facilitate the delivery of plasmid DNA into cultivated expression systems (Rader, 2008; Hacker and Wurm, 2017). Due to the scope of the technology with which products are being developed, there have been multiple definitions given for the term biopharmaceutical. However, not all definitions encompass the biological derivation or complexity of the field, whilst some are extensively long-winded and can appear confusing for the reader. As a result of this there has been many attempts to coin a definitive term.

A review by Rasmussen *et al.*, (2021) looking at the definition, categorisation, and environmental risk assessment of biopharmaceuticals defines biopharmaceuticals as, 'complex molecules derived from a biological source, with the purpose to diagnose, prevent, treat, or cure diseases or conditions of human beings'. Whilst this definition is useful for an overarching idea of what a biopharmaceutical is, it is not very specific. Therefore, for the purposes of this report, the definition given by Walsh and Walsh (2022) that categorises biopharmaceuticals as 'recombinant proteins, including recombinant antibodies, and nucleic acid-based and genetically engineered cell-based products' fits the categorisation within this thesis as it encompasses products derived from these aspects, such as vaccines. This report focuses on therapeutics currently being designed by the biopharmaceutical industry for the treatment of humans, although recombinant therapeutics are also being used in the treatment and diagnosis of other animals, namely in the food and pet industries (Gifre *et al.*, 2017; Bustamante-Córdova *et al.*, 2018).

A paper published by Hacker and Wurm (2017), detailing recombinant DNA technology to produce protein therapeutics in cultured mammalian cells, states that recombinant DNA technology refers to the transferring of foreign DNA, in forms such as plasmids, into another cell type using the process of conjugation to transform a recipient cell. Alongside the transfer of the recombinant gene with its regulatory elements, a second gene that confers the cells with a selective advantage is frequently simultaneously transferred so that after a few days of cultivation, when a selection agent is applied, only cells with both genes survive and grow (Wurm, 2004). Dihydrofolate reductase (DHFR) and Glutamine synthetase (GS) are commonly used genes for selection, with selection occurring in the absence of hypoxantine/thymidine and glutamine, respectively, to prevent non-transformed cells from growing (Wurm, 2004). The use of a second gene and agent together is known as a selection system. The introduction of foreign DNA into a host cell using a transfection system facilitates the expression of the gene by the host and the recombinant protein is produced by the host organism (Hacker and Wurm, 2017). The host that the foreign DNA is transferred into to produce the recombinant protein is known as the expression system. In biopharmaceutical production, the expression systems used can be mammalian, bacterial, fungal or plant- or insect- based. Biopharmaceuticals differ from chemically-based synthetic drugs, in that they are produced in living cells as opposed to being the products of chemical processes (Rader, 2008; Kesik-Brodacka, 2018). Due to the biological source and manufacture of biopharmaceuticals, there is an inherent diversity and complexity that is not found in small molecules or other synthetic chemical substances and, unlike a lot of traditional chemical drugs, biopharmaceuticals have the potential to be immunogenic due to the protein interaction with a specific target (Rader, 2008; Gils *et al.*, 2017).

The expression system used to produce a biopharmaceutical impacts the formation of the post-translational modifications (PTMs) that become essential structural (and potentially functional) features of the overall tertiary structure of the protein. The first cultivated mammalian host cell

line to be subject to gene transfer, and used as an expression system, were Chinese Hamster Ovary (CHO) cells (Kaufman *et al.*, 1985; Hacker and Wurm, 2017). The recombinant proteins first expressed in CHO included β-interferon and the first Food and Drug Administration (FDA) -approved therapeutic recombinant protein, tissue plasminogen activator (tPA), in 1986 (Kaufman *et al.*, 1985; Kim *et al.*, 2012; Hacker and Wurm, 2017). CHO as an expression system will be further discussed in Section 1.3.

1.1.2 Types of biopharmaceuticals

The Biopharmaceutical benchmarks 2022, the most recent of the quadrennial reviews published by Walsh and Walsh to survey the progression of the biopharmaceutical industry, summarises that allowing for withdrawals, the total number of individual biopharmaceutical products with active licences in the United States and the European Union is estimated to be 443. Monoclonal antibodies (mAbs), hormones, nuclei acid or gene-therapy based products, vaccines, colony-stimulating factors, cell-based products, enzymes, fusion products and clotting factors are included in this total product count (Walsh and Walsh, 2022). The recent COVID-19 pandemic influenced the proportions of the types of biopharmaceuticals produced, particularly placing an emphasis on vaccine production alongside the typical non-pandemic related therapeutics (Walsh and Walsh, 2022). Of the 197 biopharmaceutical products that were approved in the US and/or the EU within the four-year survey period from 2018-2022, 46% were genuinely new to the market and the remaining 54% were biosimilars (Walsh and Walsh, 2022). Biosimilars are defined in the Guideline on Similar Biological Medicinal Products produced by the European Medicines Agency (EMA) in 2014, as "A biological medicinal product that contains a version of the active substance of an already authorised original biological medicinal product. A biosimilar demonstrates similarity to the reference medicinal product in terms of quality characteristics, biological activity, safety, and efficacy based on a comprehensive comparability." The reference medicinal product (RMP) is also termed the

'originator' and refers to the initial product approved for market after being subject to and passing the safety and efficacy tests that new drugs are required to comply with (Covic and Kuhlmann, 2007). Biosimilars are discussed further in Section 1.1.2.2.

1.1.2.1 Monoclonal Antibodies

The demand for mAbs has resulted in the devotion of a significant proportion of the global biopharmaceutical manufacturing capacity being dedicated to the production of mAbs, including continuous endeavour to optimise the manufacturing process to maximise the system's capacity for production (Ecker *et al.*, 2015). The maturation of the biopharmaceutical industry will cause the volume and breadth of diseases being treated by mAbs to rise with the need for a cost-effective supply of large quantities of product for the treatment of conditions such as asthma and rheumatology (Ecker *et al.*, 2015). Although there have been many improvements to the optimisation of mAb production that have enhanced the process yields and as a result decreased manufacturing costs, the high demand for the products will necessitate further progress in this area (Ecker *et al.*, 2015). MAbs have been approved to treat conditions such as paroxysmal nocturnal haemoglobinuria or cryopyrin-associated periodic syndromes that affect a few thousands of patients to being used to treat cancers and multiple sclerosis that effect hundreds of thousands of patients to being used for the treatment of rheumatoid arthritis and asthma that effects millions of patients (Ecker *et al.*, 2015).

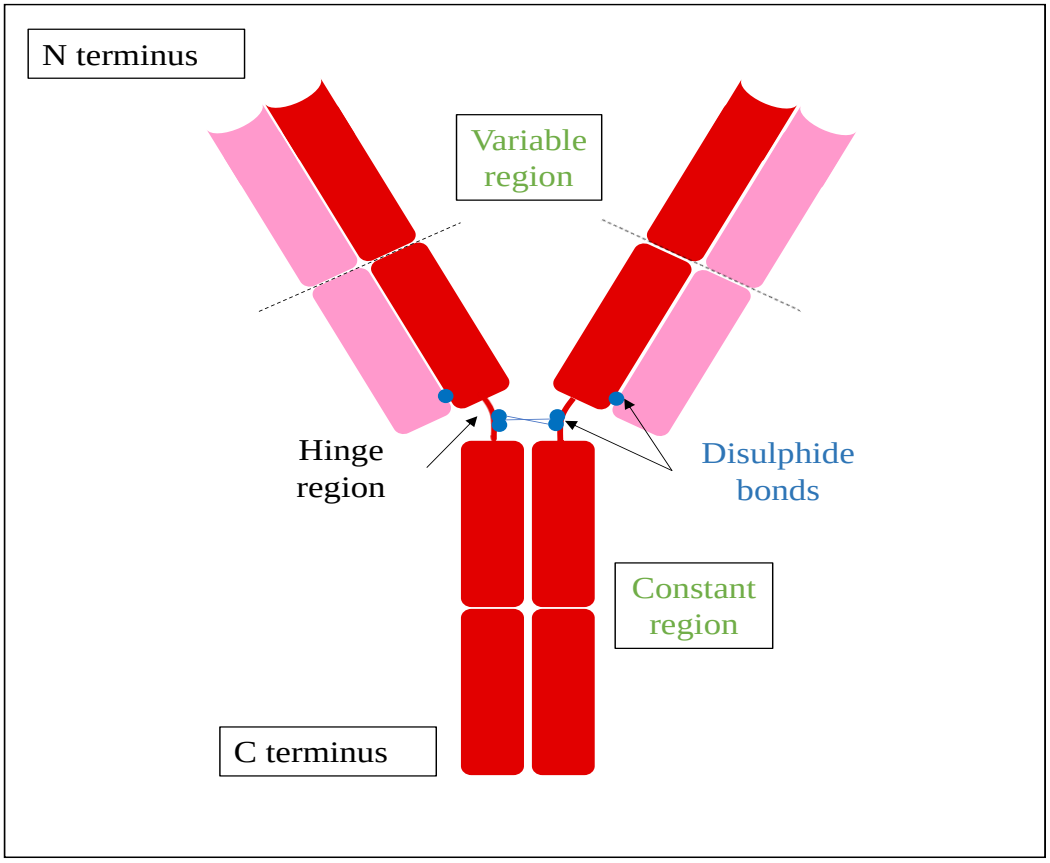

Figure 1.1. *Schematic illustration of an immunoglobulin G (IgG).*

The red represents the heavy chain and the pink represents the light chains. The variable regions in which the epitope binding sites are located are situated at the N-terminus of the antibody. The hinge region is joined through disulphide bonds to the constant region in the C-terminus.

The different subclasses of antibodies in mammalian organisms are IgM, IgG, IgA, IgE and IgD (Hanack *et al.*, 2016). Each of these classes have specialised functions within the immune response of mammalian organisms, but a key subclass for this report is that of the IgG antibodies (Hanack *et al.*, 2016). In humans, IgG are secreted in the form of globular proteins that consist of four chains in total, two light chains (molecular weights of 25 kDa) which each combine with one of the two heavy chains (molecular weights of 50 kDa) in a Y-shaped structure, that has an overall molecular weight of 150 kDa (Hanack *et al.*, 2016). The structure of an IgG is shown in Figure 1.1. Each chain is separated by variable and constant regions that

are involved in antigen binding and mediating effector functions respectively (Hanack *et al.*, 2016). The IgG subclass is comprised of the most common antibodies and are antibodies secreted by mature cells and can target corresponding antigens to label for degradation and includes the IgG1 antibody produced by the recombinant cell line in this report (Hanack *et al.*, 2016). In mammalian organisms, antibodies are secreted as part of the humoral immune response by B-lymphocytes and plasma cells (Hanack *et al.*, 2016). Depending on the lymphocytes from which antibodies originate, they can either be polyclonal or monoclonal, depending on whether they are generated from several immune cells or one immune cell with multiple different or one singular epitope, each with the affinity for one antigen (Mitra and Tomar, 2021). Both polyclonal and monoclonal antibodies have differing qualities that make them suitable for varying applications (Mitra and Tomar, 2021).

MAbs arise from one B-lymphocyte or plasma cell and target only one specific epitope on an antigen that is then replicated (Gils *et al.*, 2017). The large-scale use of mAbs in the biopharmaceutical industry originated from the development of hybridoma technology by Milstein and Kohler that led to the production of Orthoclone OKT3 (muromonab-CD3), the first therapeutic mAb to be approved by the EMA and the FDA in 1986 (Gils *et al.*, 2017). The hybridoma technique involves fusing a mouse myeloma cell with a B-lymphocyte to result in the immortalisation of a B-lymphocyte from a mouse that has been immunised against a specific antigen to secrete unlimited quantities of antibodies and can be used to produce mouse/human chimeric, humanised, and fully human mAbs (Osbourn, 2007; Gils *et al.*, 2017). The hybridoma technology that was first reported in 1975, was an early forerunner to the realisation of genetic engineering approaches involving the introduction of genes into cells to make factories for proteins that can either be secreted or used to engineer cell functions, giving way to chimeric and then recombinant proteins (Köhler and Milstein, 1975; Osbourn, 2007; Kunert and Reinhart, 2016). The previously described generation of recombinant DNA

technology in section 1.1.1, is used in the production of mAbs, as a recombinant antibody (rAb) is by nature monoclonal, as a specific gene is used from the start of the production process to express one product (Kunert and Reinhart, 2016). In this report recombinant mAbs are of key importance as an investigation is conducted to see how the secretion of these proteins by an expression system is affected in differing culture conditions and whether genes of interest are also influenced and whether these attributes are linked.

1.1.2.2 Biosimilars

The expiration of patents belonging to biopharmaceuticals that had been previously developed has led to a rise in the production of biosimilars (Gils *et al.*, 2017). Unlike the copies of chemical drugs, generics, biosimilars are not identical to their reference biopharmaceuticals due to their complex heterogeneous nature, therefore biosimilars must be subjected to evaluation before approval for therapeutic use (Gils *et al.*, 2017). As of 2022, marketing authorisation has been granted for 83 biosimilar products in the EU and 37 in the US (Walsh and Walsh, 2022). Due to the difference in licensing of these biosimilars, the revenues and cost savings vary across the global market, and although biosimilars have not enjoyed the same success in the US, the EU biosimilars marker is said to have reached €8.8 billion in 2021 with savings of €5.7 billion in comparison to the licencing of the originator products (Walsh and Walsh, 2022).

1.1.3 Market value

Since the introduction of biopharmaceutical drugs, they have revolutionised treatment of a broad spectrum of diseases and, consequently represent significant commercial importance (Kesik-Brodacka, 2018). The market value of the biopharmaceutical industry and the resultant products continue to rise, with financial reports that have not even fully considered the revenues from biosimilars that are not publicly reported indicating that global sales in 2021 reached $343 billion US (Walsh and Walsh, 2022). In the last four years, the development of COVID-19

vaccines in the form of nucleic acids had an unprecedented impact on the biopharmaceutical industry, with the cumulative revenues of Comirnaty and Spikevax reaching $54.5 billion (Walsh and Walsh, 2022). The continual expiration of patents on potential RMPs to produce biosimilars, means biosimilars are increasingly representing a greater proportion of approvals compared to previous years (Walsh and Walsh, 2022). However, in the last four years mAbs are still the most profitable product class, with sales of $217 billion in 2021, with a further $51 billion coming from non-mAb recombinant originator proteins (Walsh and Walsh, 2022). The keynote targets of these antibody-based products have been inflammatory/autoimmune conditions and cancer, each representing cumulative 2021 sales of $99.3 billion and $68.4 billion respectively (Walsh and Walsh, 2022).

1.1.4 Production

An important aspect to consider is the improvement in the manufacture capacity of the biopharmaceutical industry from the 1990s. Advancements in the form of an increase in the product yield and specific productivity of the expression systems, and the scale of manufacture have been made from a continued understanding of how cells make and secret proteins, such as antibodies. Understanding the advancements that have been made in the process and the genetic engineering fields can assist in providing a direction for further advancements by building upon what has already improved. As the production of recombinant proteins using expression systems has developed into an established practice, there has been a drive to increase both product quality and cell productivity, using strategies such as the development of basal media and feed as well as bioprocessing and the development of cell lines (Dhara *et al.*, 2018). The measurement of product quality of the recombinant protein produced is outside the experimental remit of this report, but it is an important aspect to consider. Methods of cell line, media and process engineering are no longer just focusing on improving yields, the end goal in production is to obtain a high-quality pure sample, as the ability of the protein to

perform downstream applications depends on its quality (Oliveira and Domingues, 2018). Typically, the quality of the protein sample depends on the purification strategy, but increasingly the quality control of the protein generation at the molecular level is being considered to validate the purification process (Oliveira and Domingues, 2018).

In the 1980s, after the development of the CHO cell line as an expression system, the first batch cultures were being conducted that lasted for a duration of ~ 7 days during which time cell concentrations peaked at ~ 2.0×10^6 to 3.0×10^6 cells/mL and reached final antibody titres of ~ 0.05 - 0.1 g/L (Wurm, 2004; Jayapal *et al.,* 2007). The international manufacturing company Lonza (2023), that specialises in the production of pharmaceuticals and biotechnology currently states in its website that the CHO expression system has a typical yield of 2-6 g/L in industry, but research has shown that yields of up to 10 g/L can be reached in the CHO cell line (Huang *et al.*, 2010). As also noted by Kunert and Reinhart, (2016), the increase in the specific productivity of the cells in culture has also increased the manufacture capacity of the biopharmaceutical industry. Specific productivity of batch cultures in the 1980s were ~ 10 $pg{\cdot}cell^{-1}day^{-1}$, today the highest specific productivity of CHO cell lines are ~50 $pg{\cdot}cell^{-1}day^{-1}$ but can reach ~90 $pg{\cdot}cell^{-1}day^{-1}$(Chusainow *et al.*, 2009; Wurm, 2004; Kober *et al.*, 2013; Reinhart *et al.*, 2015; Kunert and Reinhart, 2016; Torres *et al.*, 2023).

As discussed in further detail in Section 1.4, in regards to the culture of CHO specifically as an expression system, there are different types of culture techniques (Section 1.4.1) and include batch, fed-batch, and perfusion culture. Each expression system is optimised in conditions that are unique to the cell line being cultured, including the use of specific chemically define media, but due to a variety of reasons discussed further in Section 1.4, fed-batch and perfusion are most used across the biopharmaceutical industry. The refinement of large-scale bioreactor technology has also greatly contributed to the increase in the capacity to manufacture biopharmaceutical products (Erickson, 2009). Expression systems are influenced by factors

other than basal media and feed composition and addition, such as temperature, pH and osmolarity. Bioreactors assist in maintaining these factors to provide a constant optimal environment for cell growth. The use of bioreactors in the cultivation of recombinant therapeutic proteins has seen a more than 100-fold yield improvement in titres (Wurm, 2004).

Overall, the increase in the manufacture capacity that has occurred since the mid-1980s has been greatly influenced by process engineering resulting in better suited culture conditions. However, a better understanding of the molecular biology of the expression systems has also been crucial. The improvement seen in today's yields are a combination of a better understanding of factors such as gene expression, metabolism, growth and apoptosis delay in expression systems alongside process engineering (Wurm, 2004). However, there is still much more to be known about the molecular biology of cells that will help optimise the production process of biopharmaceuticals to increase product quantity and quality. This report looks at the effect of the presence of feed in culture, but as explained in further detail in Sections 1.5, 1.6, 1.7 and 1.8 also looks at specific pathways that are of interest in the secretory ability of a CHO line as an expression system.

1.2 Origin of the CHO cell line

The Chinese hamster (*cricetulus griseus*) was brought into the United States as a laboratory animal in 1948 by Hu and Watson, with dedicated breading of the animals commencing in 1951 by Yerganian at the Boston Children's Cancer Research Foundation as denoted in Figure 1.2 (Gottesman, 1987; Wurm, 2013). Figure 1.2 also shows how in 1957, a female hamster was given to Theodore Puck. Puck first conducted his research in the Department of Biochemistry at the University of Colorado where he set up the Eleanor Roosevelt Institute for Cancer Research to continue his research (Gottesman, 1987; Wurm, 2013).

CHO cell lines were first established by Puck from the trypsinization of 0.1g of ovary tissue from a Chinese hamster (Wurm, 2013). The resultant culture from the trypsinization was mainly fibroblast in type with a near diploid karyotype with 1% of the population having 21 or 23 chromosomes instead of the expected 22, a diversion in the primary cells that is not seen in primary human cells (Wurm, 2013). The close-to-diploid-like cells were then maintained in culture for 10 months, during which time a 'spontaneous immortalisation' event occurred as noted in Figure 1.2, and the resultant cells were reported to have modified to a more epithelioid morphology (Puck, 1994; Wurm, 2013). Re-cloning of the cells from this culture (that had undergone some form of 'spontaneous immortalisation') generated what is regarded to be the originator source of all current CHO lines (Puck, 1994; Wurm, 2013). Wurm states that the event itself was relatively poorly recorded/described, as it was not the intended outcome of an experiment itself, but the outcome of the event has resulted in the creation of subsequent CHO lines that have become the predominant expression system used today to produce recombinant therapeutics.

The lower half of Figure 1.2 shows how this immortalised original CHO cell line has given rise to multiple other branches of CHO lines, each arising as a result of mutational events coupled to cell selection or latterly the result of directed genome engineering. The term 'quasispecies' was devised by Wurm to denote families of related genomic sequences that are exposed to high mutation rate environments where a large proportion of the offspring is expected to carry on one or more mutations, and the CHO cell system is an example of this biological situation (Wurm, 2013; Lewis *et al.,* 2013).The initial non-standardised culture conditions of CHO cells has contributed to the high mutation rate of the cell line and resulted in the continuous remodelling of the genomic structure in both clonal and non-clonal populations to create subsequent sub-lines with great genomic and phenotypical differentiation, which has had a

significant impact on the production of proteins (Gottesman, 1987; Wurm, 2013; Lewis *et al.,* 2013; Stolfa *et al.*, 2018).

Several CHO cell lines are used in bioproduction. Work done by Lewis *et al.,* (2013) on the genomic landscapes of CHO cell lines revealed using the *Cricetulus griseus* draft genome has been conducted to generate a unifying genomic resource for CHO cells to aid in the assessment of the genotypic differences amongst CHO cell lines. As seen in Figure 1.2, while the CHO-K1 was sustained in Denver by Puck and Kao in 1968, and the CHO pro3- was sustained by Flintoff in 1976, these sublines have since given rise to subclones with similar and distinct properties to their own and readily produce mutant phenotypes (Gottesman, 1987). Alongside CHO-K1 and CHO pro3-, the CHO-S sub-line may have been adapted for growth in suspension in 1971 by Thompson and Baker, (1973) at the University of Toronto as this is where its appearance is first noted (Gottesman, 1987). This CHO-S subline is the progenitor to the cell line used in this report, hence the elaboration of its descendant subclones in Figure 1.2.

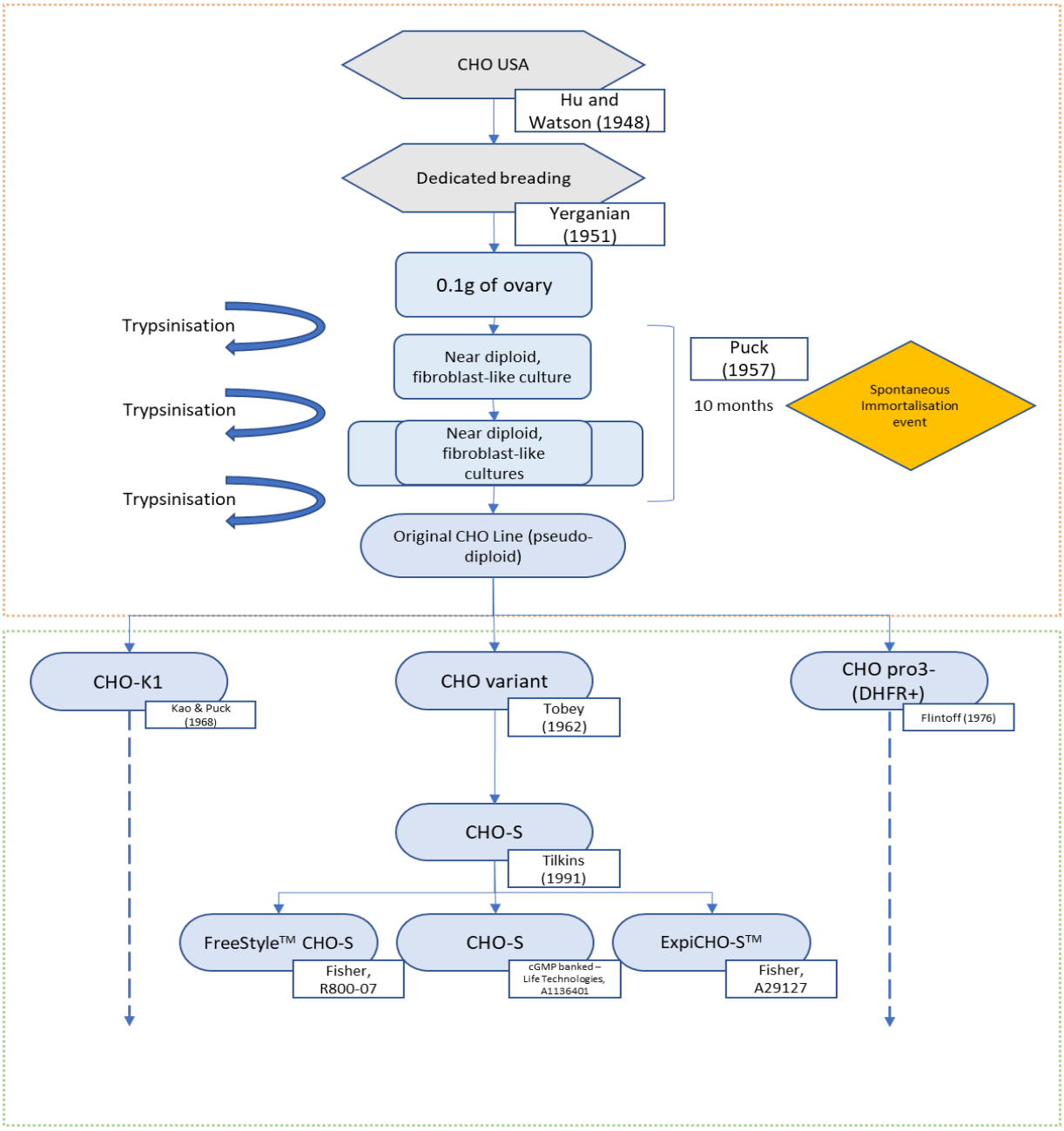

Figure 1.2. *Outline of CHO-S cell line origin.*

The figure has been adapted from Lewis et al., (2013) and Wurm, (2013). The sequence outlined by the dashed orange box depicts the sequence of events that led to the generation of the original Chinese hamster ovary (CHO) line. The 'spontaneous immortalisation' event occurred within the 10-month culture period but the exact timing is unknown. The sequence outlined by the dashed green box depicts the sequence of events that led to the generation of the CHO-S line that has led to some of the lines in use today. It also depicts the CHO-K1 and CHOpro3-(DHFR+) branches of the CHO cell line but the decedents of which have not been included to highlight the CHO-S branch that has been used in this study.

1.2.1 CHO-S

As with much of the recording of the origin of CHO cells, there is ambiguity surrounding the development of the CHO-S cell line. In 1964, Puck *et al.*, recognised that there was capacity for growth in single-cell suspension culture (Puck *et al.*, 1964; Wurm, 2013). As previously stated, the development of CHO-S was mentioned by Thompson and Baker in 1973, but there is uncertainty surrounding the origin of the development of the CHO-S cell line (Thompson and Baker, 1973; Wurm, 2013). A sister line to the Toronto CHO-K1 line is referred to as CHO pro^{-5}, from which it has been speculated by Wurm, (2013), that it is from this line which the CHO-S line could have been derived from. As well as being cultured in research labs, these CHO-S cells were eventually passed into commercial production and have been on the market since 2002 (Wurm, 2013). Following the exact lineage of the CHO-S line is challenging due to the lack of initial definitive records keeping up with the heterogeneity of the CHO and the resultant formation of sublines, which is compounded by the ownership of much of the CHO-S technology by biopharmaceutical manufactures such as Sigma Aldrich that justifiably do not wish to publish their product details.

1.2.1.1 CHO-S IgG1

As will be discussed further in Section 2.2.1 the cell line used in this report was a recombinant IgG1 producing CHO-S cell line provided by Dr Mauro Torres. The cell line was developed during a study on the overexpression of the transcription factor BLIMP1/prdm1 leading to growth inhibition and enhanced secretory capacity of CHO cells (Torres and Dickson, 2021). To produce the IgG1 CHO-S cell line, the CHO-S cells were transfected with an expression plasmid using standard electroporation before being placed in a selection medium (Torres and Dickson, 2021). The plasmid expressed human IgG1 Herceptin HC and LC sequences controlled by a CMV promoter and was purified and linearised prior to transfection (Torres and Dickson, 2021). Three weeks after seeding, fluorescence-activated cell sorting (FACS)

was used and positive IgG1 cell line was sorted using FITC-conjugated Goat Anti-Human IgG Fc for limited dilution cloning before being scaled-up from well-plates to shake-flasks (Torres and Dickson, 2021). Cells adapted to suspension with 100% viability were frozen as stocks (Torres and Dickson, 2021).

Section 1.1.1 described the concept of using selection systems to ensure that recombinant genes transfected by expression plasmids are present in cells. For this report puromycin was used as a selection agent for the plasmids introduced into the CHO-S IgG1 cell line. Puromycin is an antibiotic that mechanistically works as an aminonucleoside to disrupt translation, inducing apoptosis through interference with RNA function inhibiting protein synthesis (Lanza *et al.*, 2013; Korrapati, 2014). Part of the structure of puromycin resembles charged tRNA which can terminate a growing polypeptide chain (Lanza *et al.*, 2013). The puromycin N-acetyl transferase (pac) gene that is originally present in the bacteria *Streptomyces alboniger* confers resistance to puromycin (Lanza *et al.*, 2013). When mobilised onto a plasmid this pac gene can be used to provide resistance (Korrapati, 2014). Puromycin works as a selective agent in gram-positive bacteria and eukaryotes (Korrapati, 2014). It does not work in fungi and gram-negative bacteria due to the antibiotics low-permeability (Korrapati, 2014).

1.3 CHO as an Expression System

As mentioned in Section 1.1, expression systems are used in the production process of biopharmaceutical products. During the 2018-2022 period, mammalian cell systems continued from previous years to be the predominant expression system used in biopharmaceutical production, with CHO cells continuing to be the most frequently used expression system in recombinant antibody production (Walsh & Walsh, 2022). Other mammalian expression systems such as murine myeloma (NS0 or Sp2/0) cell lines, are also commonly used in biopharmaceutical production, but to a lesser extent (Estes and Melville, 2014; Walsh, 2018). In 2016 CHO lines were used to produce 7 of the top 10 best-selling biopharmaceuticals, and

until 2018, CHO lines had been used to produce 57 of the 68 (84%) mAb products approved overall until the year 2018 (Kesik-Brodacka, 2018; Walsh, 2018). By 2022, CHO expression systems had been used to produce 95 of the 107 (89%) individual mAbs expressed by mammalian systems (Walsh & Walsh, 2022).

As previously referred to in Section 1.1, there are alternatives such as bacterial, plant, insect and fungal expression systems, that have all been used to produce biotherapeutic products and have their own advantages, mammalian expression systems are still preferred (Dumont *et al.*, 2016). This is mainly due to the complex PTMs that most closely resemble those of humans in mammalian systems, but also a result of the rapid growth, high yield and investment (Dumont *et al.*, 2016). There are human cell lines such as the HeLa which was the first human cell line to be established, 1951, from a cervical cancer patient from whom, diploid cells were developed and still used today for the manufacture of vaccines (Dumont *et al.*, 2016). Whilst the use of human cell lines in the production of some biopharmaceuticals does occur and the possible capability of the cell lines are being investigated, they are not currently the preferred expression system due to potential human virus sequences that can impact the therapeutic product.

Starting from the time when a CHO cell line was used as the expression system to produce tissue plasminogen activator (tPA), the first recombinant therapeutic protein approved for use in 1986, CHO expression systems have retained their popularity for several reasons (Kim *et al.*, 2012). The popularity of using CHO cell lines as expression systems in manufacturing is a result of the duration in which they have been used in culture, the robustness and relative tolerance to environmental changes in manufacturing culture conditions, and the ability to express successful products with limited risk of transmission of unknown infectious agents, which has built an established safety profile and a sense of familiarity in the field (Kim *et al.*, 2012; Wurm, 2013; Dumont *et al.*, 2016). Moreover, CHO production platforms have shown the ability to produce high (3-8g/L) antibody titres at production scale, with some reports of up

to 10g/L (Kim *et al.*, 2012; Walsh & Walsh, 2022). CHO cells can also be grown in suspension culture to enable large-scale production as well as to be adaptable to serum-free media which has a better safety profile than media that contain animal derived proteins as well as conferring a greater degree of reproducibility (Kim *et al.*, 2012; Dumont *et al.*, 2016). Crucially, as previously stated, the choice of expression system used in the production of biopharmaceuticals, such as mAbs, is dictated by the PTM requirements of the product, and CHO is a mammalian expression system that can facilitate many of the more complex PTMs as the cells contain much of the machinery required to synthesise proteins with large molecular structures (Walsh & Walsh, 2022; Torres & Dickson, 2022). However, it should be noted that CHO production platforms are unable to produce certain types of human glycosylation and also produce glycans, such as α-gal and NGNA, that are not expressed in humans and may carry immunogenicity risks for therapeutic products produced (Dumont *et al.*, 2016).

Section 1.1.4 discussed how a better understanding of how the cells being used as expression systems produce proteins has led to an increase in the yield, the specific productivity, and the scalability of expression systems between the 1990s and today. To increase product titres, either the specific productivity of a cell can be increased by targeting the protein synthesis and secretion machinery or cell numbers can be increased by altering cell metabolism or reducing apoptosis to increase cell density (Prashad & Mehra, 2015). Although CHO cells are the leading production platform for manufacturing protein-based therapeutics, the efficiency of recombinant protein production is impeded by limitations in their secretory ability (Torres & Dickson, 2022). The differences in CHO cell line genotype and subsequent phenotype that limit productivity have been approached using traditional bioprocess optimisation and cell line engineering alongside the incorporation of omics-based approaches to maximise the gains of improvements (Stolfa *et al.*, 2018). The productivity of recombinant CHO lines is complex, with numerous pathways contributing to the production rate, therefore, understanding the

molecular basis of the expression systems productivity is complex (Prashad & Mehra, 2015). The high titres that have been achieved in the production of recombinant therapeutic proteins in industry are a result of the combination of high throughput cell line selection and advancements in bioreactor technology and the optimisation of culture conditions, such as feeding regimes, as discussed in Sections 1.1.4 and 1.4 (Prashad & Mehra, 2015).

1.4 Culture of CHO cells

As discussed in Sections 1.1 and 1.3, CHO cell lines are robust and adaptable, which lends them to being the primary choice in expression system. As CHO cell lines are used in the production for most biopharmaceuticals, improvements to the efficiency and the quality with which they produce recombinant proteins would increase the overall yield of usable product, saving on time and cost in production. Therefore, the way in which CHO cells have been cultured has been subject to great consideration. The culture conditions of expression systems are known to greatly impact the cell line growth and productivity and therefore have been investigated to optimise the culture process.

1.4.1 Types of cell culture techniques

Batch culture (BC) is a method of cell culture, that can be conducted with relative simplicity and ease. As described further in Section 2.2.5, during BC, cells are seeded in medium and incubated over the course of culture duration. Cell or medium samples are taken to monitor antibody production and cell growth. Under BC, recombinant protein would tend to be harvested at the end of culture as the build-up is cumulative in the medium throughout. Throughout culture, no additional supplements are added, so cell metabolism relies on the nutrients present in the medium at the time of seeding. Although this is an advantage of BC as it is the least labour intensive and complex culture method of expression systems such as CHO, it means as culture progresses, the nutrients required for cell growth and viability are consumed

and, making BC a finite process. Not only is the consumption of nutrients a limitation, the build-up of toxic by-products from cell metabolism that are not removed from the closed culture system, results in cell death.

Fed-batch culture (FBC) is an alternative method of culture. Although the initial preparation of a FBC is the same as a BC, the two culture techniques differ with the addition of nutrient-enriched feed in FBC that does not occur in BC. FBC is the most used mode of cultivation of CHO cell lines for commercial production of mAbs (Schellenberg *et al.*, 2022). The feeding regime, which encompasses feed composition and the interval with which the culture is supplemented with feed, defines the parameters of the FBC, and can either been given continuously or in bolus application (Xu *et al.*, 2023). The bolus method can be used to collect the recombinant protein expressed by the system. A predetermined volume of medium is removed from the culture, typically immediately prior to the addition of feed, that is then replenished with the same volume of feed to maintain a constant cell culture volume, as change in volume impacts cell growth. These medium samples can also be used to monitor growth and viability of the expression system in culture. FBC expression of recombinant protein is a cumulative process and a continual feed process can be implemented with the entire system sacrificed and protein harvested from the medium at the end of culture. Although the addition of feed, is a marked difference between FBC and BC, and that medium is removed to be replenished by feed and for cell viability monitoring, there is still a build-up of toxic by-products from cell metabolism in the medium as they are not removed as they are produced, this differs from perfusion – a separate method of culture discussed at the end of this section.

Studies comparing BC and FBC in CHO cell lines consistently show that as a result of the nutrient supplementation, expression systems cultured in FBC reach a higher peak cell density and length of culture duration, than in BC. This is because there are practical limitations to the amount of nutrients that can be initially supplied to a BC, these being that the available nutrients

in the medium would used up by cell metabolism as the number of viable cells increases in the culture, as well as the fact that the overconsumption by cells made possible by the addition of surplus nutrients may have adverse effect on cell health (Wong *et al.*, 2006). As a result, the avoidance of nutrient limitation in FBC results in a higher production of recombinant proteins, with reports of mAb titres of up to 10 g/L in CHO cells in FBC (Xu *et al.*, 2023). As exemplified in Section 3.1.1, there are different cellular growth phases in BC and FBC, these being the lag phase, the exponential phase, the stationary phase, and the death phase of cell growth. In FBC, outside of the increase in peak cell density and culture duration, the pattern in which these stages are conducted is similar in BC and FBC, except for the increase in the duration of stationary phase in FBC but this is a result of the increase in duration of FBC in comparison to BC (Sellick *et al.*, 2015; Xu *et al.*, 2023).

Aside from BC and FBC, there are other culture techniques for expression systems such as perfusion. These culture conditions are not explored in this report, but in large-scale bioreactors, after FBC, perfusion in is the second most common cultivation method in biomanufacturing (Bielser *et al.*, 2018). The nature of perfusion results in a high yield of harvest of recombinant protein, however, the processes involved are either labour intensive or require complex machinery. During perfusion, medium is added to the system at a constant flow rate that is identical to the rate in which the bioreactor content is removed, with the cells being retained in the bioreactor, or being bled out using a bleed stream to remove cells to maintain a steady cell concentration (Bielser *et al.*, 2018). Unlike FBC, this results in the prevention of build-up of toxic by-products and cells from entering cell death phase. Refinement to the culture techniques and machinery used in the implementation of these processes is a rapidly evolving practice.

1.4.2 Medium composition

Although the addition or removal of supplements or by-products, respectively, is not a consideration required for BC, the initial medium in which the cells are seeded must be considered. As the process of cell culture is continually refined, it has become obvious that different cell types require specific environments to thrive, one of which being the medium in which they are grown. As detailed in Section 2.2.1 the basal medium used in the culture of this IgG1 CHO-S line was CD CHO, which was subject to supplementation. Supplementation of the medium enables the specialisation of commercial medium to certain cell lines, such as IgG1 CHO-S, for cell growth optimisation in BC.

As detailed in Section 2.2.1, both BC and FBC were seeded in the same initial medium. However, the name-sake defining feature in FBC in comparison to BC is the addition of nutritional supplementation of the medium in which the expression system is seeded. The addition of feed can be used to replenish nutrients that are being consumed by cellular metabolism. As detailed in Section 2.2.6, the feed used for FBC of IgG1 CHO-S cells in this report was a mix of CHO CD EfficientFeed A and CHO CD EfficientFeed B. Pan *et al* (2017), examined the effect of using chemically-defined media on FBC of CHO cells to examine 24 different culture conditions. The study involved the use of two CHO BC suspension lines, a high peak cell density and low productivity cell line, CHO BC-G, a low peak cell density and high productivity cell line, CHO BC-P, compared in 12 different basal medium-feed combinations, one of which being the CD CHO basal medium with the addition of 1:1 (v/v) ratio Efficient Feed A + B, as used in this report (Pan *et al.*, 2017). The CD CHO EfficientFeed A+B combination reached an IgG titre of ~40mg/L and had an IgG volumetric productivity of ~35mg/L/day in the CHO BC-G cell line, and an IgG titre of ~450mg/L and had an IgG volumetric productivity of ~400mg/L/day in the CHO BC-P cell line (Pan *et al.*, 2017). These productivity levels were towards the lower end in comparison to other basal media/feed

combinations (Pan *et al.*, 2017). A study conducted by Sellick *et al.*, (2015) looked at metabolite profiling using gas chromatography-mass spectrometry (GC-MS) to define molecular loci of two feeds to improve recombinant antibody yields in a GS-CHO cell line. CD-OptiCHO medium was then either left as an unfed BC or supplemented with either CHO CD Efficient Feed A or CHO CD Efficient Feed B in FBC. In absence of feed the BC reached a cumulative cell number over the culture period of 40.84×10^6 cells/mL/day with a specific productivity from day 0-10 of 10.72 pg·cell^{-1}day^{-1} (Sellick *et al.*, 2015). In comparison in FBC, the cumulative cell number was over the total culture period was 81.17×10^6 cells/mL/day with EfficientFeed A and 90.19×10^6 cells/mL/day with EfficientFeed B and the specific productivities from day 0-10 were 13.00 pg·cell^{-1}day^{-1} and 12.36 pg·cell^{-1}day^{-1}, respectively (Sellick *et al.*, 2015). Furthermore, a study conducted by Braasch *et al.*, (2021), using a recombinant CHO line expressing human monoclonal anti-Interleukin-1β IgG1 was conducted in BC and FBC conditions to assess the impact of the addition of varying autophagy-inducing peptide (AIP) concentrations on antibody production. Autophagy is discussed further in Section 1.5, but in the study both BC and FBC were conducted in absence of AIP as controls (Braasch *et al.*, 2021). Both BC and FBC were cultured in chemically defined supplemented CD CHO medium, with a feed comprising of CD CHO Efficient Feed A and amino acid mixtures 'A' and 'B' being added to the FBC daily from Day 1 of culture (Braasch *et al.*, 2021). The specific productivity of the control in BC was 10.6 ± 0.6µg/10^6cells/day compared to 9.6 $\pm$ 1.5µg/10^6cells/day in FBC, showing the addition of feed had little impact on this parameter (Braasch *et al.*, 2021).

As with initial medium composition, the feed being used to supplement FBC can be tailored to cell line specific needs, to optimise cell growth. In CHO FBC feed composition optimisation, amino acid content is crucial. Cells can synthesise non-essential amino acids, but essential amino acids cannot be synthesised, so to save from the detrimental consequences on

recombinant protein production as a result of amino acid depletion as seen in BC in CHO, amino acids must be added in the feed medium (Xu *et al.*, 2023). The tricarboxylic acid cycle (TCA cycle) in CHO cell metabolism relies on the addition of amino acids in feed (Xu *et al.*, 2023). However, the quantity of amino acids in the feed composition must be carefully controlled, as by-products such as the build-up of ammonia from the hydrolysis of amino acids, can have a negative impact on cell proliferation at concentrations above 5mM (Yang and Butler, 2000; Xu *et al.*, 2023). Similarly, a source of carbon is needed for the TCA cycle and must be provided in the feed. In the TCA in CHO, glucose is the primary carbon source, but its consumption leads to the production of pyruvate and lactate metabolites which inhibit cell growth (Xu *et al.*, 2023). Glutamine is the secondary carbon source of the TCA in CHO, but the consumption of this too increases lactate levels (Xu *et al.*, 2023). Other feed composition elements to consider include inorganic salts, vitamins, lipids as well as others (Xu *et al.*, 2023). Another aspect to consider in FBC is not only the feed composition but the interval with which the medium is supplemented with feed. A frequent feeding regime may result in a fluctuation in the number of cells in culture, as the addition of feed and removal of culture sample decreases cell density which may influence cell growth and may not be conducive to attaining the highest yield of recombinant protein possible. Also, a more frequent feeding regime is obviously more labour intensive, which may not be favourable when running the expression system. Bolus feeding can result in the build-up of toxic by-products, but in comparison to a continuous feed strategy is relatively simple to operate, with low facility requirements and associated costs (Xu *et al.*, 2023).

1.4.3 The effect of feed on gene expression in CHO

From previous studies, such as that of Sellick *et al.*, (2015), FBC has been shown to result in a longer culture duration, higher peak cell density and a greater yield in antibody production from CHO expression cell lines (Alhuthali *et al.*, 2021). This is a result of having nutrients

available for cell metabolism. A study conducted by Wong *et al.*, 2006, used a recombinant human interferon gamma (IFN-γ) CHO cell line and subjected it to transcriptional profiling to follow the sequential regulation of apoptosis in culture, to determine differential expression of apoptosis signalling genes in BC and FBC. For both BC and FBC during the exponential phase of cell growth there was little change in the apoptosis-related genes, however, at the transition to the stationary phase of culture there was shown to be an increase in the up-regulation of initiator genes in the death-receptor and mitochondria-mediated apoptosis pathways (Wong *et al.*, 2006). The death phase of cultures saw the up-regulation of executioner apoptosis genes which are discussed further in Section 1.8.3 (Wong *et al.*, 2006).

1.5 Cell death

Cell death is the end of life for unicellular organisms, but an essential process for the physiological growth and development of multicellular organisms, from which expression systems are generated (Chen *et al.*, 2018). Having cells as an expression system that survive for longer or are resistant to processes that may activate cell death, could be an advantage for maximising the output of a cell factory system. To increase the output of recombinant proteins, understanding the mechanisms behind the signalling pathways that lead to cell death could be used to generate a greater yield from culture as mediating factors that lead to cell death and consequently stop protein production, could be mitigated. As previously discussed in Sections 1.1, 1.3 and 1.4 engineering of cell lines is used to increase the manufacture capacity of the biopharmaceutical industry. Looking at the cell death process in closer detail may enable us to establish whether it influences the protein synthetic machinery that could be altered to increase the quantity and quality of the output of cells as expression systems. It also provides context for Sections 1.6, 1.7 and 1.8 in which we look at the capacity of cells, especially CHO, to respond to stress that might result in the causation of cell death. The capacity of cells to respond to stress can be indicated by the measurement of markers, such as proteins that are involved in

stress responses including that of the unfolded protein response (UPR), a concept which is discussed in more detail in following sections.

The classification by which cell death occurs is determined by its morphological appearance, the enzymological criteria, functional aspects, or immunological characteristics (Kroemer *et al.*, 2009). Through the activation of multiple specific signalling pathways, the mechanisms of cell death display distinct morphological features, as will be described below (Chen *et al.*, 2018). However, there is interplay between these pathways which can be activated simultaneously and in a multicellular organism can operate in adjacent cells to respond to cellular stresses (Chen *et al.*, 2018).

Conventionally, at a basic level there was wrongly considered to be only two forms of cell death, un-programmed (UCD) and programmed (PCD) (Cui *et al.*, 2021). These categories were initially represented by the terms necrosis and apoptosis, respectively. As a result of more detailed research, cell death has further sub-classifications (with other potential mechanistic variants being proposed) including that of necroptosis, which while not discussed in detail in this report, has similar morphological appearance to necrosis but is programmed, which goes against the traditional classifications of necrosis (Khan *et al.*, 2021). Presently, the *predominant* morphologies associated with cell death are necrotic and apoptotic, with autophagy being a degradation mechanism that can induce autophagy-dependent cell death, if necessary (Chen *et al.*, 2018). There is now known to be programmed forms of necrotic cell death (such as necrosis), but it was generally considered to be an 'accidental' or 'uncontrolled' form of cell death, and is marked by an increase in cell volume with swelling of organelles to the extent that the cellular plasma membrane ruptures, resulting in the loss of cellular intracellular contents (Kroemer *et al.*, 2009; Khan *et al.*, 2021). Necrosis is typically characterised in the absence of apoptotic or autophagic markers (which will be outlined below), but biochemically necrosis can be circumvented through the genetic or pharmacological inhibition of receptor

interacting protein kinase 1 (RIP1/RIPK1) (Kroemer *et al.*, 2009). Necrosis is not being considered in relation to the work described in this project due to its lack of involvement in the regulation of the cellular internal environment by processes such as proteostasis.

Apoptosis induced by nutrient limitations is a well-known mechanism of cell death impacting cell culture (Kim and Lee, 2002; Braasch *et al.*, 2021). Apoptosis, alongside autophagy, is a molecular process that maintains homeostasis at an organismal and cellular level (Fan and Zong, 2013). Kerr *et al.*, (1972) first coined the term apoptosis to refer to a mechanism of controlled cell deletion processes that work in opposition to mitosis in an actively programmed manner, initiated or inhibited by a variety of stimuli in the cellular environment. Since its derivation, the term apoptosis has almost become synonymous with PCD, but this is misleading as there are other forms, such as the previously mentioned autophagy-dependent cell death and necroptosis, pyroptosis, and ferroptosis, that do not share apoptotic morphological features (Cui *et al.*, 2021). These other forms of PCD differ from classical apoptosis through their initiation signalling or through the balance of effector executioners. Pyroptosis, is a lytic inflammatory cell death mediated by inflammatory caspases, while ferroptosis, is an iron-dependent form of PCD that is characterised by an accumulation of intracellular reactive oxygen species (Cui *et al.*, 2021). Apoptosis is now generally considered to be a caspase-mediated PCD that is characterised by the rounding of the cell with retraction of pseudopods and a reduction in the volume of the cell followed by chromatin condensation and nuclear fragmentation with little to no modifications to cytoplasmic organelles (Chen *et al.*, 2018; Kroemer *et al.*, 2009). *In vivo* plasma membrane blebbing would occur at late stages before the cell is engulfed and destroyed by phagocytes.

The mediation of activating signals of apoptosis can be via extrinsic pathways, typically triggered by the binding of extracellular ligands to receptors, or by intrinsic pathways that are typically initiated by stimuli produced from within the cell itself (Wong *et al.*, 2006). These

differences in the stimuli have led to morphologically similar subtypes of apoptosis, distinguished by the biochemical routes by which they are activated (Kroemer *et al.*, 2009). The activation can occur via either the death receptor-mediated, the mitochondria-dependent or endoplasmic reticulum (ER) stress-induced, apoptosis pathways (Chen *et al.*, 2018). In cell culture, increased apoptosis has been linked with a decrease in cell productivity, product quality, growth and viable cell density (VCD) (Krampe and Al-Rubeai, 2010).

As previously alluded to, autophagy is the cellular process by which cytoplasmic contents are degraded and the constituents recycled (Feng *et al.*, 2014). In mammals macroautophagy, microautophagy and chaperone-mediated autophagy, are the three kinds of autophagy that occur in these multicellular organisms and are distinct based on mechanism by which the uptake of cytoplasmic material occurs during these processes (Feng *et al.*, 2014). In this report on the culture of the unicellular mammalian expression system, CHO, we focus on macroautophagy, as the primary form of autophagy. Macroautophagy is the process by which material is sequestered by two-membraned structures that contain degenerating organelles known as 'autophagosomes' for degradation by lysosomes (Kroemer *et al.*, 2009). The fusion of the autophagosome and lysosomes results in the formation of autolysosomes, in which the catabolic process of the degradation of the autophagosome inner membrane and its luminal contents by hydrolases occurs (Kroemer *et al.*, 2009). In microautophagy, there is no autophagosome in the process, the hydrolases enter directly through the breaking of the cellular membrane (Kroemer *et al.*, 2009). Autophagic cell death occurs in the absence of chromatin condensation with the incidence of autophagic vacuolisation of the cytoplasm and differs from apoptotic cell death as there is little to no association with phagocytes (Kroemer *et al.*, 2009).

Evidence of apoptosis occurring in cell culture was found by Al-Rubeai *et al.*, (1990) during electron microscopy of hybridoma cells regarding mAb production (Krampe and Al-Rubeai, 2010). Since, apoptosis has been shown to be induced in BC, FBC and perfusion cultures and

has been shown to be triggered by nutrient deprivation, environmental stress factors such as pH fluctuations, high osmolarity, oxygen deprivation, accumulation of reactive oxygen species as well as exposure to hydrodynamic forces (Krampe and Al-Rubeai, 2010). Macroautophagy (autophagy) has also been implicated in mammalian cell culture. Autophagy has been implicated in cellular stress responses, working in conjunction with apoptosis (Zustiak *et al.*, 2008). Autophagy-dependent cell death can occur when apoptosis has been inhibited (Zustiak *et al.*, 2008). Both apoptosis and autophagy have been evidenced in cell culture of recombinant CHO lines, such as in instances of nutrient deprivation (Hwang and Lee, 2008; Krampe and Al-Rubeai, 2010). As a result, apoptosis and autophagy have been targets of cellular engineering in CHO cell lines. In a CHO-DG44 cell line, transient over-expression of the anti-apoptotic gene bcl-2 resulted in the yield of adequate mAb increasing by 70-270% (Majors *et al.*, 2009; Krampe and Al-Rubeai, 2010). Furthermore, a study conducted by Kim *et al.*, (2009) was able to delay both apoptotic and autophagic-cell death in a recombinant CHO-EPO cell line in nutrient deprived conditions through the overexpression of another anti-apoptotic protein, Bcl-xl (Krampe and Al-Rubeai, 2010). As previously mentioned in Section 1.4.2, a study by Braasch *et al.*, (2021) targeted autophagy using culture conditions to improve mAb productivity of a CHO cell line, through the addition of AIP in BC and FBC. The study found that addition of 1-4μM increased productivity in a concentration dependent manner, despite negative impacts on cell growth and viability, but provides overall support for the modulation of autophagy in the improvement of CHO cell culture (Braasch *et al.*, 2021).

1.5.1 Proteostasis

As previously referred to, homeostasis is the property of a system, such as an entire organism or cell, in which variables are regulated to ensure the internal conditions are relatively constant (Torday, 2015). There are three key aspects of homeostasis, a *sensor* to detect change, a *feedback* mechanism and an *effector* to implement changes in the regulated condition (Torday,

2015). Due to the nature of homeostasis, there are many subsystems within its regulation. One such subdivision is protein homeostasis or 'proteostasis', the regulation of a cell's internal environment in the regards of proteins, to sustain a healthy proteome (Hoppe and Cohen, 2020). The proteome is all the proteins expressed in a cell type or organism (Balchin *et al.*, 2016; Hoppe and Cohen, 2020). The quality control signalling pathways of the proteostasis network are discussed in the Section 1.7, but it is the breakdown of these pathways that lead to apoptosis and autophagy as previously described.

1.6 Secretory pathway

As discussed in Section 1.1.4, there has been a significant increase in the manufacture capacity of the biopharmaceutical industry and, as discussed further in 1.4, the optimisation of culture conditions has greatly impacted this. Reiterating Sections 1.1, 1.3-1.5, alongside culture optimisation, genetic engineering of cell lines is a mechanism the has been used to increase manufacture capacity. Cell line engineering relies upon an understanding of the molecular biology of expression systems, such as CHO. Cell line engineering has previously been targeted towards enhancement of transcription and translation in expression systems, but increasingly the secretory pathway is being investigated in the capacity to increase protein production (Le Fourn *et al.*, 2014).

Due to the nature of the production mechanism, the secretory ability of an expression system is fundamental in its capacity to produce antibodies. In mammalian cells, protein secretion begins with translocation of the polypeptide into the ER, the ER lumen is where protein folding and maturation occurs before the protein is translocated to the Golgi apparatus for additional modifications, such as glycosylation if required, before the protein is secreted into the extracellular environment (Zhou *et al.*, 2018). How the secretory pathway in CHO cell lines impacts recombinant protein expression is an area that has been reviewed by Torres *et al.*, (2022). Phenotypically, secretory bottlenecks are characterised by a dissociation between the

recombinant mRNA abundance and cell specific productivities (Schröder and Friedl, 1997; Schröder *et al.*, 2002; Coats *et al.*, 2020; Torres *et al.*, 2022). Secretory bottlenecks in recombinant protein production arise as a result of CHO cells being pushed to the limit of the cellular capacity to manufacture proteins, lacking dedicated machinery to accommodate for increased protein secretion (Torres *et al.*, 2022). The mechanisms by which these bottlenecks arise at the molecular level are specific to the cell-line used and recombinant protein being expressed (Torres *et al.*, 2022). However, these mechanisms have been associated with three stages of the secretory pathway, *protein synthesis and/or translocation, early ER processing* which encompasses protein folding and assembly, and *protein trafficking* between the ER-Golgi interface (Torres *et al.*, 2022). As discussed in further detail in the upcoming sections, 1.7 and 1.8, the focus of this report will be on molecular events at the early ER processing stage of recombinant protein production and the quality control mechanisms in place within the cell.

1.7 ER Stress

As eukaryotes, mammalian cells contain membrane-bound organelles including the nucleus, the Golgi apparatus, mitochondria and the ER. The ER is a large lacework-like organelle that extends throughout the cell cytoplasm, in close proximity to and interacting with all other organelles, most notably the nuclear envelope with which it is physically interlinked (Zhao *et al.*, 2022). The roles served by the ER include the synthesis, folding and transport of proteins (Almanza *et al.*, 2019; Zhao *et al.*, 2022).

As described in Section 1.6, in mammalian systems the secretion pathway starts with the translocation of the developing protein into the ER (Prashad & Mehra, 2015; Zhu & Lee, 2015). The synthesis and folding of proteins is fundamental to cell function and survival. In mammalian cells, roughly a third of all proteins present in the cell during translation are targeted to the ER (Zhao *et al.*, 2022). Proteins that are translocated to the ER undergo PTMs, such as N-linked glycosylation and disulphide-bond formation, to support their folding

(Meusser *et al.*, 2005). Errors can occur in the protein folding process. These errors may happen for different reasons, examples of which include, spontaneous errors in transcription and translation, mutations, toxicity in the cellular environment, the complexity that arises as a result of multiple energetically favourable intermediate states being involved before the final protein confirmation, as well as other cellular stresses (Jahn and Radford, 2005; Vembar and Brodsky, 2008). If errors in protein folding go unchecked there can be dire consequences, in humans unchecked errors in protein folding have been implicated in many disease states, such as Alzheimer's and Parkinson's disease (Jahn and Radford, 2005; Zhao *et al.*, 2022). In cell culture unchecked errors in protein folding leads to aggregate formation, and can ultimately result in cell death or deformity (Jahn and Radford, 2005; Zhao *et al.*, 2022). The ER protein quality control system has evolved to deal with misfolded proteins, particularly in instances of ER stress (Jahn and Radford, 2005; Zhao *et al.*, 2022). ER stress is a status in which there is an accumulation of misfolded proteins in the ER (Zhao *et al.*, 2022). It is induced by many cellular scenarios such as calcium deprivation, impaired glycosylation, and nutrient deprivation (Zhao *et al.*, 2022). During ER stress, the cell responds with events that regulate ER chaperones and proteins in the degradation system to prioritise cell survival as a part of proteostasis, as previously referred to in Section 1.5.1 (Zhao *et al.*, 2022). The proteostasis of the ER is dependent on the coordination of three regulatory pathways, ER-assisted folding (ERAF), ER-associated protein degradation (ERAD) and the unfolded protein response (UPR) as well as the involvement of autophagy and apoptosis (Prashad & Mehra, 2015). The interrelation between these pathways are summarised in Figure 1.3.

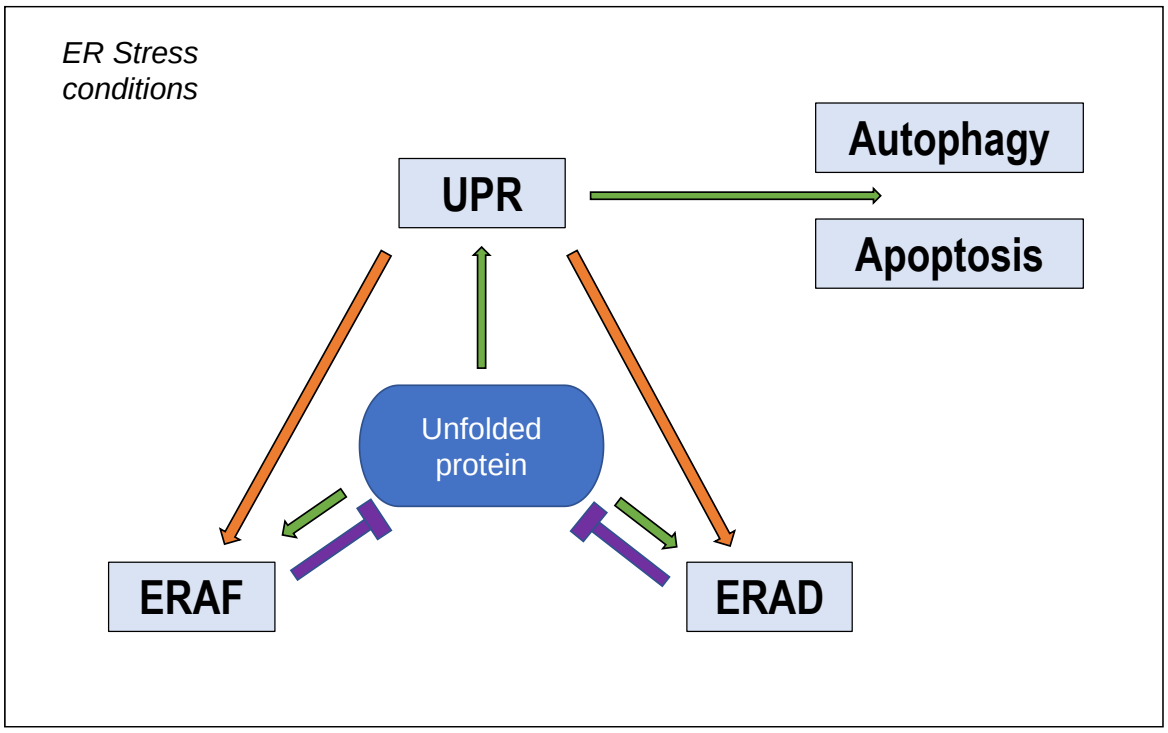

Figure 1.3 *A simplified schematic of the interrelationship of signalling pathways and responses during ER stress in cell culture.*

Accumulation of unfolded protein in the endoplasmic reticulum (ER) results in the activation of the endoplasmic reticulum -assisted folding (ERAF), endoplasmic reticulum associated degradation (ERAD) and unfolded protein response (UPR) signalling proteins. ERAF used chaperone proteins to promote refolding of proteins that are misfolded and in the ERAD pathway proteins that are extensively damaged are degraded by the 26S proteosome. The activation of the UPR pathway leads to the increased transcription of ERAF and ERAD components such as chaperones. Downstream signalling of the UPR is also involved in the activation of autophagy and apoptosis under severe or prolonged ER stress.

1.7.1 ERAF, ERAD and UPR

Protein export relies on ERAF pathways, which use chaperones and folding catalysts, to direct folding in both the luminal and cytosolic domains of proteins, as well as metabolites and other small molecules that by binding stabilise proteins for export (Wiseman *et al.*, 2007). Chaperones involved in the folding of ER luminal domains include BiP, GRP94 components and the calnexin/calreticulin cycle (Wiseman *et al.*, 2007). The folding catalysts involved in

the ERAF pathways include protein disulfide isomerases (PDIs) and cis/trans peptidyl-prolyl isomerases (Wiseman *et al.*, 2007). In multicellular organisms these luminal chaperones and folding catalysts also work in conjunction with cytosolic chaperones, such as Hsc-Hsp40/70 and Hsp90 members, for the coordination of cytosolic domain formation in transmembrane proteins (Wiseman *et al.*, 2007).

The proteins that make it through the monitoring of the ER quality control mechanisms continue on the secretory pathway, instead of becoming targets of the ERAD pathway (Vembar and Brodsky, 2008; Meusser *et al.*, 2005). The ERAD eliminates un/mis-folded proteins from the ER by targeting proteins for degradation by the ubiquitin-proteasome system (UPS) (Meusser *et al.*, 2005). Steps involved in the ERAD pathway include, the recognition of the protein for degradation, the targeting of the recognised protein, retrotranslation initiation followed by ubiquitylation alongside further retrotranslocation and finally proteasomal targeting and degradation (Vembar and Brodsky, 2008). Firstly, soluble proteins, integral membrane proteins and polypeptides that are misfolded or otherwise have not been successfully post-translationally modified and members of multiprotein complexes that are unassembled are potential ERAD substrates (Vembar and Brodsky, 2008). These substrates are recognised by cytoplasmic and luminal chaperones and the associated factors previously mentioned in the ERAF pathway – Hsp70 family members, calnexin and calreticulin and PDIs (Vembar and Brodsky, 2008). A mechanism by which potential ERAD substrates are recognised by chaperones, is through the detection of the exposed hydrophobic domains of misfolded proteins, as discussed further in the context of BiP in Sections 1.8.1 and 1.8.2.1 (Rutkowski and Kaufman, 2004; Jahn and Radford, 2005; Vembar and Brodsky, 2008). Once a ERAD substrate is recognised it is targeted to E3 ligases and/or retrotranslocation machinery in the cytoplasm where retrotranslocation is initiated, by the cell-decision cycle-48 complex and other components (Vembar and Brodsky, 2008). As proteins exit the retrotranslocation

machinery, they are marked for degradation by the incidence of polyubiquitination by E3 ubiquitin (Vembar and Brodsky, 2008). In the cytoplasm, the polyubiquitinated substrate is recognised by the 19S cap receptors of the 26S proteosome before de-ubiquitinating enzymes remove the tag and the substrate can be threaded into the catalytic 20S core of the proteosome and broken into peptide fragments (Vembar and Brodsky, 2008).

The UPR pathway is closely linked to the ERAD pathway, with the UPR inducing the transcription of a subset of factors required for ERAD. As a key focus of this report, the details of the UPR are elaborated on further in Section 1.8, and in terms of responding to and regulating the ER stress, the UPR is critical. The direct interaction between the misfolded proteins and titration of BiP from transmembrane sensor proteins in the ER, is the defining mechanism by which the UPR regulates ER stress, but other factors that are induced by the UPR regulate other mechanisms to reduce ER stress (Vembar and Brodsky, 2008). These include ER expansion from upregulated lipid synthesis, an increase in the concentration of molecular chaperones required for PTMs, a reduction in protein translation and ER translocation, increase protein transportation through the secretory pathway (Vembar and Brodsky, 2008).

Other pathways are interlinked with the ERAF, ERAD and the UPR pathways to reduce ER stress, including the previously discussed autophagy and apoptosis (Section 1.5). Particularly against the incidence of protein aggregation, autophagy serves as an alternate mechanism in the reduction of ER stress to the ERAD pathway (Vembar and Brodsky, 2008). When ERAD is at capacity or compromised, ER-stress-induced-autophagy ensues where portions of the ER, proteins and protein aggregates are engulfed by autophagosomes and transported to the lysosome or vacuole and degraded (Vembar and Brodsky, 2008). Alternatively, if ER stress is prolonged and unresolvable, which the cell recognises through phases of UPR-mediated signals, the apoptotic pathway can be activated which results in cell death (Szegezdi *et al.*, 2006). ER stress may link to apoptosis either by the induction of the apoptotic pathway through

the cleavage and activation of caspase-12, a caspase localised to the ER membrane or through the UPR inducer and ER kinase PERK in a signalling cascade that forms a key branch of the UPR (Vembar and Brodsky, 2008).

1.8 UPR Pathway

As previously mentioned in Section 1.7, misfolded proteins that do not pass the quality control mechanisms of the ER, are either sent back through the folding cycle (ERAF) or marked for degradation via the ERAD pathway (Chakrabarti *et al.*, 2011). Instances of severe or prolonged ER stress triggers the UPR. The pathways involved in the UPR have been summarised in Figure 1.4, and are involved in the induction of a wide variety of events, including the shutting down of protein translation to minimise the load on cells and the increase of chaperone quantities at the transcriptional level to enhance folding capacity. These processes have been postulated to have evolved to control proteostasis in the instance that un-/mis- folded proteins have accumulated in the ER to a potentially toxic concentration (Schröder, 2006; Prashad & Mehra, 2015; Zhu &Lee, 2015). The UPR is a scalable response that can ultimately eliminate unhealthy cells from the wider population by inducing apoptosis (Schröder, 2006; Prashad & Mehra, 2015). At a superficial level, the UPR can be broken down to be seen as performing three functions, *adaptation,* where proteostasis is attempted to be re-established through the induction of chaperone expression and the attenuation of translation, *alarm* where several signal transduction events lead to the removal of the previously implemented translational block as well as a decrease in the expression of pro-survival factors before, *apoptosis* which alongside autophagy can occur after the alarm phase if the ER stress is not reversed (Chakrabarti *et al.*, 2011).

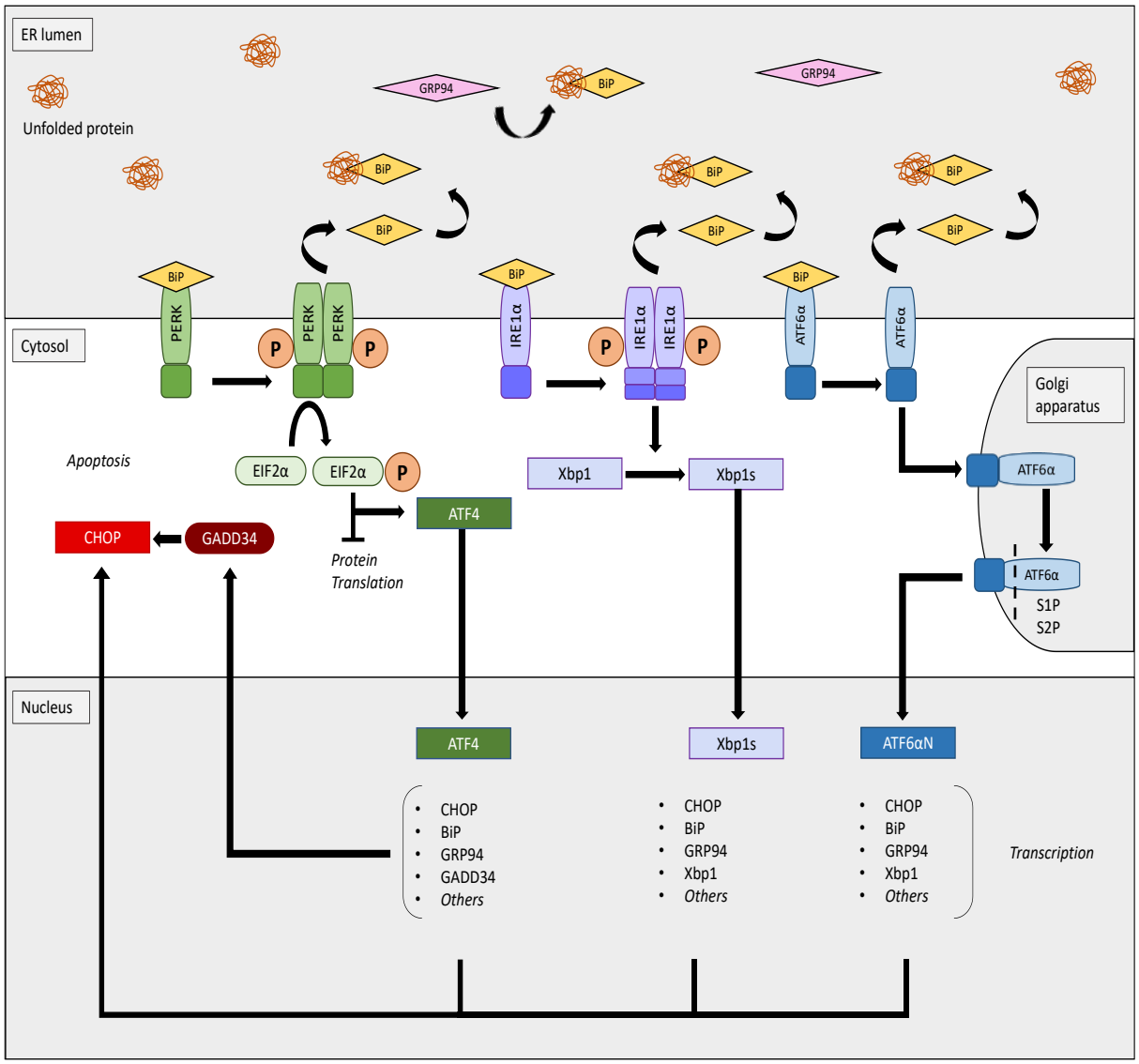

Figure. 1.4 *A simplification of the unfolded protein response (UPR) with emphasis on the roles of GRP94, BiP, Xbp1 and CHOP.*

The figure has been adapted from Prashad and Mehra, 2015 and Torres et al., 2022. The endoplasmic reticulum (ER) chaperones BiP and GRP94 are shown acting sequentially in the ER lumen to target unfolded proteins. The preferential binding of BiP to the built unfolded proteins in the ER that are causing ER stress, initiates the downstream pathways of the signal transducers PERK, IRE1α and ATF6α.

1.8.1 Signal transduction cascades of the UPR

There are three ER stress sensor arms the UPR pathway that detect the deviation from the tolerable concentration of unfolded proteins in the ER. The activation of these sensors, lead to alterations in the activity of the ERAF, ERAD and UPR. The three transmembrane receptors that initiate the pathways that comprise the UPR are Protein Endoplasmic Reticulum Kinase (PERK), Inositol-requiring enzyme 1 (IRE1) and Activating Transcription Factor 6 (ATF6) and the activity of each sensor pathways can be modulated by the interaction with Binding immunoglobulin Protein (BiP), as shown in Figure 1.4 (Chakrabarti *et al.*, 2011; Torres et al., 2022). The role of BiP in the UPR and associated pathways is discussed further in Section 1.8.2.1.

1.8.1.1 PERK

Figure 1.4 shows the role of key factors in the signalling pathway, including PERK. The protein kinase domain of PERK is held in an inactive state by engagement with BiP but exposed hydrophobic domains on newly synthesised proteins in the ER can result in competition for binding with BiP. If this does occur, PERK is released from its interaction with BiP and PERK dimerises and autophosphorylates (Chakrabarti *et al.*, 2011). When autophosphorylated, the cytoplasmic region of the serine/threonine kinase of PERK phosphorylates eukaryotic translation initiation factor 2 subunit-α (eIF2α). This reversible covalent modification of eIF2α acts to temporarily decrease the initiation of synthesis of new polypeptide chains through the reduction of translation, to reduce protein production and subsequently reduce the load of misfolded proteins and decrease ER stress (Nishitoh, 2012; Hetz *et al.*, 2020; Park *et al.*, 2021). In addition to slowing down of general translation, this modification to eIF2α generates selective recognition of elements within specific mRNA species by phospho-eIF2 and translation of a group of proteins, including activating transcription factor 4 (ATF4), is stimulated (Hetz *et al.*, 2020). Figure 1.4 depicts that ATF4 activates the expression of multiple

genes as well as upregulating protein phosphatase 1 (PP1), the regulatory subunit of growth arrest and DNA damage protein 34 (GADD34) (Hetz *et al.*, 2020). By this mechanism ATF4 contributes to a feedback loop that decreases its expression as PP1 and GADD34 form a complex that facilitates the dephosphorylation of eIF2α (Hetz *et al.*, 2020). Therefore, the expression of GADD34 is fundamental to the resumption of protein production if ER stress is eradicated to terminate the expression of other UPR genes activated by ATF4 that are involved in responses such as protein synthesis, apoptosis, and autophagy (Hetz *et al.*, 2020).

1.8.1.2 IRE1

The key factors involved in the IRE1α branch of the UPR signalling cascade are depicted in the centre of Figure 1.4. IRE1α is the most evolutionary conserved ER membrane protein in the UPR, of which there are two isoforms of IRE1α, which is expressed in the majority of tissues, and IRE1β, which is only present in airway mucous cells and intestinal epithelial cells (Junjappa *et al.*, 2018). Like the activation of PERK (Section 1.8.1.1), IRE1α is activated, when BiP, which in non-ER-stress states is bound to the inactive IRE1α protein, preferentially binds to hydrophobic domains in unfolded proteins in instances of ER stress as shown in Figure 1.4 (Park *et al.*, 2021). The structure of the ER type-I transmembrane IRE1α protein has an N-terminal ER luminal domain and a C-terminal cytosolic domain that has dual enzymatic activities, with both kinase and endoribonuclease functions (Chou and Elrod, 1999; Junjappa *et al.*, 2018).

The IRE1α serine/threonine kinase is also an endoribonuclease, and the luminal activation of IRE1α enables IRE1α to dimerise and trans- autophosphorylate, to induce a conformational change that activates the RNase domain, inciting its ability to cleave RNA (Hetz *et al.*, 2015; Hetz *et al.*, 2020; Park *et al.*, 2021). As shown in Figure 1.4, in the cytosol the activated RNase portion of IRE1α recognises the stem-loop structure of X-box-binding protein 1 (Xbp1) mRNA and cleaves the associated 26 intronic nucleotides within the Xbp1 RNA to shift the reading

frame for the translation of Xbp1s – a stable and active transcription factor (Hetz *et al.*, 2015; Park *et al.*, 2021). The specificities of Xbp1 are discussed in Section 1.8.2.3, but by regulating the expression of Xbp1, the IRE1 branch of the UPR responds to ER stress by increasing survival signals as well as pro-apoptotic signals (Prashad & Mehra, 2015).

1.8.1.3 ATF6

Figure 1.4 shows the ATF6 arm of the UPR on the right-hand-side. The ER-resident type-II transmembrane protein ATF6 has two homologous proteins in mammals, ATF6α and ATF6β (Park *et al.*, 2021). Both isoforms have conserved basic leucine-zipper and DNA binding domains but the isoforms have different transcriptional activation domains, and where AFT6α is a potent activator of ER stress-response genes, ATF6β is a poor activator of the same ER stress-response genes while also repressing ATF6α induction (Thuerauf *et al.*, 2004). Like the type-I membrane protein, type-II transmembrane proteins are single-pass, but instead of a luminal or otherwise extracellular N-terminus and a cytoplasmic C-terminus as seen in type I, a type II typically has a cytoplasmic N-terminus and a luminal or otherwise extracellular C-terminus – however in this instance the C-terminus is embedded in the ER or Golgi membrane (Chou and Elrod, 1999). ATF6 is activated by the same mechanism of BiP dissociation as PERK and IRE1α (Sections 1.8.1.1 and 1.8.1.2). However, unlike PERK and IRE1 where the dissociation of BiP primes the transmembrane proteins for oligomerisation and auto-transphosphorylation, for ATF6, the dissociation of BiP reveals an ER export motif (Hetz *et al.*, 2015). Proteins move between cellular compartments via the process of protein translocation, by which both AFT6 isoforms move from the ER to the Golgi apparatus. As shown in Figure 1.4, in the Golgi apparatus ATF6α it is cleaved by site-1 and site 2 protease (S1P and S2P) to release the cytoplasmic N-terminal region of ATF6α, ATF6α(N), that is an active transcription factor that contains a b-ZIP domain (Park *et al.*, 2021). ATF6α(N) migrates to the nucleus from the Golgi apparatus where it binds to the cis-acting ER stress response

element (ERSE) and ER stress response element II (ERSE-II), in the promoter region of target genes (Park *et al.*, 2021). Target genes that contain this element include ER chaperones, such as BiP and Glucose regulated protein 94 (GRP94) and downstream transcription factors such as Xbp1 and C/EBP homologous protein (CHOP), shown in Figure 1.2 (Park *et al.*, 2021).

1.8.2 Genes of interest

In the interest of measuring cellular response to the culture environment, for genes were selected for further analysis using RT-PCR and qRT-PCR within this study. The mRNA transcripts of genes that code for proteins associated with the UPR, that have been examined in further detail are, BiP, GRP94, Xbp1 and CHOP, collectively referred to as the genes of interest (GOI) in this report. As shown in Figure 1.4, these four proteins are involved across various stages of the UPR but due to the complex interplay between the pathways, some are also involved in the ERAF, ERAD, autophagy and apoptosis pathways in the overall response to ER stress in the conservation of proteostasis. Although, there are many proteins involved in the signalling pathways previously described, these genes have been selected as they each have been researched to varying degrees, but enough work has been conducted to know that their expression has implications for the cellular response to ER stress. Work conducted by Torres *et al.*, (2021), on the effect of temperature on the expression of UPR-/ERAD- related genes and the impact on recombinant protein production in a CHO cell line, identified that each of the four genes were significantly upregulated after treatment with tunicamycin, a UPR-inducing pharmacological agent. The role of each protein is multifaceted, the chaperone proteins BiP and GRP94 could be regarded as being highly involved in the pro-survival response of the signal transduction network, whereas the transcription factors Xbp1 and CHOP act further downstream in the response and are involved in the pro-apoptotic side of the response. A more comprehensive review of this area would have also included pro-survival downstream target, but due to the time constraints of the project only four genes were examined in detail, the

emphasis being placed on the pro-apoptotic side of the response to examine cellular capacity to respond to ER stress before the induction of apoptosis through the measurement of ER markers.

1.8.2.1 Role of BiP in the UPR

As previously referred to in Section 1.7.1, the dissociation of BiP from the hydrophobic domains of the transmembrane sensor proteins PERK, IRE1 and AFT6 is required for the activation of the UPR pathway (Rutkowski and Kaufman, 2004). As the concentration of unfolded luminal proteins increases, BiP migrates from these sensor proteins to form interactions with the hydrophobic domains that are exposed in the unfolded proteins, as shown in Figure 1.4 (Rutkowski and Kaufman, 2004).

A chaperone is a protein that interacts with, stabilises, or assists another protein to obtain the conformation in which it is functionally active, without being present in the final state (Hartl *et al.*, 2011). There are several classes of molecular chaperones in cells that exist in protein families, that are termed stress proteins or heat-shock proteins (HSPs) due to their upregulation under stress conditions in which the concentration of partially folded aggregate-prone proteins increases (Hartl *et al.*, 2011). In multicellular organisms, the folding of small proteins can be challenging *in vivo* due to the crowded nature of the cytosol, with reports of the total cytosolic protein concentration reaching 300-400g l^{-1}, increasing the likelihood with which aggregation will occur of non-native proteins (Hartl *et al.*, 2011). Crowding also occurs in this manner in the separate membrane compartments within a singular cell during culture as misfolded proteins accumulate in the lumen of the ER. The concentration dependent manner with which partially or misfolded proteins aggregate is due the exposure to the solvent of the hydrophobic amino-acid residues and regions in the unstructured polypeptide backbone that is buried in the native state of the protein (Hartl *et al.*, 2011). In terms of chaperone classification, there are small HSPs, HSP40, HSP60, HSP70, HSP90, HSP100 classes that are determined based on

their molecular weight (Hartl *et al.*, 2011). BiP, also referred to as glucose-regulated protein 78 (GRP78) or heat shock 70kDa protein 5 (HSPA5) is a member of the HSP70 class of chaperone protein. The structure of BiP consists of a nucleotide binding domain (NBD) in the N-terminal, a hydrophobic acidic linker, and a substrate-binding domain (SBD) in the C-terminal (Pobre *et al.*, 2019). The acidic linker controls the allosteric interaction between the NBD and the SBD (Pobre *et al.*, 2019). The ATPase cycle of BiP, involves the SBD with an open residue lid being docked on the NBD in the ATP-bound form. ATP hydrolysis results in the undocking of these domains and the closing over of the SBD with the residue 'lid' results in a high on/off rate for client interaction (Pobre *et al.*, 2019). This structure of BiP that enables the high on/off rate for the interaction with client proteins is fundamental to both the role of BiP as a chaperone and as a regulator of the activation of the three sensory arms of the UPR.

As the most abundant chaperone protein in the ER, BiP has a wide variety of client proteins to chaperone in instances of ER stress, as well as having a pivotal role in the activation of the sensor proteins PERK, IRE1 and ATF6 as described previously in Section 1.8.1. The activation of these signalling cascades initiates multiple mechanisms of restoring proteostasis in the ER, not in the least the upregulation of the transcription of BiP by transcription factors such as ATF4 Xbp1s and ATF6αN at the culmination of the PERK, IRE1 and ATF6 pathways as shown in Figure 1.4, which further contributes to the chaperone activity of BiP, contributing to the pro-survival response of the UPR.

Aside from the sensory activation and the chaperoning activity of BiP, BiP also has a role in calcium buffering in the ER lumen (Groenendyk and Michalak, 2004). Calcium has a role in ER homeostasis, in response to external stimuli calcium is released from the lumen of the ER into the cytosol via the inositol-1,4,5-triphosphate receptor and the ryanodine receptor channels, most of the released calcium is taken back up into the ER via the sarcoplasmic-endoplasmic-reticulum Ca^{2+}-ATPase (SERCA) pumps (Groenendyk and Michalak, 2004). This

output and uptake of calcium is fundamental to the regulation of many of the signalling cascades involved in the ER and throughout the cell, including the UPR. The capacity of BiP for binding and subsequently sequestering calcium is relatively low compared to other ER luminal chaperones, 1-2 mole of calcium per mole of protein, but being the most abundant chaperone, it contributes up to 25% of the total calcium storage capacity of the ER (Groenendyk and Michalak, 2004). The association of BiP with non-native proteins is stabilised by high calcium concentrations which is possibly involved in the binding of the two (Groenendyk and Michalak, 2004).

A study conducted by Kyeong and Lee (2022), developed a fluorescence-based UPR monitoring system in a CHO-K1 and a recombinant CHO-K1 derived line, using BiP expression in an endogenous reporter system. The study found that basal BiP expression levels affect recombinant protein productivity, suggesting that high BiP expression levels are correlated with high mAb productivity (Kyeong and Lee, 2022).

1.8.2.2 Role of GRP94 in the UPR

The second most abundant glycoprotein in the ER is the 94-kilodalton glucose regulated protein, GRP94 is a soluble, obligate dimer and ubiquitously expressed chaperone that is the only member of the heat shock protein (HSP) 90 family that is ER resident (Eletto *et al.*, 2010). All HSP90 members have four domains, an N-terminal domain (NTD), an acidic linker domain (LD), a middle domain (MD) and a C-terminal domain (CTD) (Eletto *et al.*, 2010). GRP94 is an ATPase with nucleotide binding site in the NTD, but the LD, mediates the conformational changes needed for ATP hydrolysis and residues from MD is needed for the hydrolytic activity of the ATPase. The constitutive dimerisation of GRP94 is dependent on the CTD (Eletto *et al.*, 2010). *In vivo*, the ATPase activity is necessary for chaperoning activity, in the instances of client proteins such as insulin-like growth factor (IGF) (Eletto *et al.*, 2010).

As shown in Figure 1.4, like BiP, GRP94 is a chaperone protein that directs the folding and assembly of membrane and secreted proteins (Eletto *et al.*, 2010). The variety in the structure of membrane and secretory proteins necessitates the need for a variety in chaperone systems (Eletto *et al.*, 2010). Through this mechanism of chaperoning, GRP94 contributes to quality control of the ER by assisting the folding of proteins. GRP94 also maintains ER homeostasis by interacting with components in the protein folding machinery of the ER, storing calcium, and assisting in the targeting of proteins to ERAD (Eletto *et al.*, 2010; Zhu and Lee, 2015). Up-regulation of GRP94 is often used as a hallmark of ER stress, with high levels present in secretory tissues (Eletto *et al.*, 2010; Zhu and Lee, 2015). Unlike other ubiquitous luminal chaperones such as BiP, PDI and calreticulin, GRP94 has a smaller client list making it more selective (Eletto *et al.*, 2010; Zhu and Lee, 2015). Whilst the client selectivity and late folding intermediate interactions suggest unique ER chaperone functions, a common feature of GRP94 clients, other than the presence of disulphide bonds, is yet to be discovered (Eletto *et al.*, 2010). GRP94 governs advanced folding intermediates for clients such as insulin-like growth factor I (IGF-I) and insulin-like growth factor II (IGF-II), which subsequently depend on GRP94 for their maturation. IGFs are UPR target genes and mediators, the IGF signalling pathway is pro-growth and anti-apoptotic, and IGF maturation is dependent on GRP94. IGF-I increases chaperone reserves by potentiating the IRE1 and PERK branches of the UPR.

Aside from the role as an ER chaperone, GRP94 also assists in regulating calcium concentration in the ER. ER quality control mechanisms are coupled to the use and storage of calcium as signalling pathways involved are changed by the in or out flux of calcium ions, which is shown by the use of the agent thapsigargin to induce ER stress and the subsequent UPR through the inhibition of calcium SERCA pumps (Eletto *et al.*, 2010). Most ER calcium is stored to bound proteins, with one GRP94 molecule able to bind 16-28 calcium atoms, as one of the major luminal calcium binding proteins (Eletto *et al.*, 2010). Alongside the UPR,

GPR94 is known to assist in the ERAD pathway through the interaction with OS-9, a soluble ER resident protein that distinguished between folded and unfolded proteins (Eletto *et al.*, 2010).

As mentioned in Section 1.8.2, a study conducted by Torres *et al.*, (2021), showed the expression of GRP94 to be significantly upregulated after treatment of a CHO cell line with tunicamycin, a pharmacological agent that induces UPR expression by blocking the initial step of glycoprotein synthesis in the ER, causing an accumulation of unfolded glycoproteins in the ER (Torres *et al.*, 2021; Oslowski and Urano, 2011).

1.8.2.3 Role of Xbp1 in the UPR

As discussed in Sections 1.8.1.2 and 1.8.1.3 and shown in Figure 1.4, Xbp1 is a transcription factor involved in the IRE1α and ATF6 branches of the UPR. Figure 1.4 shows how the active IRE1α recognises and cleaves Xbp1 to shift the reading frame for the translation of Xbp1s. The Xbp1 transcript, when expressed in unspliced form generates a weak transcription factor but which when spliced by IRE1α generates a much more active transcription factor, Xbp1s (Park *et al.*, 2021). The ATF6α signalling cascade results in the transcription of Xbp1 by ATF6αN, shown in Figure 1.4. This propagates the UPR as Xbp1s is an effective transcription factor that increases ER-folding capacity by transcribing ER chaperones and folding enzymes as well as increasing the transcription of ERAD components (Hu et al., 2019; Park *et al.*, 2021). The genes that are targets of Xbp1s transcription contain the cis-acting elements ER stress response element (ERSE), ER stress response element II (ERSE-II) and the unfolded protein response element (UPRE) (Park *et al.*, 2021). ERSE is found in the promotor of the Xbp1s target genes such as Hspa5, Hsp90b1 and Calr - ER chaperones that assist with protein folding, as well as CHOP (Section 1.8.2.4) (Park *et al.*, 2021). The ERSE-II consensus sequence is found in the promoter of Herpud1 and the consensus sequence of UPRE is found in the promoter region of genes such as Kruppel-like factor 9 (KLF9) which promotes calcium release and apoptosis by

increasing the transcription of ER calcium storage regulator transmembrane protein (TMEM38B) and inositol 1,4,5-trisphosphate receptor type 1(ITPR1) (Park *et al.*, 2021).

As mentioned previously in Sections 1.8.2 and, elaborated on in Section 1.8.2.2, the treatment of a recombinant CHO cell line with the pharmacological agent tunicamycin, saw a significant increase in Xbp1 expression (Torres *et al.*, 2021). Furthermore, genome wide-analysis has shown Xbp1 to have many target genes involved in pathways outside the UPR. Interestingly, Xbp1 has been shown to be highly involved in the differentiation of B cells into plasma cells and the production of antibodies by plasma cells in humans (He *et al.*, 2018; Park *et al.*, 2021; Iwakoshi *et al.*, 2003). A study conducted by Becker *et al.*, (2008) showed that expression of the active spliced form of human Xbp1 in a recombinant IgG CHO cell line increased cell line productivity.

1.8.2.4 Role of CHOP in the UPR

There are three primary pathways by which ER-stress induced apoptosis occurs, these being the IRE1/ASK1/JNK, the caspase-12 kinase and the CHOP pathways (Hu *et al.*, 2019; Oyadomari and Mori, 2004). CHOP, also known as DDIT3 or GADD153, is a 29 kDa bZIP transcription factor involved in ER-stress induced apoptosis (Nishitoh, 2012; Kim *et al.*, 2008). CHOP protein contains two functional domains at the N-terminal, which is the transcriptional activation domain and the C-terminal, which is the basic leucine zipper (bZIP) domain (Hu *et al.*, 2019). CHOP operates at the union of the PERK, AFT6 and IRE1 pathways (Kim *et al.*, 2008; Nishitoh, 2012). The activation of these sensory proteins activates transcription factors such as ATF6, ATF4 and Xbp1s for which the gene promoter of CHOP contains binding sites (Zhu and Lee, 2015; Kim *et al.*, 2008). CHOP is a pro-apoptotic factor, and the induction of CHOP expression induces the expression of other pro-apoptotic proteins such as the pseudokinase tribbles homolog 3 (TRB3) (Kim *et al.*, 2008; Prashad and Mehra, 2015; Hu *et al.*, 2019). The binding of CHOP to TRB3 inhibits the ERK pro-survival pathway, thus

promoting apoptosis (Hu *et al.*, 2019). CHOP functions as a transcriptional repressor by inhibiting the expression of genes responsive to C/EBP family transcription factors by forming heterodimers by bZIP-domains with the transcription factors themselves (Ubeda *et al.*, 1996). CHOP transcriptionally decreases the expression of B-cell leukaemia/lymphoma 2 (BcL-2) by directly decreasing BcL-2 transcription as well as increasing the transcription Bcl-2 Interacting Mediator of cell death (BIM) which also functions to inhibit BcL-2 (Kim *et al.*, 2008). Beclin is an autophagy protein that is inhibited by directly binding to the anti-apoptotic protein BcL-2 (Kim *et al.*, 2008). If there is a reduction in the expression of BcL-2 then beclin is not suppressed and autophagy can occur (Kim *et al.*, 2008).

As in the previous Sections in 1.8.2, the treatment of a recombinant cell line with the UPR-inducing pharmacological agent tunicamycin resulted in a significant increase in CHOP expression in a CHO cell line (Torres *et al.*, 2021).

1.8.3 UPR in CHO

A key focus of this report is how the UPR may be influenced by changes in CHO cell culture conditions and how this may affect antibody production. As reviewed by Torres *et al.*, (2022), there is a dynamic upregulation of the expression of UPR and ERAD related components in CHO expression systems during recombinant protein production (Prashad and Mehra, 2015). This may be a result of complex PTMs required for the expression of therapeutic protein with complex molecular architecture which may put pressure on the ER processing machinery that induces ER stress and induces the UPR and the ERAD pathways (Torres *et al.*, 2022). As referred to in sections 1.8.2.1-1.8.2.4, UPR-associated proteins have been examined in CHO to assess the correlation between gene and UPR expression, as potential targets for cell line engineering to optimise CHO cell lines as expression systems (Kyeong and Lee, 2022; Torres *et al.*, 2021; Becker *et al.*, 2008).

As previously detailed, the UPR-related genes, BiP, GRP94, Xbp1 and CHOP have been chosen to reflect the status of the UPR through BC and FBC duration in IgG1 CHO-S cells. As detailed in Section 1.4.2, the lack of or presence of feed has been shown to influence cell growth and specific productivity in other CHO cell lines. Cells cultivated in BC and FBC are continuously using cellular machinery to producing recombinant proteins, therefore there is a potential increase in load on the ER, shown in the increase in specific productivity between BC and FBC by Braasch *et al.*, (2021), as discussed in Sections 1.4.2 and 1.5 (Prashad and Mehra, 2015). The production of complex recombinant proteins and an increasing load may result in ER stress. As the UPR is an ER stress response, its activation could signify the status of cell health in culture. If there is a correlation between the expression of these GOIs and changes in IgG1 CHO-S growth, viability, or productivity this may be an indication of causation and therefore the associated gene could be used as a biomarker for cell health and/or productivity.

Previously, studies have investigated the expression of these GOIs in CHO cell culture (see also Section 1.4.3) as well as the effects of feed on gene expression in CHO cell lines. The study conducted by Wong *et al.*, 2006, found that ER-mediated apoptosis signalling genes such as Ire1, BiP and p38MAPk and Caspase-7/-12 were either not differentially expressed or down-regulated in BC and FBC and the mRNA response was therefore not influenced by feeding in this instance. However, the CHO IFN-γ cell line used in the study to compare apoptosis signalling in BC and FBC, had a specific productivity of ~1 $pg \cdot cell^{-1} day^{-1}$ which could be considered relatively low and therefore ER stress due to misfolding would not be an issue in the induction of apoptosis (Wong *et al.*, 2006). The study did not include representatives from the PERK and AFT6 pathways in their microarrays but did include BiP which was shown not to be differentially expressed (Wong *et al.*, 2006). Ire1 and p38MAPk, a protein involved in the activation of CHOP, where shown to be down-regulated (Wong *et al.*, 2006).

1.9 Aim

The aim of this report is to contribute to a better understanding of the molecular biology of the recombinant CHO-S IgG1 cell line to generate information that could potentially contribute to the improvement of the manufacture capacity of the biopharmaceutical industry. The development of biopharmaceuticals using recombinant technology requires expression systems such as CHO cell lines, to produce recombinant therapeutic proteins, such as mAbs. Culture conditions and cell line engineering impact the protein yield and quality as well as the specific productivity of expression systems. Research into the molecular biology of quality control mechanisms in mammalian cells, specifically CHO cells, has been investigated. From this, it has been identified that the secretory ability of recombinant proteins by CHO cells is impaired by inherent cellular pathways such as the UPR. The UPR was examined and BiP, GRP94, Xbp1s and CHOP were identified as GOI that could serve as potential biomarkers for the activation of the UPR and the subsequent consequences on antibody secretion in mammalian expression systems such as CHO.

1.9.1 Objectives

The objectives by which this aim will be achieved are firstly, to study the growth and IgG1 production of the recombinant CHO-S cell line in BC and FBC, to assess the effect of the addition of feed to these parameters. The second objective of this report is to develop methods to assess the expression of a set of UPR-relevant proteins, using PCR and Western blotting techniques. This then leads to the third objective which is to examine the expression of these UPR-relevant proteins in BC and FBC. Finally, the relationship between the expression of the UPR-relevant proteins, the specific productivity of the cell line and the overall IgG1 yield will be assessed in response to FBC conditions. Knowing this information would enable a rationalisation towards the engineering of cells and their processes to ensure better yield of quality.

Chapter 2: Methodology

2.1 Materials and Equipment

All chemicals and reagents were of analytical grade or cell culture grade and obtained from standard sources.

2.1.1 Preparation of solutions

All solutions were prepared in MilliQ water (ddH_2O), which had been filtered using the Advantage A10 Water Purification System (Merck Millipore) unless otherwise stated. All solutions used in the processing of RNA were made in NFW (Nuclease-Free Water (Qiagen)). Solutions were stored at room temperature and pressure (RTP), unless otherwise stated.

2.1.2 pH measurements

Measurements of the pH of solutions used were made using a calibrated digital pH meter SevenEasy (Mettler Toledo) with a glass electrode. The meter was calibrated according to the manufacturer's instructions prior to use. Adjustment to the final working pH was done by adding slowly adding either hydrochloric acid (HCl) or sodium hydroxide (NaOH) as appropriate, unless stated otherwise.

2.1.3 Primer Design

Table 2.1. *Primer sequences used in PCR reactions.*

Name	*Sequence (5'→3')*
BiP Forward	GCGCATTGATACCAGGAACG
BiP Reverse	GAGGGCCTGCACTTCCATAG
GRP94 Forward	AGGAAAACCGGGAAGCAACA
GRP94 Reverse	GCCCGTTTGGTATGCTTGTG
Xbp1s Forward	CTCGCTTGGGAATGGATGTG
Xbp1s Reverse	GGTAGACCTCTGGGAGTTC
CHOP Forward	CACCATACCTGAAAGCAGAA
CHOP Reverse	ACCTCCTGCAGATCCTCATA
β-actin Forward	GCTCTTTTCCAGCCTTCCTT
β-actin Reverse	GAGCCAGAGCAGTGATCTCC

PCR primers were designed using the NCBI PrimerBLAST tool and synthesised by Eurofins Genomics. The quantity of a target gene was calculated by normalisation to β-actin. Forward and reverse primers were diluted in NFW to a concentration of 100µM as per manufactures instruction.

Regarding Xbp1, the primers designed and used in the RT-PCR and qRT-PCR analysis conducted in this report were specifically designed for the detection of spliced Xbp1 (Xbp1s). Subsequently, in Section 3.4, the gene of interest is referred to as Xbp1s throughout.

2.1.4 Antibodies

Table 2.2. *Antibodies used in Western blot analysis.*

GOI	Primary IgG	Primary IgG quantity used (µl)	Secondary IgG	Secondary IgG quantity used (µl)
ERK2	Mouse monoclonal (50µg/0.5ml)	10	Goat anti-Mouse (1mg/ml)	1
BiP	Goat polyclonal (200µg/ml)	5	Donkey anti-Goat (1mg/ml)	1
Xbp1	Goat polyclonal (200µg/ml)	10	Donkey anti-Goat (1mg/ml)	1

Both primary and secondary antibodies were kindly provided by Mauro Torres. The primary antibodies were obtained from Santa Cruz Biotechnology. The secondary antibodies were obtained from LI-COR.

The antibodies used in the western blots conducted in this report in the detection of Xbp1, detect both the unspliced and spliced form. Subsequently, in Section 3.5, the gene of interest is referred to as Xbp1 throughout.

2.2 Mammalian cell culture

2.2.1 Cell maintenance and harvesting

All cell culture medium and additives were either sterilised by the manufactures prior to purchase. A Class II Biological Safety Cabinet (BSC), was used to perform all cell culture procedures.

The cell line used in this project was a IgG1 CHO-S cell line which was developed as described in Torres and Dickson, 2021. A 1×10^6 vial of the IgG1CHO-S was kindly provided by Mauro

Torres for use in this project. In culture, cells were grown in 50ml spin tubes that were bought sterile from the manufacturer (Corning Incorporated). The medium used in all cultures was CD CHO supplemented with 4% (v/v) Glutamax, 1% (v/v) HT supplement, 1% (v/v) Pluronic acid and 0.125% (v/v) Puromycin (Complete Medium). The Lab-Therm LT-X KuhnerSHAKERX used to incubate the cultures was set to 37°C, 230rpm, 70% humidity and 5.0% CO_2.

Spin tubes were seeded at 0.2×10^6 cells/ml to a volume of 10ml. To maintain cell stocks cultures were sub-cultured during exponential growth, typically on day 4 of culture. To seed cells, counts were performed (see Section 2.2.2) and the appropriate volume of cells to harvest 2×10^6 cells was transferred to a flacon tube and centrifuged in a U-32 centrifuge (Boeco, Germany) 1500rpm for 10 mins. 10ml of Complete Medium was added to the pellet which was resuspended into a fresh 50ml spin tube. Cultures were then incubated as described above.

2.2.2 Measuring cell growth and viability

To measure cell growth and viability, 50µl cell culture (medium and cells) was placed into a microcentrifuge tube and 10µl was mixed with 10µl Trypan Blue solution (0.4%, Sigma), to conduct Trypan Blue exclusion (Strober, 2015). This was viewed under a visible light microscope (20× magnification) in a bright line haemocytometer (Neubauer, Germany). Viable cells appear as a clear circular object whereas cells that have breached membranes and are no longer viable have blue stained nuclei. Cells were counted by eye to determine total and viable cell concentration.

In instances where the cell count was greater than 30 cells per haemocytometer quadrant cell samples were diluted with PBS prior to counting.

2.2.3 Cryopreservation

After 3 days of culture cells in exponential growth 1×10^7 cells were harvested by centrifugation (Sigma 1-14 Microfuge at 2000rpm, 5 mins). Freezing medium (Complete

Medium [Section 2.2.1], supplemented with 10% (v/v) DMSO) was prepared during the centrifugation period. The supernatant was removed and the cell pellet was resuspended in freezing medium and mixed thoroughly with 1ml freezing medium before being placed in a labelled cryovial. The vials with placed in the -80°C freezer overnight before transfer to liquid nitrogen for longer-term storage. Multiple portions of cell stocks were generated by scaling-up the harvest cell numbers.

2.2.4 Cell revival

A cryovial of frozen cells (Section 2.2.3) was thawed by placing in a water bath (37°C) and after 60s the cryovial was transferred to the tissue culture hood where 1ml pre-warmed Complete Medium was slowly pipetted into the vial and mixed until the cell pellet and medium were homogenous before being transferred to a sterile 1.5ml Eppendorf. The cell suspension was centrifuged (Sigma 1-14 Microfuge at 1000rpm, 5 mins). After centrifugation, the supernatant was removed and the cell pellet was resuspended in 10ml Complete Medium in a 50ml spin tube and cultured (Section 2.2.2) for a minimum of 3 passages before use in other applications. The sub-culture regime and the associated seeding densities of these passages were as previously described (Section 2.2.1).

2.2.5 Batch culture

BC was carried out in 50ml spin tubes at a total volume of 20ml Complete Medium (Section 2.2.1). Cells from maintenance culture (Section 2.2.1) were seeded to a density of 0.2×10^6 cells/ml at the start of BC and culture was progressed in the Lab-Therm LT-X KuhnerSHAKERX (See Section 2.2.1) with cells numbers and viability assessed by light microscopy and trypan blue exclusion (Section 2.2.2). BC was stopped when cell viability dropped below 70%. For sampling of culture supernatant or cells, a volume of culture was removed from the spin tubes and centrifuged (Boeco U-32 centrifuge 1500rpm, 10 mins) and

supernatants and cell pellets were separated and stored at -20˚C and -80°C respectively for later analysis of metabolites, IgG secretion, protein, and RNA. At early stages of culture, when cell densities were low, in order to harvest the number of cells required to attain the quantity (1×10^7) for detection of cellular protein and RNA species, an entire spin tube would be sacrificed for each harvest (Evie *et al*, 2017).

2.2.5.1 Tunicamycin treatment

In triplicate, 50ml spin tubes containing 10ml Complete Medium (see Section 2.2.2) were seeded at 1.0×10^7 cells/ml. The tubes were treated with 10µl of the antibiotic tunicamycin and left to incubate for 6.5 hrs in the Lab-Therm LT-X KuhnerSHAKERX (See Section 2.2.1) as previously described. To collect samples, supernatant and pellet were harvested after the treated Complete Medium was transferred to 50ml falcon tubes before being centrifuged (Boeco U-32 centrifuge 1500rpm, 10 mins).

2.2.6 Fed-batch culture

Cells were cultured and supernatant and cell samples stored as described for BC (Section 2.2.5) with cells in a basal medium of Complete Medium and 1ml feed (1:1 mix of CHO CD EfficientFeed A and CHO CD EfficientFeed B) added to shake tubes every other day from day 2 onwards. Prior to the addition of 1ml feed, 1ml was removed from culture to maintain culture volume over time. The removed culture was used for generation of samples for supernatant and cellular analyses. Culture was stopped when cell viability dropped below 70%.

2.3 Determining IgG1 concentration by ELISA

The quantification of IgG1 production was determined using an IgG enzyme-linked immunoassay (ELISA). The cumulative amount of secreted IgG1 in the medium (for collection see Sections 2.2.5 and 2.2.6) was determined using a sandwich ELISA method that had been previously developed in house.

Solutions required for the assay were prepared. To prepare Phosphate buffered saline (PBS) solution 10 PBS tablets (Sigma P4417) were dissolved in 2L MilliQ water. Wash buffer was prepared using, 1ml of Tween20 was added to 1L of the PBS solution. The blocking buffer prepared consisted of, 1.5g of marvel milk powder added to 50ml of wash buffer (PBS-0.1% Tween20). The sample buffer consisted of 0.5% (w/v) marvel milk powder in wash buffer (PBS-0.1% Tween20). TMB (3,3′,5,5′-Tetramethylbenzidine) diluent was used as the visualising agent in the IgG ELISA. To make the diluent two solutions were prepared. For Solution 1, 4.25g of dibasic sodium phosphate was dissolved in 150ml of MilliQ water. For Solution 2, 2.625g of citric acid was dissolved into 125ml of MilliQ water. These solutions were combined to form the TMB diluent in the way of 128.5ml of Solution 1 and 121.5ml of Solution 2 was added to 250ml of MilliQ water and the pH of the resultant solution adjusted to pH 5.2 (See Section 2.1.2). The 2M sulphuric acid was prepared by adding 11ml of sulphuric acid to 89ml of MilliQ water.

The concentration of IgG1 in each sample was determined by comparing the absorbance to that of a standard curve. To make the first standard, 4.2µl of IgG molecule was added to 495.8µl, the resultant concentration being 100ng/µl. 10µl of this standard was further diluted in 990µl of sample buffer to create a standard of a concentration 1ng/µl. A further 12 standards were prepared using a 1:2 dilution series of the 1ng/µl standard, the final concentration being 0.024ng/100µl.

To prepare capture antibody solution, 7.7µl of Goat Anti-Human IgG Fc capture antibody was diluted in 10ml PBS, 100µl was then added to each well of a 96 well plate. The plate was then left to incubate for 1hr at RTP on a platform shaker set to 110rpm. After incubation, the plate

was washed 3 times using 200µl per well of wash buffer. The plate was tapped after each wash, to remove excess buffer. After washing, 150µl of blocking buffer was added to each well using the multichannel pipette. The plate was left to incubate on a SSL1 Orbital Shaker (Stuart) at 110rpm for 1hr at RTP. The plate was then again washed 3 times using 200µl per well of wash buffer, tapping the plate after each wash to remove the buffer.

In triplicate, 100µl of either each standard or sample was added to the appropriate wells, as well as 100µl in triplicate of sample buffer. The plate was left to incubate at RTP for 1hr on a SSL1 Orbital Shaker (Stuart) at 110rpm. The plate was then washed and tapped 3 times, as previously described. The secondary antibody was prepared by adding 1µl of mouse anti-human kappa-HRP antibody to 15ml of sample buffer, 100µl of was added to each well and the plate left to incubate for 1 hour at RTP on a SSL1 Orbital Shaker (Stuart) at 110rpm. The plate was then washed and tapped 3 times, as previously described.

The detection reagent was prepared by adding 5µl of hydrogen peroxide to 12ml of TMB diluent before the addition of 1 TMB tablet (Sigma-Aldrich) immediately before use. After a brief vortex, 100µl of the reagent was added to each well. The plate was left to incubate for 10 minutes in the dark at RTP. After the incubation period, 100µl of 2M sulphuric acid was added to each well of the ELISA plate. The plate was then immediately read in the Varioskan LUX Multimode Microplate Reader (ThermoScientific) at a wavelength of 450nm. The IgG1 concentration of the samples and the specific productivity at each timepoint was calculated using the sample absorbance and the standard curve using Microsoft Excel.

2.4 Metabolite assessment

2.4.1 Glucose Assay

The basis of the glucose assay is the formation of a red quinone complex measured spectrophotometrically at 505nm. Glucose and glucose oxidase were reacted in a two-step reaction to form the Quinone complex via hydrogen peroxide as follows:

$$\text{Glucose} + O_2 + 2H_2O + \text{GOD} \rightarrow \text{Gluconate} + 2H_2O_2$$

$$2H_2O_2 + \text{Phenol} + \text{4-amino antipyrine} + \text{HRP} \rightarrow \text{quinone complex} + 4H_2O$$

The glucose assay working reagent consisted of 100ml 150mM phosphate buffer (pH 7.5) supplemented with 2mg 4-amino antipyrine, 8µl of 1.07g/mL Liquified Phenol (Sigma-Aldrich), 56mg glucose oxidase and 1mg Horseradish peroxidase. The addition of the phenol solution was carried out in a fume hood.

Glucose standards were prepared from a 1M glucose solution, serially diluted in a 1:2 dilution to produce 12 standards ranging from 50mM to 0.0245mM. Onto a 96 well plate, 2µl of standard or sample was loaded in triplicate. 200µl glucose assay working reagent was added to each well using a multichannel pipette. The plate was incubated at 37°C for 10 mins red colour formation was read in a Varioskan LUX Multimode Microplate Reader (ThermoScientific) at a wavelength of 505nm.

2.4.2 Lactate Assay

The reaction of the conversion of lactate to pyruvate by lactate dehydrogenase (LDH) also reduces NAD^+ to NADH:

$$\text{Lactate} + \text{NAD} \leftrightarrow \text{pyruvate} + \text{NADH}$$

$$\text{Pyruvate} + \text{Hydrazine} \rightarrow \text{hydrazine-pyruvate complex}$$

The basis of the lactate assay is that NADH strongly absorbs ultraviolet light at 339nm with the extinction coefficient 6220 $M^{-1}cm^{-1}$. The determination of lactate concentration was therefore possible using a standard curve.

A 200mM glycine solution and a 200Mm NaOH solution were prepared, by dissolving 1.5g of glycine in 100ml MilliQ water and by dissolving 0.79g of NaOH in 100 ml of MilliQ water, respectively. To produce 100ml of the assay buffer, 5ml of 200mM glycine solution, 1.86ml of 200mM NaOH solution and 730µl of 1.032 g/mL hydrazine monohydrate was added to 92.6ml of MilliQ water. The addition of the hydrazine monohydrate was conducted in the fume hood.

Lactate standards were prepared from a 50mM lactate solution, serially diluted in a 1:2 dilution to produce 12 standards ranging from 50mM to 0.0245mM. The 50mM lactate stock solution 56mg of Sodium L-lactate was dissolved in 10ml MilliQ water. Onto a 96 well plate, 1.7µl of standard or sample was loaded in triplicate. 300µl of assay buffer was added using a multichannel pipette and mixed manually. 100µl of LDH was diluted in 460µl of MilliQ water, 1.9µl of the resultant LDH solution was then added to each well using the multichannel pipette. The plate was incubated at RTP for 60 mins in the dark before being read in a Varioskan LUX Multimode Microplate Reader (Thermo Scientific) at a wavelength of 340nm.

2.4.3 Ammonia Assay

A phenol and a hypochlorite reagent were prepared in a fume hood. The phenol reagent was prepared by mixing 5ml of phenol (0.106M) with 495ml of MilliQ water. To this, 25mg of

sodium nitroferricyanide III (0.17mM) was added and the resultant solution mixed. For the hypochlorite reagent, 2.5ml of sodium hypochlorite (1M) solution was added to 450ml of MilliQ water. To this, 2.5g of sodium hydroxide (0.125M) was added and the total volume of the solution being adjusted to 500ml with MilliQ water. Both containers were wrapped in foil to limit the exposure to light before being stored in the fridge at 4˚C.

Ammonia standards were prepared from a 50mM ammonium chloride solution and serially diluted in a 1:2 dilution to produce 12 standards ranging from 50mM to 0.0245mM. The 1M ammonium chloride solution was prepared by dissolving 0.53g of ammonium chloride (53491 g/mol) in 10ml of MilliQ. 1M ammonium chloride solution was diluted to 50mM by taking 500µl of the 1M solution and diluting with 9.5ml MilliQ water.

In triplicate, 1.5µl of each standard and sample was transferred to a 96 well plate. 150µl of each reagent was added to each well and the plate manually mixed. The plate was then read in the Varioskan LUX Multimode Microplate Reader (Thermo Scientific) at a wavelength of 630nm.

2.5 Analysis of mRNA expression

2.5.1 RNA isolation

Triplicate cell pellets of each timepoint were stored at -80˚C. To conduct cell lysis, the pellets were thawed at RTP and 1000µl of Trizol (T75) was added and pipetted until homogeneous and incubated for 5 mins at RTP.

For phase separation, 200µl of chloroform, was added to the samples and manually shaken for 2 minutes before being incubated for 5 mins RTP. The samples were pelleted in a Mikro 200R

centrifuge (Hettich) for 15000 rpm, 15 mins at 4˚C. After centrifugation, 350µl of the upper aqueous phase was transferred to a new 1.5ml Eppendorf.

To precipitate the RNA, 500µl of isopropanol was added to the 350ul of RNA solution, manually shaken and incubated at RTP for 10 mins before centrifugation (Mikro 200R centrifuge, 15000 rpm, 15 mins at 4˚C). The supernatant was then removed from the samples, taking care not to disturb the pellet. The RNA pellet was washed with 700µl of 70% ethanol. The pellet was briefly vortexed (VX-200 Vortex Mixer) and centrifuged (Mikro 200R centrifuge, 15000 rpm, 10 mins at 4˚C). The supernatant was removed after centrifugation and the pellet air-dried in the fume hood. The RNA was then re-dissolved in 40µl NFW. The concentration and purity of the samples were determined using a NanoDrop 2000/2000c Spectrophotometer (ThermoFisher).

2.5.2 DNase I treatment

The amount of RNA required for 10µg was calculated from the ng/µl determined by the NanoDrop 2000/2000c Spectrophotometer. In a PCR reaction tube, the required volume of RNA for each sample was combined with, 5µl DNase I (NEB) and 10µl DNase reaction buffer. The solution was made up to 100µl using NFW. The samples were placed in the ^{3}Prime (Techne) machine for a programme of incubation, 37°C for 30 mins followed by 75°C for 10 mins in a 1 cycle programme.

2.5.3 cDNA synthesis by Reverse Transcription (RT)

A cDNA synthesis kit (Bioline) was used to prepare an RT+ and RT- for each sample. In a PCR tube for every RT+, 10µl of DNase treated RNA was combined with 1µl of Oligo dT, 4µl of RT Buffer, 1µl dNTP, 1µl Inhibitor, 1µl of RT enzyme and 2µl of DEPC water. In a PCR tube for every RT-, 10µl of DNase treated RNA was combined with 1µl of Oligo dT, 4µl of

RT Buffer, 1µl dNTP and 4µl of DEPC water. The PCR were then incubated in the Techne ^{3}Prime machine for 45 mins at 42°C followed by 5 mins at 85°C in a 1 cycle programme.

2.5.4 RT-PCR

PCR (Promega) followed cDNA synthesis. For each, 2µl of cDNA was combined with 1µl of a 1:10 dilution of forward primer (See Section 2.1.3), 1µl of a 1:10 dilution of reverse primer (See Section 2.1.3), 5µl of buffer, 2.5µl of $MgCl_2$, 1µl of dNTP, 0.5µl of GoTaq enzyme and 12µl of NFW. All enzymes were kept on ice. The PCR tubes were then incubated in the ^{3}Prime (Techne) machine. The programme of incubation was, 94°C for 5 min, 30 cycles of 94°C for 30 s, an annealing temperature of 57°C for 30 s, 72°C for 30 s. After 13 cycles, there was an incubation period of 72°C for 10 mins to complete the programme. The expression of the housekeeping gene β-Actin was used to normalise gene expression, as referenced in Table 2.1.

2.5.4.1 Preparation of the Agarose Gel

To prepare the gel, a 1% solution of Molecular Biology Grade Agarose in 1×TAE (tris-acetate-EDTA) was made by adding 1g of agarose to 100ml of 1×TAE. The 1×TAE was prepared by the dilution of 50×TAE (2.0M Tris Acetate and 100mM N_2EDTA) in MilliQ water. The solution was manually mixed and microwaved until boiling. 2.5µl of safe view was added immediately after microwaving and manually mixed. The agarose was poured into a mould, with a holder in place to make wells for the addition of the samples into the gel, and left to set.

2.5.4.2 Running the RT-PCR

To prepare the ladder (NEB ladder kit), 4µl of NFW was combined with 1µl of gel loading dye and 1µl of DNA ladder. To run the RT-PCR, the agarose gel was placed in the hold and covered to the max fill line in 1×TAE. 5µl of the ladder was pipetted into the first well of the gel with 10µl of each sample into the predetermined remaining wells. The electrodes were then inserted

and 90V was ran across the gel for 45 mins using a PowerPac Basic (BIO-RAD). The gel was then imaged using a ChemiDoc MP Imaging System (BIO-RAD).

2.5.5 Quantitative RT-PCR

A primer master mix, containing both forward and reverse primers (See Section 2.1.3) in a 1:10 dilution in NFW (20µl:20µl:160µl) was prepared. A total of 10µl was added to each well, 1.25µl of forward primer, 1.25µl of reverse primer, 2.5µl of 1:5 diluted cDNA (in NFW) and 5µl of SYBR Green. The qPCR plate was covered with an opticover and briefly centrifuged using a 5804R centrifuge (Eppendorf). RT-The plate was then run in a QuantiStudio 3 Real-Time PCR System (ThermoFisher). The programme set in the QuantStudio Design & Analysis Software v1.4 consisted of a hold stage (50˚C/2 min, 95 ˚C/10 min), a PCR stage ((95 ˚C/15 sec, 57 ˚C/1 min, 72 ˚C/1 min) × 40) and a melt curve stage (95˚C/15 sec, 60˚C/1 min). As with RT-PCR in Section 2.5.4, the expression of the housekeeping gene β-Actin was used to normalise gene expression, (Table 2.1)

2.6 Analysis of protein expression

The proteins were extracted for western blot analysis after being separated via Sodium Dodecyl Sulfate-Polyacrylamide Gel Electrophoresis (SDS-PAGE).

2.6.1 Protein extraction of intracellular proteins

Cells were harvested as described in Sections 2.2.5 and 2.2.6. Cell pellets containing ~1 × 10^6 cells, from BC and FBC that had previously been frozen at -80˚C were thawed at RTP to cast reducing gels. The pellets were washed by resuspension in 1ml of 1× PBS and centrifugation (Sigma 1-14 Microfuge at 2000rpm, 5 min) at RTP. The pellets were resuspended in 2× SDS-PAGE sample buffer (of 62.5mM Tris-HCL, pH 6.8, 25% glycerol, 2% SDS, 0.01% bromophenol blue). Immediately before use, 5% (v/v) β-mercaptoethanol was. Per sample, 20µl of sample buffer, 20µl of MilliQ water was added. The cell lysates were passed through

a syringe and a 21g needle to sheer the cells. The samples were briefly vortexed (VX-200 Vortex Mixer) before a 5 min incubation (QBD2 heat block (Grant Scientific) at 95˚C, 5 min) before being cooled at RTP.

2.6.2 SDS-PAGE

SDS-PAGE separating (1.5M Tris-HCl at a pH of 8.8 with 150µl of 10% (w/v) SDS), stacking (0.5 M Tris-HCl at a pH of 6.8, with 150µl of 10% SDS) and running buffers were prepared. The running buffer was prepared using Bio-Rad 10× Tris/Glycine/SDS Buffer (buffer concentrate) for SDS applications. 1L of working buffer was made by adding 100ml buffer concentrate to 900ml nanopure water, mixed to produce a final concentration of a 1× solution (25mM Tris, 192mM glycine, and 0.1% (w/v) SDS, pH 8.3).

The Mini-PROTEAN Tetra System (Bio-Rad) was used to conduct SDS-PAGE. A separating gel was overlaid by a stacking gel. The separating gel was prepared in a 50ml falcon tube, and, for two gels, consisted of 5.05ml MilliQ water, 6.2ml Protogel solution (30% [w/v] Acrylamide) and 3.75ml separating buffer. In the fume hood, polymerisation was initiated by adding 150µl of 10% (w/v) APS (ammonium persulphate) and 15µl of TEMED (tetramethylethylenediamine). 7ml of the separating buffer was added to each gel cast using a 10ml stripette. To remove bubbles, 20µl of isopropanol was added to the gel casts. Once the separating gel had set, the gel cast was removed from the mould and tapped to remove all isopropanol that would prevent the stacking gel from setting. The gel cast was then re-inserted to the mould.

The stacking gel was prepared in a 50ml falcon tube, and, for two gels, consisted of 6ml MilliQ water, 1.6ml Protogel solution (30% [w/v] Acrylamide) and 2.5ml stacking buffer. In the fume hood, polymerisation was initiated by adding 100µl of 10% (w/v) APS and 10µl of TEMED. The stacking gel was used to fill the remailing space in the gel casts using a 5ml stripette. A

1.5mm diameter comb was inserted into the top of each gel casts. Once set, the glass casts were placed into the cassette to run. The combs were removed from the gels in preparation for the loading of the ladder and samples.

To conduct electrophoresis, the cassettes and container were filled with 1× SDS-PAGE Running Buffer. To well 1 of each gel, 5µl of ladder was loaded. 20µl of each sample was loaded to predetermined wells. The Mini-PROTEAN Tetra System (Bio-Rad) was set to run using the PowerPac Basic (Bio-Rad) at 60Vfor 30 minutes, followed by 200V until the dye had reached the bottom of the tank (~30 min).

2.6.3 Western blot analysis

1L of transfer buffer was prepared from 100ml 10x Tris/Glycine Buffer concentrate, 200ml methanol and 700ml MilliQ water, mixed thoroughly to produce a 1× transfer buffer (final concentration 25mM Tris, 192mM Glycine, and 20% (v/v) methanol, pH 8.3).

In a tray of 1× transfer buffer a 'sandwich' was prepared. On a hinged grid with a sponge on either side, 5 pieces of filter paper placed on sponge. A nitrocellulose membrane was pre-soaked in transfer buffer and placed on top of one side of the filter paper. The gel was then removed from the cassette and casts and placed on top of the membrane and rolled flat to displace bubbles. The grid sandwich was then closed and pressed together tightly and placed in the cast box in the correct orientation for transfer and filled with transfer buffer to submerge the grids. The proteins were then transferred using the PowerPac Basic (Bio-Rad) cast box at 0.3V for 2 hrs at 4˚C.

For membrane blocking, 30ml of blocking buffer (5% milk PBS-Tween20) was prepared. The membranes and gels were removed from the casting sandwiches and, using the gel as a guide, the outline of the nitrocellulose membrane was cut. The gel was discarded and the membrane was then transferred to a container for blocking. Using a 10ml stripette, 10ml of blocking buffer

(5% milk PBS-Tween20) was added to the blot box, which was labelled and incubated on a SSM3 Mini Gyro-Rocker (Stuart) at 60 rpm for 1 hr.

To a 15ml falcon tube, 10ml of blocking buffer (5% milk PBS-Tween20) was added with the primary antibody. The antibodies used are described in Table 2.2. The tubes were mixed on the SRT6D Roller Mixer (Stuart) at 60rpm for 10 min. The blocking buffer was removed from the blot box and membrane and washed out twice with wash buffer (Section 2.3). To the membrane, the appropriate antibody solution was added (Table 2.2) and incubated on a SSM3 Mini Gyro-Rocker (Stuart) for 2 hrs at 60 rpm.

To a 15ml falcon tube, 10ml of blocking buffer (5% milk PBS-Tween20) was added with 1µl of a secondary antibody (Table 2.2) and mixed on the SRT6D Roller Mixer (Stuart) at 60rpm for 10 min. The primary antibody solution was removed from the blot box and membrane and washed out twice with wash buffer (Section 2.3). To the membrane, the appropriate secondary antibody solution was added (Table 2.2) and incubated on a SSM3 Mini Gyro-Rocker (Stuart) for 2 hrs at 60 rpm.

After incubation, the membrane was then washed three times using wash buffer (Section 2.3) before being imaged using the ChemiDoc MP Imaging System (Bio-Rad).

2.7 Statistical Analysis

The data presented, unless otherwise stated, are the normalised means from one to three independent experiments conducted in three biological replicates, with error bars representing the standard error of the mean (SEM). Unless otherwise stated, Microsoft Excel was used to calculate the R^2 values (coefficient of determination) for linear regression of the trend lines. Results were graphed and calculated using GraphPad Prism (9.5.1) where stated. Significance was determined either via the Student's t-Test with two-tailed independent samples or through

the use of a one-way analysis of variance (ANOVA), where appropriate. Mean values that were shown to be of significant difference are indicated by asterisks (*P<0.05, **P<0.001).

2.7.1 Calculations

The equations used to calculate the results relayed in the corresponding figures are as follows.

2.7.1.1 Figure 3.2: Specific Growth Rate

$$\mu = \frac{\ln\left(\frac{x}{x_0}\right)}{\Delta t}$$

Where:

μ = specific growth rate, hr^{-1}

x = viable cell density at the second timepoint, $\frac{cell}{ml}$

x_0= viable cell density at the original timepoint, $\frac{cell}{ml}$

Δt = the difference in time between the two timepoints, hr

2.7.1.2 Figure 3.3: Cell Doubling Time

$$td = \frac{\ln(2)}{\mu}$$

Where:

td = cell doubling time, hr

μ = specific growth rate, hr^{-1}

2.7.1.3 Figure 3.6: Specific Productivity

Step 1:

$$IVCD = (VCD_1 + VCD_2) \cdot (T_1 + T_2) \cdot 0.5$$

Step 2:

$$IVCD^{(t)} = \sum_{t=1} IVCD_{t-1} + IVCD_t$$

Step 3:

$$qP = \left(\frac{titre}{IVCD}\right) \cdot 10^{-3} \cdot 10^{9} \cdot 24$$

Where:

$IVCD$ = Integral viable cell density, $\frac{cell \cdot hr}{ml}$

VCD_1 = Viable cell density at timepoint 1, $\frac{cell}{ml}$

VCD_2 = Viable cell density at timepoint 2, $\frac{cell}{ml}$

T_1 = Time 1, hr

T_2 = Time 2, hr

t = Time, hr

$titre$ = Antibody titre, $\frac{mg}{l}$

qP = Specific productivity, $pg \cdot cell^{-1} day^{-1}$

Chapter 3: Results

3.1 Cultivation techniques

BC (Section 2.2.5) was used to characterise recombinant CHO-S cell growth in a closed system. As discussed in Chapter 1, the use of both BC and FBC each have relative merits. In this section, the concept that the addition of feed to replenish nutrients (Section 2.2.6) in a FBC extends productivity by increasing overall cell growth is explored.

3.1.1 Growth and Viability

Knowing the way in which IgG1 CHO-S cells grow in BC and FBC is the cornerstone of this project. Looking at different culture techniques to better understand factors that impact cell growth is fundamental to understanding how to make recombinant protein production more efficient for use in the biopharmaceutical industry.

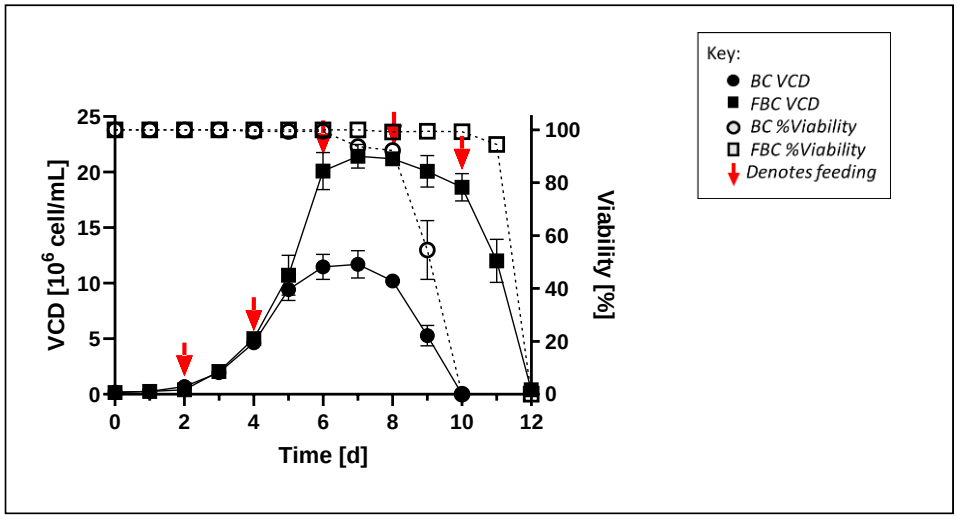

Figure 3.1. *VCD and percentage viability for the CHO-S IgG1 cell line in BC and FBC. Viable cell density (VCD) in batch culture (BC) is represented by a full circle with a full line, VCD in fed-batch culture (FBC) is represented by a full square with a full line, Viability BC is represented by an empty circle with a dashed line and Viability FBC is represented by an empty square with a dashed line. The intervals at which an addition of 1ml of feed consisting of Efficient Feed A and Efficient Feed B in a 50:50 ratio (section 2.2.6), was added to the supplemented CD CHO medium for FBC are denoted by a red arrow. The experimental values represent the mean of three biological replicates and error bars indicate ± SEM.*

As can be seen in Figure 3.1, the addition of feed greatly impacts the VCD of IgG1 CHO-S cells in culture. The overall growth pattern between BC and FBC is similar in both cultures, with the FBC reaching a just under two-fold greater VCD at peak density (BC ~11.7 × 10^6 cell/mL, FBC ~21.4 × 10^6 cell/mL) and the duration of the culture being extended by 48hrs. As all other factors other than the addition of feed remained constant between the cultures, the difference in VCD and percentage viability is a result of the addition of the nutrient supplementation.

The growth of the recombinant CHO-S IgG1 cell line used in this work (Section 2.1.1) in BC has been recorded and published in Torres and Dickson (2022). The trend in growth of cells in this previous publication is similar to that depicted in Figure 3.1, with lag, log, stationery, and decline phases. After beginning BC at a similar VCD (~0.2 × 10 cell/ml), peak VCD were similar, ~10 × 10 cell/ml in the publication and ~11.5 x 10 cell/ml in Figure 3.1. A difference between the BC, is that despite a similar lag phase from 0 hours to 72 hours, there is a delay in the log phase of the BC in Figure 3.1, with the culture in the Torres and Dickson (2022) publication reaching peak VCD after 120 hours. In the BC of this thesis, there is also a more prominent stationary phase from 120 hours to 192 hours whereas the cells described in the publication follow the log phase with a peak after 120 hours which precedes an immediate decline phase after 144 hours (Torres and Dickson, 2022). A possible explanation for the prolonged stationary phase for the BC conducted in this report in comparison to the BC of the same cell line in Torres and Dickson (2022) is a difference in medium composition. As described, the stationary phase is the phase in cell culture where cell growth is no longer exceeding cell death before cell growth slows and begins to drop off in the decline phase (Jaishankar and Srivastava, 2017). A depletion in nutrients in the BC medium is a factor in the longevity of this phase (Jaishankar and Srivastava, 2017). The Complete Medium (Section 2.2.1) in this study consists of the same components as the medium used in the Torres and

Dickson (2022) paper, other than the use of Glutamax in this study as opposed to the L-glutamine used in the publication. Using Glutamax as a glutamine supplement in the medium has been shown to extend cell culture duration (Zhao *et al.*, 2016). Therefore, the difference in culture duration of the same IgG1 CHO-S cell line may be explained by the difference in medium supplementation.

The profile of viability change of the CHO-S IgG1 cells in this study (Figure 3.1) and in the Torres and Dickson (2022) publication, is similar. Despite slight differences in the timing of log phase and extended stationary phase in Figure 3.1, in both BC, the percentage viability remained at 100% until after the peak in VCD. After the peak in VCD, the viability declined sharply. However, the percentage viability decreases to 0% over 72 hours in Figure 3.1, whereas in Torres and Dickson (2022) the percentage viability decreases to 0% over 48 hours. Comparatively, the duration of each culture for this study and in Torres and Dickson (2022) was 240 hours and 168 hours, respectively.

As described in Section 1.4.2, there are multiple feeds and regimes that have been used in FBC of CHO cell lines other than the feeding strategy described in Section 2.2.6. As previously mentioned in Section 1.4.2, work conducted by Pan *et al* (2017), examined the effect of using chemically-defined media on FBC of CHO cells to examine 24 different culture conditions. Although the effect is not recorded on the exact same cell line, the addition of 1:1 (v/v) ratio Efficient Feed A + B (See Section 2.2.6) increased cell growth (Pan *et al.*, 2017). The increase in peak cell density between BC and FBC is seen in the control cultures of the previously referred to (Section 1.4.3) study of Braasch *et al.*, (2021), which increased from ~9.2×10^6 cells/mL in BC to $20.2 \pm 1.7 \times 10^6$ cells/mL in FBC.

A paper published by Pan *et al.*, (2017), which investigated the metabolic characterisation of a CHO cell size increase phase in FBC looked at the cell growth as part of the study (Pan *et al.*,

2017). The paper reports an addition phase for the CHO cell FBC (Pan *et al.*, 2017). Rather than the typical lag, exponential, stationary and death phase the paper reports that as a result of the increase in cell size there is the lag phase, an exponential phase where the *concentration increases but the cell volume remains constant*, a phase where the cell *concentration stays approximately constant and the cell size increases nearly linearly*, a stationary phase where the biomass concentration is constant and viability is over 80% and a death phase where viability declines below 80% (Pan *et al.*, 2017).

A paper published by Reinhart *et al.*, (2015) aiming to standardise some of the commercially available CHO cell culture media proficiency in antibody production used an IgG-producing CHO DG44 cell line as a model for BC and FBC. In this publication, the CD CHO medium (See Section 2.2.1) used in this report was used comparatively in BC but not included in the FBC experimentation. The report found that in the un-supplemented CD CHO medium, cells grew to concentrations of 2.6×10^6 cells/mL after 12 days, with the highest peak lactate concentration of 2.2 g/L and the highest specific glucose consumption rates.

Findings from the presentation of Reinhart *et al.*, (2015), looking at the influence of cell culture media and feed supplements on cell metabolism and IgG quality in CHO-S and CHO-K1 and CHO-DG44, showed that the basal medium of the culture greatly influenced production (Reinhart *et al.*, 2015). It was found that in general FBC was prolonged in comparison to BC, with higher peak densities and up to six-fold greater antibody titres (Reinhart *et al.*, 2015). Additionally, the un-supplemented CD CHO was used as the basal medium used in the Complete Medium (Section 2.2.1). This was compared in the study to ActiCHO^{TM} P medium which was shown to produce higher peak densities in the CHO-S cell line as well as the CHO-K1 and CHO-DG44.

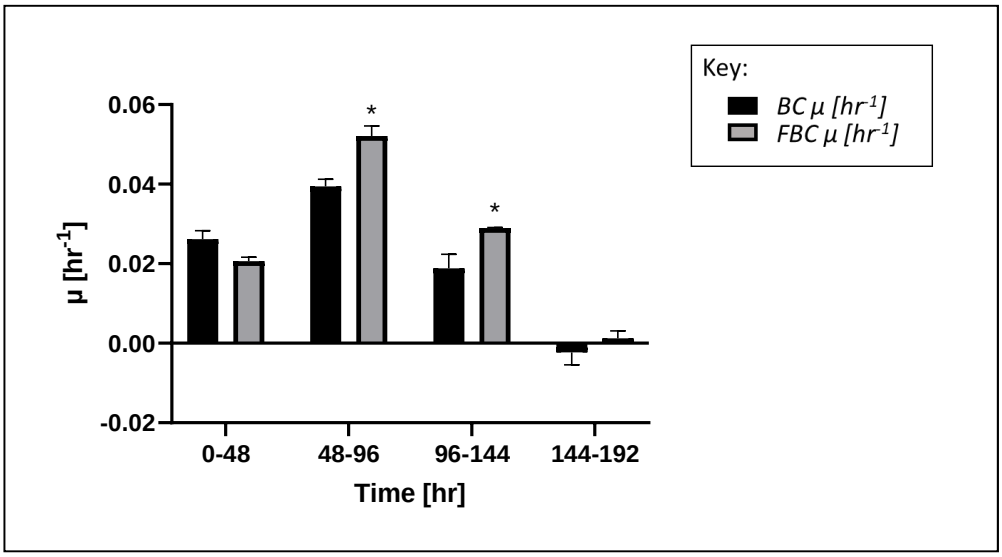

Figure 3.2. *Specific Growth Rate (μ) for the CHO-S IgG1 cell line in BC and FBC.*

*The calculation of μ is described in Section 2.6.batch culture (BC) is represented by the black bars, and fed-batch culture (FBC) is represented by the grey bars. The Experimental values represent the mean of three biological replicates and error bars indicate ± SEM. Significance was determined via the Student's t-Test with two-tailed independent samples. Mean values that were shown to be of significant difference are indicated by asterisks (*P<0.05).*

The Specific Growth Rates (μ) for BC and FBC are depicted in Figure 3.2. In Figure 3.2, the μ for BC and FBC between each 48-hour interval of the culture is compared and significance tested. The μ of FBC was found to be significantly greater that the μ of BC between 48-96 and 96-144 hours. In Torres and Dickson (2022), the same CHOS IgG1 cell line had mean specific growth rate of ~0.03 h^{-1}. Although the publication does not differentiate between the different phases of culture, the mean μ of the BC across all time periods is ~0.02h^{-1}.

A recent paper from Torres *et al.*, (2023) that looks at the effect of long-term culture and how it promotes changes to growth, gene expression, and metabolism in CHO cells that are independent of production stability. In this paper the same recombinant IgG1 CHO-S cell line is used in the development of stable (D8H3) and unstable (D7H12) cell lines (Torres *et al.*, 2023). The μ in this paper was calculated for early and late-stage culture in both cell lines and

in D8H3 was ~0.8^{-d} in early culture and ~0.9^{-d} in late culture (Torres *et al.*, 2023). In the D7H12 the μ remained relatively constant at ~0.9^{-d} in both early and late-stage culture (Torres *et al.*, 2023). In the paper published by Torres, M. *et al.* (2021) looking at the metabolic profiling of CHO cell cultures at different working volumes and agitation speeds using spin tube reactors used the same IgG1 CHO-S cell line as this report and found in BC the μ to be 0.487 ± 0.004.

Figure 3.3 shows the Cell Doubling Time (td) of BC and FBC. The results of the two-tailed

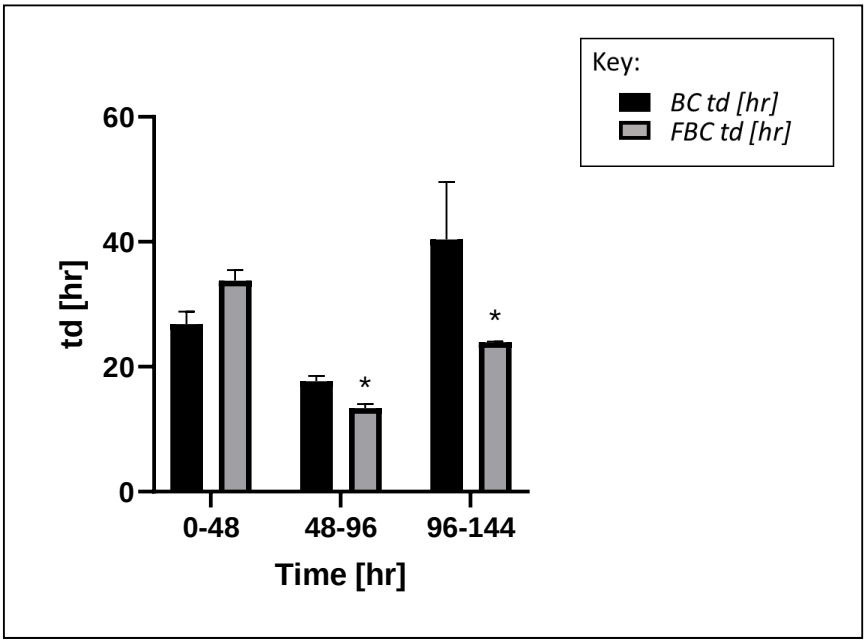

Figure 3.3. *Cell Doubling Time (td) for the CHO-S IgG1 cell line in BC and FBC.*
*Batch culture (BC) is represented by the black bars, and fed-batch culture (FBC) is represented by the grey bars. The experimental values represent the mean of three biological replicates and error bars indicate ± SEM. Significance was determined via the Student's t-Test with two-tailed independent samples, as described in Section 2.6. Mean values that were shown to be of significant difference are indicated by asterisks (*P<0.05).*

independent t-test showed that the td of FBC was significantly different from the BC during hours 48-96 of culture. As shown in Figure 3.1, this is immediately following the first feed for the FBC at the start of the exponential phase of cell growth for both cultures. The td is the lowest for both cultures at this interval as it is the time period in which the cells are undergoing

the greatest period of growth following the lag phase. The μ depicted in Figure 3.2 shows that there is significant difference in growth rate during both 48-96 and 96-144 intervals, which as td is the inverse of doubling time, both the same periods are significantly different as expected. Although, the td for both BC and FBC has been calculated and compared in this study as a separate parameter to characterise culture growth and for the use in comparison to cell productivity, when examining the relationship between specific growth rate and cell doubling time as a parameter for tumour growth, cell td was found to be unsuitable reasons including the fact that mean td can over or underestimate average growth rate (Mehrara *et al.*, 2007).

The relationship between specific growth rate and cell doubling time and the impact on cell specific productivity and titre is presented in Section 3.2.

3.2 Quantification of IgG production

As explained in the introduction (Section 1.4), CHO cell lines are the predominant expression system to produce biopharmaceuticals in industry. More knowledge on antibody production by CHO cells is fundamental to increasing the efficiency of antibody production. Increased efficiency would lead to a higher yield of protein being harvested for therapeutic use in the biopharmaceutical industry. Therefore, understanding the effect of feed in this recombinant CHO-S cell line in the production of IgG1 antibody by sampling BC and FBC is an important aspect of cell line characterisation.

3.2.1 IgG1 Titre

The titre of IgG1 is the cumulative amount of IgG1 in the sample produced by the viable cells present in culture.

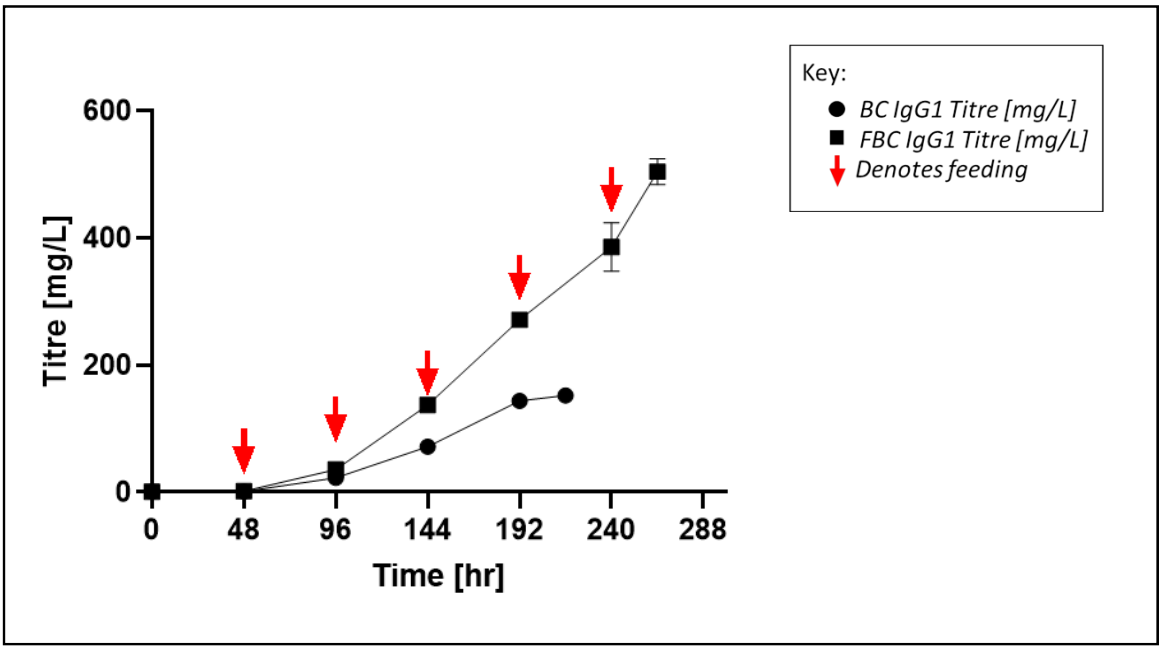

Figure 3.4. *IgG1 production for the recombinant CHO-S IgG1 cell line in in BC and FBC. Quantified using an immunoglobulin G enzyme-linked immunosorbent assay (IgG ELISA) (Section 2.3). IgG1 production in batch culture (BC) is represented by the circle line and IgG1 production in fed-batch culture (FBC) is represented by the square line. The experimental values represent the mean of three biological replicates and error bars indicate ± SEM. Error bars have been included on all data points but are only large enough to be visible outside of the denoting symbols at 240 hr and 264 hr of FBC. The intervals at which an addition of 1ml of feed consisting of Efficient Feed A and Efficient Feed B in a 50:50 ratio, was added to the supplemented CD CHO medium for the FBC are denoted by a red arrow.*

As described in Sections 2.2.5 and 2.2.6, during BC and FBC, respectively, medium samples were collected and stored at -20˚C for analysis. These samples were analysed using the IgG ELISA described in Section 2.3. Figure 3.4 shows the IgG1 titre for both BC and FBC for the duration of the cultures. Knowledge of factors that affect IgG1 titre of the CHO-S cell line is fundamental to the cell line as an expression system for recombinant protein production.

Figure 3.4 shows that IgG1 titres for both culture processes increased throughout culture duration. As shown in Figure 3.1, the duration of BC and FBC were 240 hr and 288 hr respectively. Figure 3.4 shows that the last time point analysed using the IgG1 ELISA was at 216 hr and 264 hr for BC and FBC, as seen in Figure 3.1, these are the last days of culture and VCD and viability are in steep decline. The titre increasing in both cultures despite the decrease in VCD and viability, would suggest that antibodies are still being released by the remaining viable cells that is contributing to the cumulative titre in the medium. Figure 3.4, depicts how from 0-96hr the titre for both BC and FBC are similar, however from 144hr onwards the cumulative FBC titre is visibly greater than BC IgG1 titre. As discussed further in Figure 3.5, the final BC IgG1 titre is ~150mg/L and FBC is ~500mg/L. The titre from the BC conducted at the same rpm and volume as this report (see Section 2.2), using the IgG1 CHO-S cell line was found to be ~200mg/L after 10 days of culture (Torres et al., 2021).

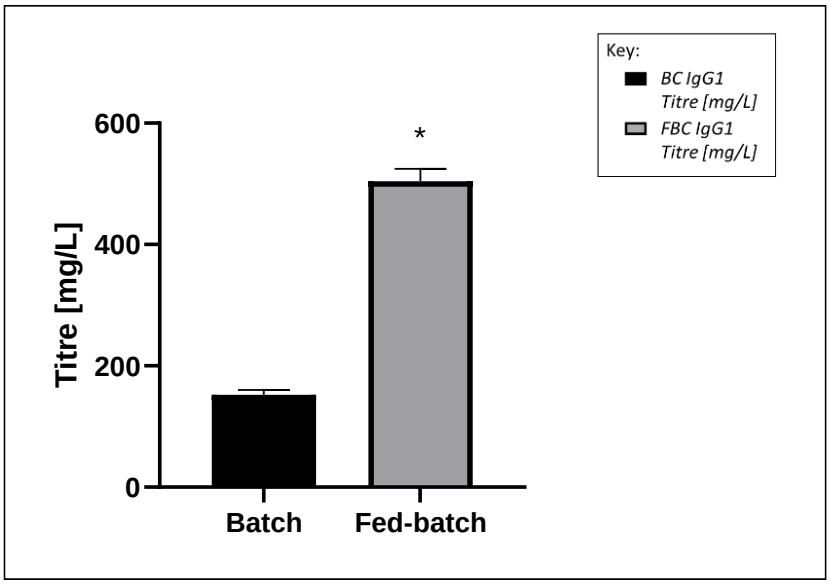

Figure 3.5. *A comparison of IgG1 titre for the CHO-S IgG1 cell line at the end of BC and FBC.*

*Quantified using an immunoglobulin G enzyme-linked immunosorbent assay (IgG ELISA). The titres were determined using a standard curve. The black bar represents the IgG1 titre of batch culture (BC) on Day 9 and the grey bar represents the IgG1 titre of fed-batch culture (FBC) on Day 11. The experimental values represent the mean of three biological replicates and error bars indicate ± SEM. Significance was determined via the Student's t-Test with two-tailed independent samples. Mean values that were shown to be of significant difference are indicated by asterisks (*P<0.05).*

Figure 3.5 is a comparison of the titres at the final timepoints analysed by IgG ELISA for BC and FBC. As the antibody accumulates in the medium as culture progresses the final recorded sample is a cumulative measure. As seen in Figure 3.5, the IgG1 titre is significantly greater when CHO-S cells are cultured in FBC in comparison to BC. The final FBC titre of ~500mg/L is over 3-fold greater than the final BC titre of ~150mg/L. This is significant as when looking at a cell line as an expression system, it is beneficial to maximise the productivity of the cell line so more protein can be harvested in the most efficient manner. These results indicate that the addition of feed increases overall CHO-S cell productivity. From here, the IgG1 titres were then used to calculate the specific productivity for BC and FBC, as seen in Figure 3.6, to assess the effect of the addition of feed on this parameter.

3.2.2 Specific Productivity

The Specific Productivity (qP) of the IgG1 recombinant CHO-S cell line was calculated as a parameter that determines the productivity of individual cells rather than the entire culture. The calculation of qP is described in Section 2.6.

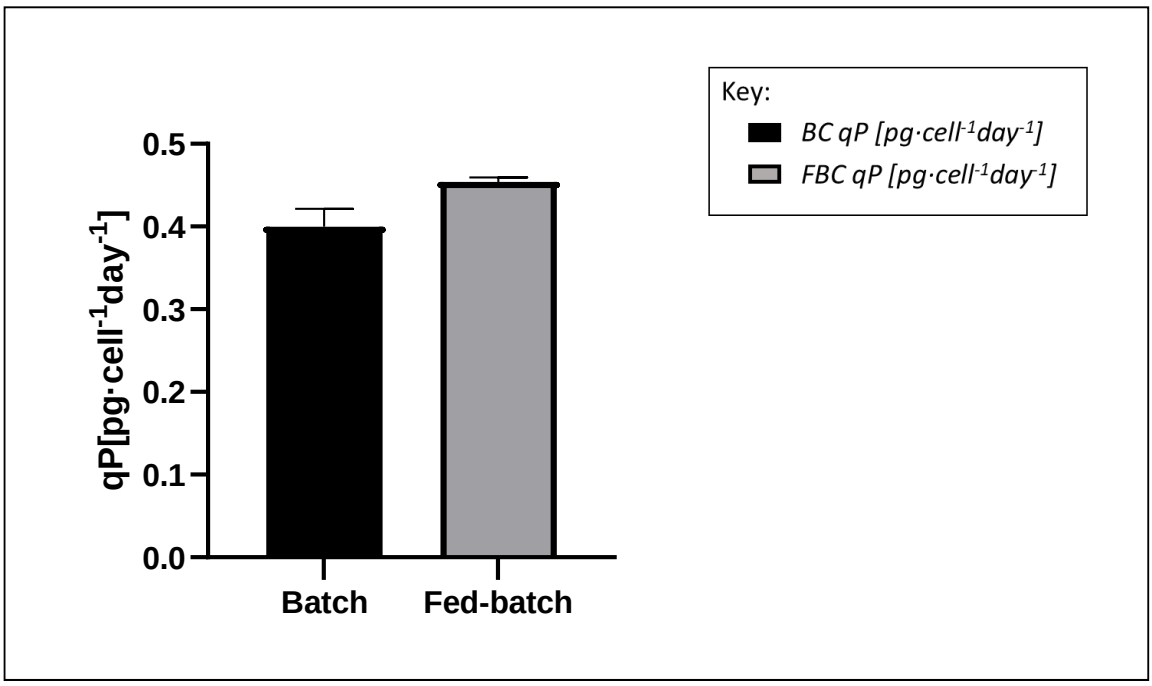

Figure 3.6. *Shows the Specific Productivity for the CHO-S IgG1 cell line for the summation of BC and FBC.*

*The specific productivity of batch culture (BC) is represented by the black bar and the specific productivity of fed-batch culture (FBC) is represented by the grey bar. Significance was determined via the Student's t-Test with two-tailed independent samples. Mean values that were shown to be of significant difference are indicated by asterisks (*P<0.05).*

Figure 3.6 depicts the Specific Productivities (qP) for IgG1of BC and FBC, these were ~0.385pg·cell^{-1}day^{-1} and ~0.454 pg·cell^{-1}day^{-1}, respectively. The cumulative product titres denoted in Figures 3.4 and 3.5 are cumulative and although is an important parameter for cell-line characterisation is affected by qP to a great extent (Zalai *et al.*, 2016). Specific productivity

(qP) in recombinant cell culture quantifies the rate of protein expression per cell and time unit, therefore delivering time-resolved which can be used to provide the information on the kinetics of protein synthesis (Zalai *et al.*, 2016).

As seen in Figure 3.6, the difference between the specific productivity between the cultures is slightly greater in FBC but this difference is not significant. This shows that the cells capacity to produce antibody in a given time is not impacted by the addition of feed. Therefore, the significant difference in titre seen in Figure 3.5 is a consquence of other factors. An explanation could be that the addition of feed directly influences cell growth, as seen in Figure 3.1, and this increased growth in FBC is conducive to more cells producing antibody that accumulates in the medium with little to no impact on an individual cell's capability to produce IgG1. Although an increase in qP as a result of feed addition have been reported in CHO, such as that of Sellick *et al.*, (2015), where with feed addition, qP was enhanced by 25–30%, there are also studies that do not produce the same findings. As with this report, an increase in qP as a result of feed addition is not observed in the studies conducted by Reinhart *et al.*, (2019) and Braasch *et al.*, (2021).

The qP was determined for the previously mentioned D8H3 (stable) and the D7H12 (unstable) cell lines derived from the same recombinant IgG1 CHO-S cell line used in this study, were developed by Torres *et al.*, (2023). For both cell lines the qP is determined at early and late culture passages (Torres *et al.*, 2023). For the D8H3 the qP is around 9 $pg \cdot cell^{-1}day^{-1}$ in early culture and 8 $pg \cdot cell^{-1}day^{-1}$ in later culture (Torres *et al.*, 2023). For the D7H12 the qP is around 9 $pg \cdot cell^{-1}day^{-1}$ in early culture and 5 $pg \cdot cell^{-1}day^{-1}$ in later culture (Torres *et al.*, 2023). Furthermore, a paper from Reinhart *et al.*, (2019) looking at the bioprocessinupdateg of recombinant CHO-K1, CHO-DG44, and CHO-S as to whether CHO expression hosts favour monoclonal antibody production or biomass synthesis also calculated the specific productivity of a recombinant CHO-S cell line in CD CHO basal medium for BC, FBC and perfusion

conditions (Reinhart *et al.*, 2019). In BC the CHO-S was found to have a qP of 14.0(±0.6) $pg \cdot cell^{-1}day^{-1}$, FBC 13.8 (±0.5) $pg \cdot cell^{-1}day^{-1}$, and perfusion 16.2(±2.8) $pg \cdot cell^{-1}day^{-1}$ (Reinhart *et al.*, 2019).

3.3 Metabolic Analysis

The metabolic analysis of the BC and FBC of the IgG1 CHO-S cell line is fundamental to the characterisation of cell health. Used in combination with cell growth (Section 3.1) and productivity (Section 3.2) metabolic analysis can be used to better understand changes or exhibition of cell culture phenotype. As described in Section 2.4, glucose, lactate and ammonia enzymatic assays were conducted in this report. Enzymatic assays are used to identify a particular substrate to prove its presence or lack of in a sample and to determine the amount of the specified substrate in the sample.

3.3.1 Glucose assay

Glucose is a primary fuel for heterotrophic organisms, and is therefore used to derive energy in the mammalian IgG1 CHO-S cell line.

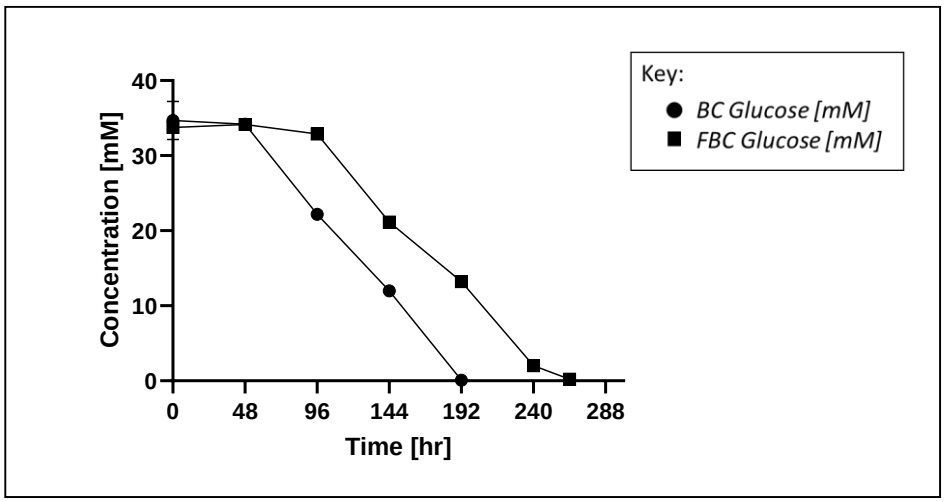

Figure 3.7. *The change in glucose concentration throughout BC and FBC of the CHO-S IgG1 cell line.*

Batch culture (BC) is represented by the circle line and fed-batch culture (FBC) is represented by the square line. Values were calculated using the enzymatic glucose assay described in Section 2.4.1.1. The experimental values represent the mean of three biological replicates and error bars indicate ± SEM. Error bars have been included on all data points but are only large enough to be visible outside of the denoting symbols at 0 hr in BC. These results were graphed and calculated using GraphPad Prism (9.5.1).

Figure 3.7 shows the trends in glucose concentration in both BC and FBC. There is a similar trend between BC and FBC, with the glucose concentration for both cultures decreasing throughout, despite the addition of glucose that occurred within the feed supplementation. At 0hrs both BC and FBC have a glucose concentration of ~33mM, which remains similar for both cultures after 48hr. At the next sampling of BC at 96 hr there has been a steep decrease in glucose concentration to ~22mM. This decrease of ~10mM every 48hr until the glucose concentration has reached 0mM after 192hr. Looking at the growth data in Figure 3.1, at 168hr BC VCD peaks and the percentage viability has begun to decrease slightly from 100%. At 192hr BC VCD is decreasing and percentage viability continues to decrease. The lack of glucose in the medium correlates with the decrease in VCD and percentage viability which both reach 0, 48hr after glucose is no longer present in the medium.

FBC differs from BC in that after 96hr there is a minimal decline in glucose concentration to ~32.5mM from ~33mM after 48hr. As stated previously and in Section 2.2.6, the addition of feed to the FBC occurred after sampling throughout the duration of culture. This shows at this stage in the culture, glucose that would be consumed from the Complete Medium in BC is being replenished by the addition of feed. However, despite the addition of feed every 48hr from 48hr onwards (see Section 2.2.6) the addition of feed has little impact on the trend in which way the glucose concentration decreases. Like the BC consumption of glucose, from 96hrs there is a ~10mM decrease in glucose concentration every 48hr, despite the addition of feed, containing glucose, at the same time intervals. From looking at Figures 3.1, 3.4 and 3.7 the increased growth and productivity of the FBC results in the consumption of glucose as quickly as its added to the medium via feed.

As referred to in Section 3.1.1, the presentation of Reinhart *et al.*, (2015), looking at the influence of cell culture media and feed supplements, found that the FBC strategies influenced the cell-metabolic rates of nutrient consumption and by-product formation (Reinhart *et al.*, 2015). This included the finding that in the basal CD CHO media used in this report, cell-specific glucose consumption rates were 30-55% higher in the CHO-S, CHO-DG44 and CHO-K1 cell lines.

3.3.2 Lactate assay

Im mammalian cell culture, the metabolite lactate is primarily a waste product that is formed as a byproduct of glycolysis (Torres *et al.*, 2018).

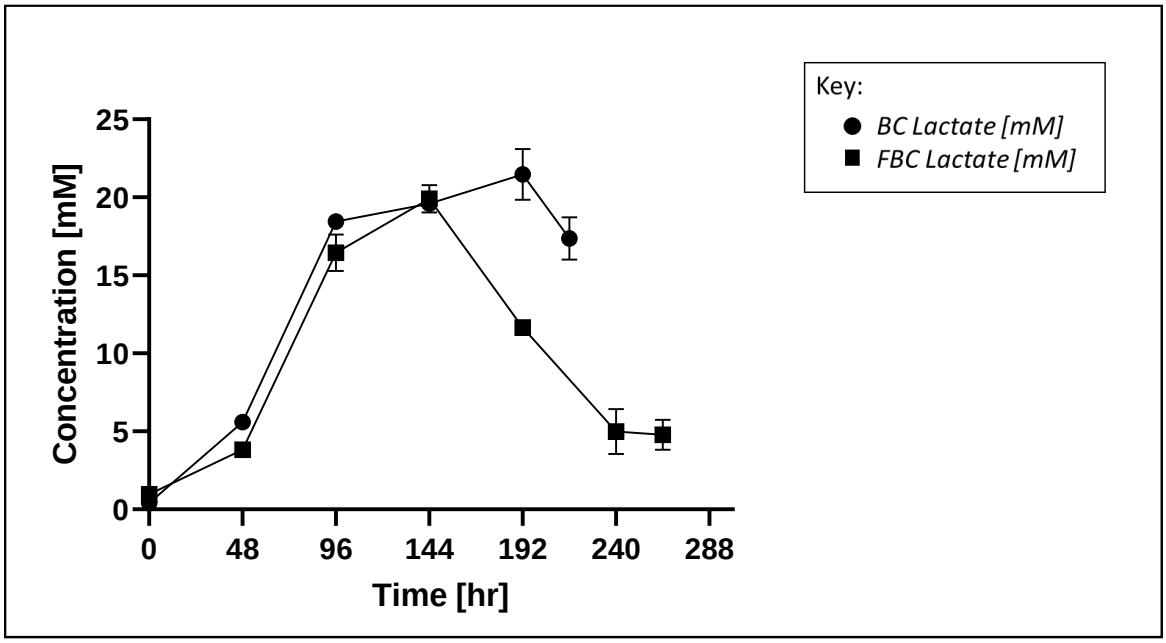

Figure 3.8. *The change in lactate concentration throughout BC and FBC of the CHO-S IgG1 cell line.*

Batch culture (BC) is represented by the circle line and fed-batch culture (FBC) is represented by the square line. Values were calculated using the enzymatic lactate assay described in Section 2.4.1.2. The experimental values represent the mean of three biological replicates and error bars indicate ± SEM. These results were graphed and calculated using GraphPad Prism (9.5.1).

Figure 3.8 shows lactate concentration of the medium in BC and FBC. In both BC and FBC the lactate concentration at 0hrs is ~0mM. Despite the addition of feed in the FBC, until 144hr the trend in changes in lactate concentration is similar between BC and FBC. Although, FBC has a slightly lower lactate concentration at 48 and 96hr, both BC and FBC from 0hr there a relatively small increase at 48hr to ~5.5mM and ~4mM followed by a large increase at 96hr to ~18mM and ~16mM. At 144hr, both BC and FBC have a lactate concentration of ~20mM. As

seen in Figure 3.1, both BC and FBC are in lag and log phase from 0hr to 144hr, during which time VCD is increasing. Despite the VCD of FBC being ~8mM greater than BC at 144hr, the lactate concentration of the medium is the same.

As can be seen from Figures 3.1 and 3.8, in comparison to BC, the FBC grows for a longer period and to a higher VCD yet begins to use lactate earlier than BC. Theoretically, the addition of a feed containing pyruvate may be expected to increase the concentration of lactate in the medium from its breakdown (Sellick *et al.*, 2011). However, as shown in a study into the metabolite profiling of recombinant CHO cells and the design of tailored feeding regimes to enhance the production of the recombinant IgG4 antibody conducted by Sellick *et al.* (2011), showed that the addition of feeds containing amino acids and pyruvate decreased medium lactate amounts. The working explanation for such change in lactate concentration in the medium is that the addition of feed promotes the greater efficiency of the TCA cycle which facilitates effective use of the nutrients available, in this incidence lactate (Sellick *et al.*, 2011). In terms of the influence of medium on lactate profiles in BC and FBC, the presentation of Reinhart *et al.*, (2015) found that the three CHO cell lines investigated with different media and feed strategies converted glucose to lactate with different efficiencies, with the CHO-S cell line converting 10-15% of glucose into lactate (Reinhart *et al.*, 2015).

From 144hr to 192hr there is an increase in lactate concentration in the BC that is not seen in the FBC. During the same time period there is a sharp decrease in lactate concentration from ~20mM to ~12mM. This decrease is compounded by a further decrease from 192hr to 240hr to ~5mM, where it is maintained to the last day of FBC at 264hr. Although the last day of BC, 192hr to 216hr, does also see a decrease from ~22mM to ~17mM, the lactate concentration at the end of BC remains much higher than at the end of FBC.

3.3.3 Ammonia assay

In mammalian cell culture, the metabolite ammonia is a predominantly a waste product that accumulates as a result of the breakdown of glutamine (Schneider *et al.*, 1996).

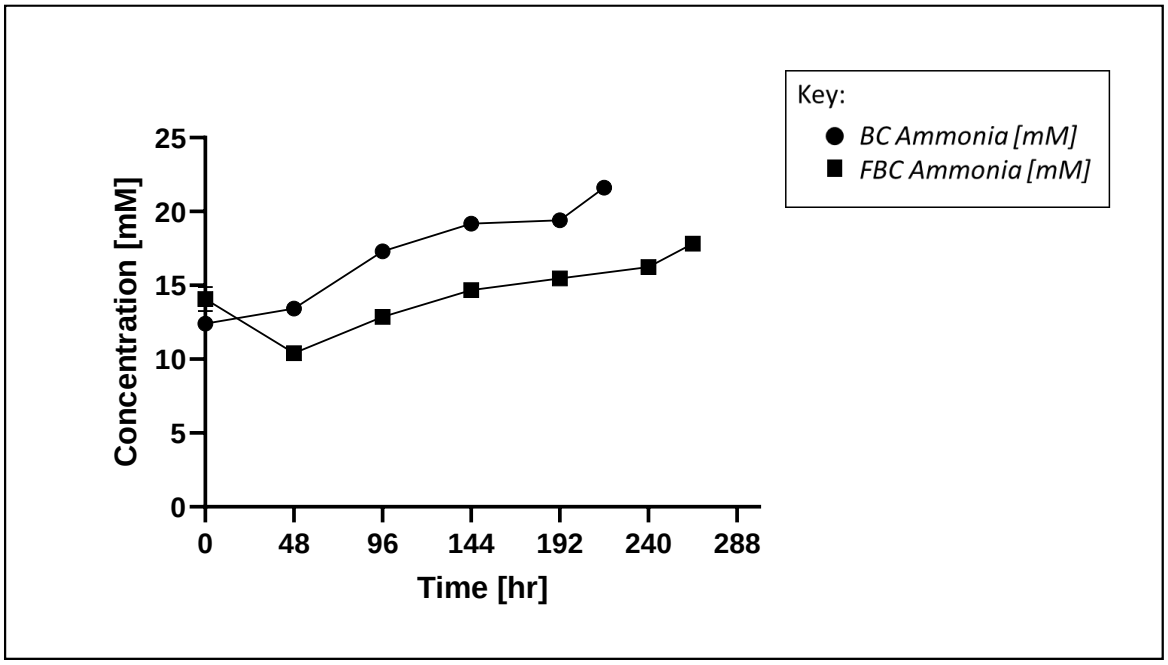

Figure 3.9. *The change in ammonia concentration throughout BC and FBC of the CHO-S IgG1 cell line.*

Batch culture (BC) is represented by the circle line and fed-batch culture (FBC) is represented by the square line. Values were calculated using the enzymatic ammonia assay described in Section 2.4.1.3. The experimental values represent the mean of three biological replicates and error bars indicate ± SEM. These results were graphed and calculated using GraphPad Prism (9.5.1).

Figure 3.9 shows the difference in ammonia concentration throughout BC and FBC to follow a similar trend despite the presence of feed. Both cultures start at a similar ammonia concentration, BC ~6mM and FBC ~7mM, which is as to be expected as directly after seeding at 0 hrs there is no difference in Complete Medium composition (see Section 2.2.1). The ammonia concentration in BC appears to steadily increase from ~6mM at 0 hrs to ~10mM at the last sample has been taken after 216hrs. As shown in Figure 3.1, 216 hrs is the second to

last day of BC at which point both VCD and percentage viability are in steep decline. For the last day of BC at 240hrs, the ammonia concentration has not been recorded, given that the cells were not at all viable at this timepoint (Figure 3.1) a sample was not taken, however given the relatively steep rise from 192hrs to 216hrs knowing the ammonium concentration at 240hrs in BC may have been of interest.

Despite a slight decrease in the FBC ammonia concentration, after 48 hrs the ammonia concentration remains similar between the cultures. This is expected as from 0hrs to 48hrs there is no difference in the culture processes between BC and FBC and in FBC, feed was added to the Complete Medium after sampling (Section 2.2.6). As stated in Figure 3.9, the experimental values represent the mean of three biological replicates and error bars indicate ± SEM, of which these are the most notable at 0hrs for the FBC. The trend in FBC ammonia concentration being a steady increase throughout culture, with a slightly steeper increase on the second to last day of culture (Figure 3.1) at 264hrs, is the same as seen in BC. However, the ammonia concentration in FBC remains lower at each timepoint with a more gradual increase from ~7mM to ~9mM. From the lowest to the highest ammonia concentration BC has an increase of ~4mM whereas FBC has a lower increase of ~2mM.

3.4 Analysis of mRNA expression

After the characterisation of growth, productivity, and metabolite analysis of the IgG1 CHO-S cell line in BC and FBC in Sections 3.1, 3.2 and 3.3, a closer look at the expression of UPR-related genes throughout culture duration was undertaken. As previously stated in Sections 1.6, 1.7 and 1.8, in has been identified that the UPR is involved in the incidence of secretory bottlenecks that impact cellular capacity to produce recombinant antibodies. The rationale behind analysing the expression of the four GOI in particular, was explained in Section 1.8.2.

3.4.1 RT-PCR

Figure 3.10 shows RT-PCR for each gene in BC, using both RT+ cDNA and RT- cDNA. The samples were analysed using β-Actin as a housekeeping gene for comparison. β-Actin is always expressed in viable CHO cells as part of the cytoskeleton, therefore, if the cDNA used in the RT-PCR with β-Actin primers (Section 2.1.3) is viable then a positive result should be seen. β-Actin is a loading standard, and the extent of the resultant band reflects the quality of the RT-PCR reaction. A positive result in RT-PCR is a strong white band at the expected molecular weight which can be deduced from the base-pair ladder that has been run alongside the samples. Such result can be seen in lanes 1-9 of Figure 3.10. Lanes 10-18 are lanes run with the same sample timepoints but without the reverse transcription enzymes in the cDNA synthesis steps. These are run as a negative control, as there are no reverse transcription enzymes cDNA synthesis should not occur and therefore there should be no product seen in the RT-PCR, as seen in Figure 3.10. Although run for the other samples, RT- have not been included in the other RT-PCR figures for simplicity.

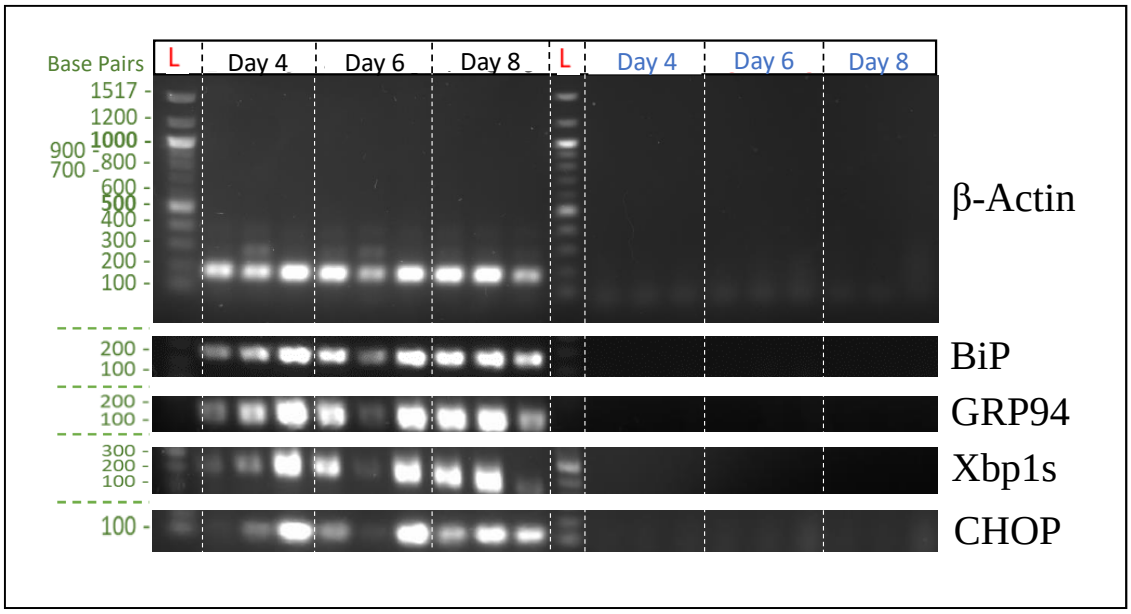

Figure 3.10. *RT-PCR gel of the CHO-S IgG1 cell line in batch culture (BC).*

Each lane has been marked at the top of the gel. As described in Section 2.5.3, the cDNA used in reverse transcription polymerase chain reaction (RT-PCR) was synthesised by reverse transcription (RT). As previously stated, for every sample timepoint a sample containing the RT enzymes (RT+) and a sample in which the RT enzymes were omitted (RT-), were prepared. At the top right-hand side, the lanes containing the RT+ samples are labelled in black as 'Day 4', 'Day 6' and 'Day 8' with each timepoint being conducted in triplicate. At the top left-hand side, the lanes containing the RT- samples are labelled in blue as 'Day 4', 'Day 6' and 'Day 8' with each timepoint being conducted in triplicate. The ladder is marked 'L' for both the RT+ and RT-, with the left-hand side of the image denoting the base pairs marked by the NEB 100 bp ladder. The lanes labelled 'Day 4' contain RT+ day 4 BC sample replicates A/B/C. The lanes labelled 'Day 6' contain RT+ day 6 BC sample replicates A/B/C. The lanes labelled 'Day 8' contain RT+ day 8 BC sample replicates A/B/C. The lanes labelled 'Day 4' contain RT+ day 4 BC sample replicates A/B/C. The lanes labelled 'Day 6' contain RT+ day 6 BC sample replicates A/B/C. The lanes labelled 'Day 8' contain RT+ day 8 BC sample replicates A/B/C.

Down the RHS of the figure, the genes for which the RT-PCR has been carried out are labelled. β-Actin is the housekeeping gene used to assess the cDNA quality of expression. The genes BiP, GRP94, Xbp1s and CHOP are the unfolded protein response (UPR) associated genes previously described. For primer design see Section 2.1.3.

RT-PCR is a methodology that can be used to test the quality of the cDNA produced from the

samples (Section 2.5). As can be seen in Figure 3.10, when looking at β-Actin in BC each triplicate for days 4, 6 and 8 produce a positive result in the form of a white band showing that cDNA has been synthesised at these timepoints. Although RT-PCR is not quantitative, any variation in the intensity of the band is a result of variation in the quality of the product in the samples. Therefore, the quality of the cDNA used in the RT-PCR may impact the PCR output. As β-Actin is the housekeeping gene, the intensity of the bands should be the sample throughout culture although day 4 replicate A, day 6 replicate B and day 8 replicate C are perhaps slightly less intense than the rest of their cohort.

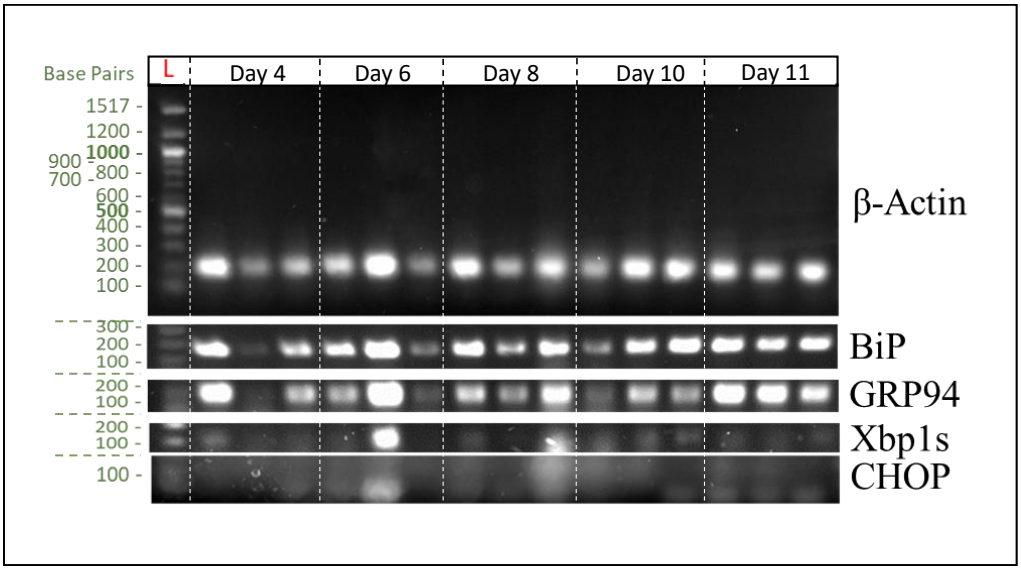

Figure 3.11. *RT-PCR of the CHO-S IgG1 cell line in fed-batch culture (FBC).*

*Each lane has been marked at the top of the gel. As described in Section 2.5.3, the cDNA used in reverse transcription polymerase chain reaction (RT-PCR) was synthesised by reverse transcription (RT). As previously stated, for every sample timepoint a sample containing the RT enzymes (RT+) and a sample in which the RT enzymes were omitted (RT-), were prepared. The RT- samples have been discounted from the image for simplicity, see Figure 3.10. The RT+ of FBC are labelled 'Day 4', 'Day 6', 'Day 8' 'Day 10' and 'Day 11' denoting the timepoint at which the samples were harvested, accordingly. The lanes labelled 'Day 4' contain RT+ day 4 BC sample replicates A/B/C. The lanes labelled 'Day 6' contain RT+ day 6 BC sample replicates A/B/C. The lanes labelled 'Day 8' contain RT+ day 8 BC sample replicates A/B/C. The lanes labelled 'Day 10' contain RT+ day 10 BC sample replicates A/B/C. The lanes labelled 'Day 11' contain RT+ day 11 BC sample replicates A/B/C. The ladder is marked '**L**', with the left-hand side of the image denoting the base pairs marked by the NEB 100 bp ladder.*

Down the right-hand side of the figure, the genes for which the RT-PCR has been carried out are labelled. β-Actin is the housekeeping gene used to assess the cDNA quality of expression. The genes BiP, GRP94, Xbp1s and CHOP are the unfolded protein response (UPR) associated genes previously described. For primer design see Section 2.1.3.

RT-PCR is also a method by which the effectiveness of the primers can be observed. If the primers designed (Section 2.1.3), were of poor quality the band would either not exist or be drawn out across the gel. By comparing the RT-PCR of multiple genes using the same cDNA,

any issues with a specific primer pair can be identified. As can be seen in Figure 3.10, the primers used for β-Actin, BiP, GRP94, Xbp1s and CHOP were all effective, hence likely to be useful for qRT-PCR quantification.

Figure 3.11 shows the results of the RT-PCR for the proteins, β-Actin, BiP, GRP94, Xbp1s and CHOP for samples taken from the IgG1 CHO-S cell line in FBC. Figure 3.10 only depicts the lanes containing the RT+ samples, rather than the RT+ and RT- samples seen in Figure 3.11. As seen in Figure 3.10, no bands were produced in the RT- lanes 10-18 which was the case for all gels, which have subsequently been excluded from the figures. As can be seen in Figure 3.11, when tested for the housekeeping gene, β-Actin, a product is visible in every lane, although there is some variation in the product quality. Points that are notably less defined are the samples in lanes 2, 6, 8 and 10, which are samples from day 4 replicate B, day 6 replicate C, day 8 replicate B and day 10 replicate A.

The intensity of the band seen in the samples for BiP and GRP94 are extremely similar throughout FBC. However, despite the same cDNA being used in the RT-PCR for all proteins in the FBC and the same primers being used as shown in Figure 3.10 for the RT-PCR of the FBC samples, qualitatively there is a slight difference in band intensity for Xbp1s and CHOP

for FBC samples. Bands are hardly visible for any sample other than lanes 5 and 9, samples from day 6 replicate B and day 8 replicate C, which are still only barely visible in CHOP.

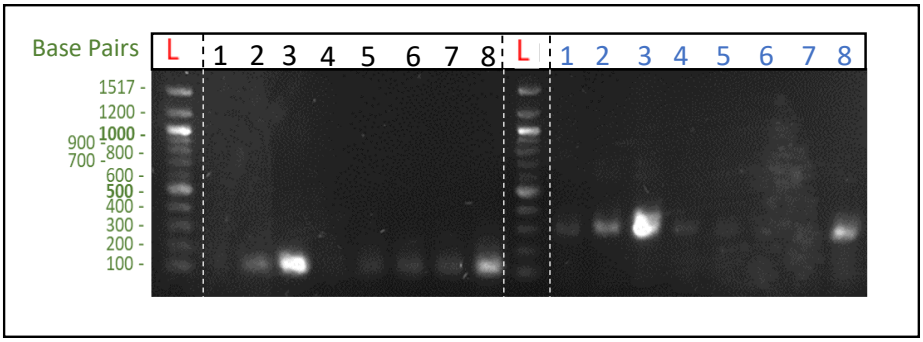

Figure 3.12. *Reverse transcription positive (RT+) Biological Replicate 'A' for Xbp1s and CHOP of the CHO-S IgG1 cell line in batch culture (BC) and fed-batch culture (FBC).*

The reverse transcription polymerase chain reaction (RT-PCR) was conducted as described in Section 2.5.4.

*At the top right-hand side of the image, the lanes containing the Xbp1s samples are marked in black numbers from '1-8'. At the top left-hand side, the lanes containing the CHOP samples are marked in blue numbers from '1-8'. The ladder is marked '**L**', with the left-hand side of the image denoting the base pairs marked by the NEB 100 bp ladder. For both proteins, lanes 1, 2 and 3 contain samples from days 4, 6 and 8 from BC accordingly. Lanes 4-8 contain FBC samples from days 4, 6, 8, 10 and 12 in that numerical order. For primer design see Section 2.1.3.*

Following on from the results of Figures 3.10 and 3.11, RT-PCR was again conducted for the Xbp1s and CHOP in BC and FBC, using of cDNA from only one experiment set, labelled Biological Replicate A, to focus the passage of time using the same cDNA. Although RT-PCR is not quantitative, a qualitive difference in protein expression can be observed as culture progresses. For both Xbp1s and CHOP, in BC and FBC the mRNA content appears to increase with culture duration. The most intense bands for both proteins are lanes 3 and 8, with lane 3 being the most intense overall. Referring to Figure 3.1, day 8 in BC is the beginning of the decline phase and by day 12 in FBC the VCD and viability is zero. It is to be expected that the

expression of Xbp1s and CHOP correlates due to their roles in the UPR explained in Section 1.8.2.

3.4.2 Quantitative RT-PCR

Following the establishment of effective primers and quality cDNA in the samples from BC and FBC. Quantitative RT-PCR (qRT-PCR) was conducted as described in Section 2.5.5, to calculate the difference in expression between the timepoint and cultivation techniques. This is a key aspect of the project to understand how the expression of UPR-related proteins is impacted by BC and FBC. As described in Section 2.5.5, the GOI in qRT-PCR were normalised using the expression levels of β-Actin in the same samples.

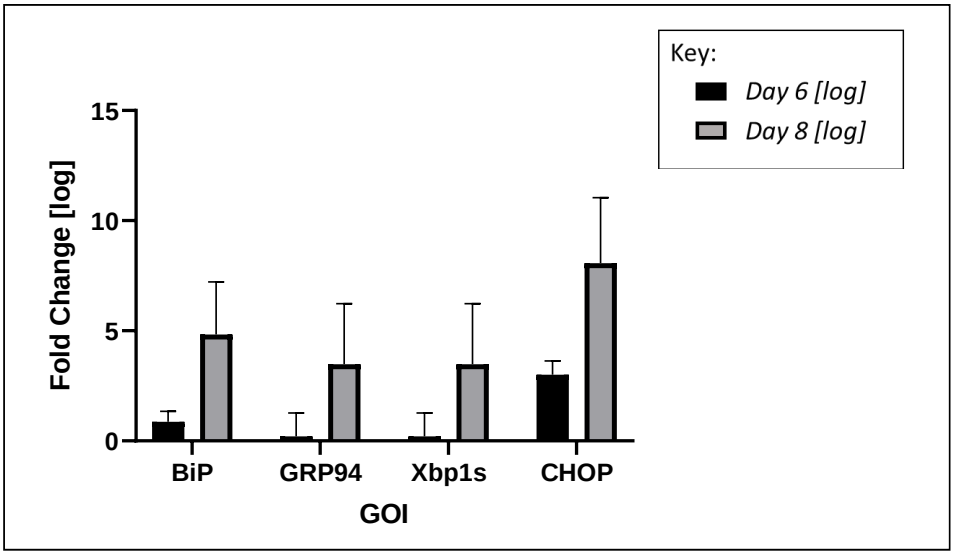

Figure 3.13. *Quantitative reverse transcription polymerase chain reaction (qRT-PCR) depicting the differential expression values for Days 6 and 8 of batch culture (BC) in comparison to Day 4 expression levels in the CHO-S IgG1 cell line.*

The fold change between day 4 and day 6 is for each gene of interest is depicted by the black bars, and the fold change between day 4 and day 8 is for each gene of interest is depicted by the grey bars. Significance was determined via the Student's t-Test with paired samples. The lack of significance between the two timepoints for each of the genes of interest is indicated by the absence of asterisks in the figure. The experimental values represent the mean of three biological replicates and error bars indicate ± SEM.

Figure 3.13 depicts the difference in the fold change of expression in BC between days 6 and 8 when both compared to the expression levels on day 4 of culture for each gene of interest. Although the difference in the fold change of expression when comparing day 8 to day 6 in BC is significant overall, for the individual genes of interest none of the differences are significant between days 6 and 8 when compared to day 4. Although, the difference in fold-change between days 6 and 8 in comparison to expression levels on day 4 is greatest in BiP and CHOP. All four of the GOIs have a greater level of expression on day 8 than on day 6. Looking at

Figure 3.1, the VCD and percentage viability of BC on days 6 and 8 are either side of the log phase of the culture, with a slight decline in both VCD and percentage viability on day 8.

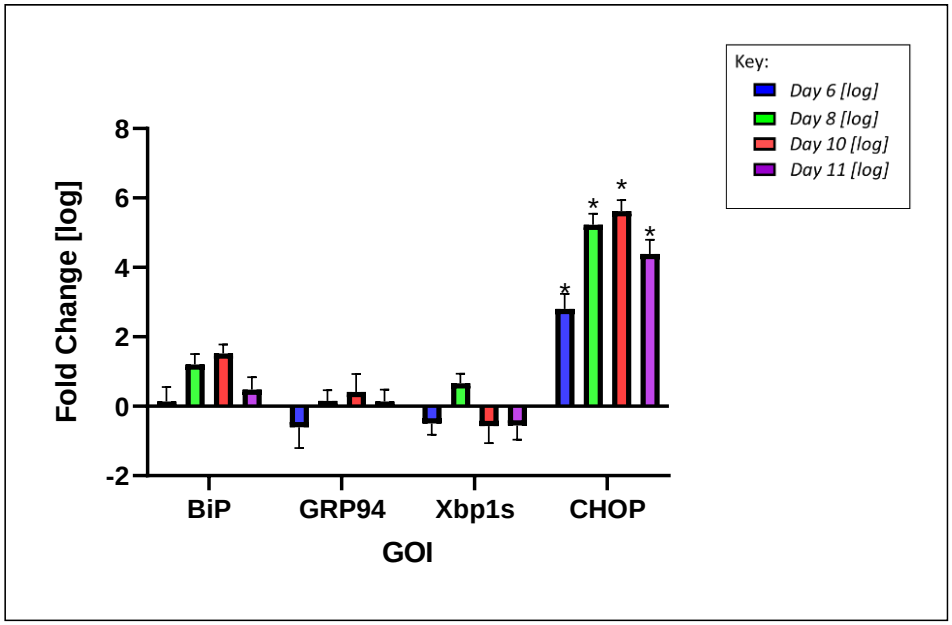

Figure 3.14. *Quantitative reverse transcription polymerase chain reaction (qRT-PCR) depicting the differential expression values for Days 6, 8, 10 and 11 of fed-batch culture (FBC) in comparison to Day 4 expression levels in the CHO-S IgG1 cell line.*

The fold change between Day 4 and Day 6 for each gene of interest is depicted by the blue bars, the fold change between Day 4 and Day 8 the green bars, the fold change between Day 4 and Day 10 the pink bars, and the fold change between Day 4 and Day 11 the purple bars. Significance has been determined using a separate one-way analysis of variance (ANOVA) for each of the genes of interest. The experimental values represent the mean of three biological replicates and error bars indicate ± SEM.

Figure 3.14 shows the fold change in the difference between the expression levels of the genes on interest for days 6, 8, 10 and 11 of FBC in comparison to the expression levels on day 4 of culture. The general trend in the fold change of expression for each of the GOIs is an increase until day 10 followed by a decrease on day 11. Looking at Figure 3.1 in tandem with the results in Figure 3.14, the VCD of the FBC peaks before day 8 on day 7 and then steadily declines in plateau phase before a steep decline in both VCD and percentage viability from day 10 to a

VCD and percentage viability of 0 by day 12. Therefore, on day 11 the VCD and viability is decreasing but the culture is still viable.

The expression of BiP and CHOP is consistently greater for the duration of culture than on day 4, with both genes following the trend of increasing to day 10 until decreasing slightly on day 11. Although, GRP94 also follows the same trend in the fold change of expression overall, initially the expression of GRP94 is greater on day 4 than day 6, before being more highly expressed on days 8, 10 and 11. This is unlike the trend in expression in BC, seen in Figure 3.13, the expression is greater at day 6 than day 4. The only gene that does not follow the trend in expression is Xbp1. Unlike the other GOI, the fold change in expression of peaks on day 8 at ~0.5 fold greater than day 4 rather than day 10. Not only this, the fold change in expression in comparison to expression levels on day 4 is the same for days 6, 10 and 11, with the levels on day 4 being ~0.5-fold greater. Like GRP94, in BC (Figure 3.13) the expression of day 6 is greater than day 4, whereas as seen in Figure 3.14, this is not the case in FBC.

When the individual data sets for each gene were significance tested using a one-way ANOVA, the difference in the fold change of CHOP was the only data set to prove significant. The greatest fold change is also seen in the levels of expression in CHOP, which peaks at day 10 at ~5.5-fold increase. As described earlier, the trend in the CHOP data set follows the increase to a peak on day 10 followed be a slight decrease on day 11.

When comparing Figures 3.13 and 3.14, the expression levels of BC and FBC using day 4 as a bench mark value, across both culture techniques the difference in BiP and CHOP appears to be the most pronounced increase.

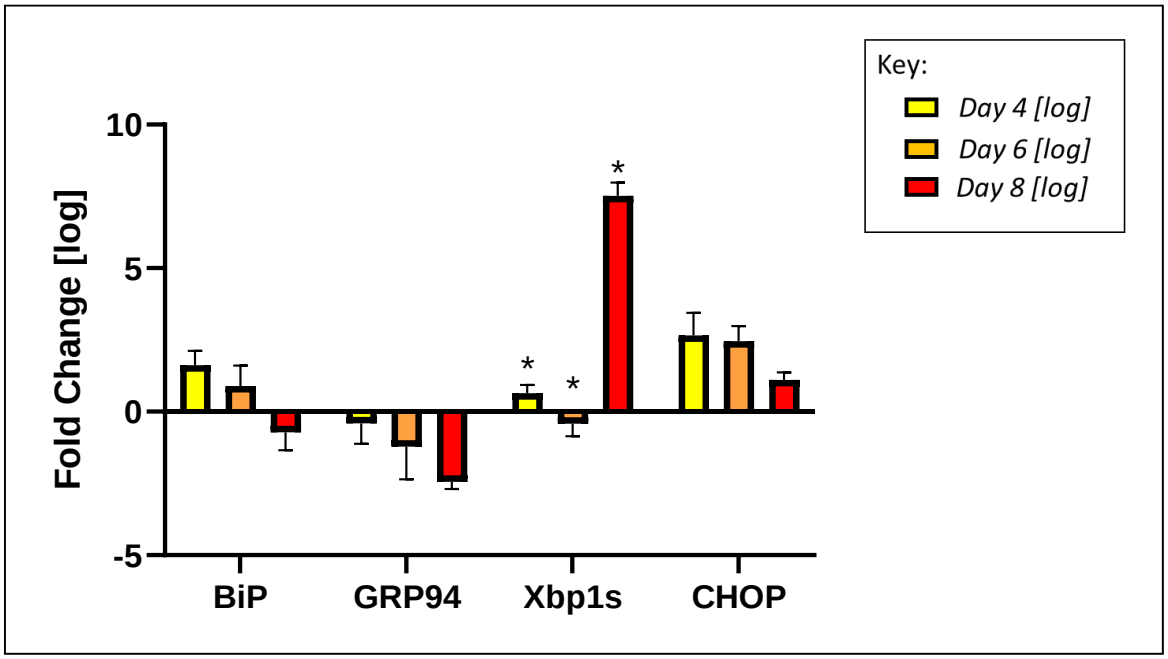

Figure 3.15. *A comparison of the fold change in expression for each of the genes of interest for days 4, 6 and 8 between batch culture (BC) and fed-batch culture (FBC) in the CHO-S IgG1 cell line.*

Day 4 is yellow, Day 6 is orange, and Day 8 is red. Significance has been determined using a separate one-way analysis of variance (ANOVA) for each of the genes of interest. The experimental values represent the mean of three biological replicates and error bars indicate ± SEM.

Figure 3.15 shows the difference in expression levels between BC and FBC for days 4, 6 and 8 for each of the genes of interest. In this analysis, for each timepoint, the expression levels for the genes in FBC are compared to expression levels of the genes in BC which has been used as the baseline expression for the comparison.

As seen in Figure 3.15, the general trend for BiP is as culture progresses from day 4 to days 6 and 8, the expression levels in FBC decrease in comparison to BC. The average expression for day 4 and 6 is ~1 fold greater in FBC than BC whereas for day 8 the expression levels for FBC

were ~1 fold less than in BC. The same trend in the fold change of expression levels can be seen in CHOP in Figure 3.15. Unlike, the expression levels for BiP, in CHOP the expression is greater in FBC than BC so there is a positive fold change at each timepoint. For days 4 and 6 the change in expression levels between BC and FBC are ~2.5 fold, for day 8 it is around 1-fold. The general trend for GRP94 seen in Figure 3.15 is also a decrease in the fold change in expression level in FBC in comparison to BC, although unlike the expression of CHOP, GRP94 expression is greater in BC than FBC for each of the timepoints. Looking at Figure 3.1, this trend in difference in expression levels for these three genes seen in Figure 3.15 maybe a result of a difference in VCD in BC in comparison to FBC.

As described in Figure 3.15, a one-way ANOVA was used to determine the significance between the fold change between BC and FBC for days 4, 6 and 8 for each of the genes on interest. The fold change in the expression levels of Xbp1s is the only gene to have a significant difference between days 4, 6 and 8. It is also the only gene of interest to not demonstrate a decrease in the fold change of expression levels BC to FBC. The indifferent expression of BiP between BC and FBC in a recombinant cell line is supported by the Wong *et al.*, (2006) study, which investigated the expression of apoptosis-related genes in a recombinant CHO cell line (see Section 1.8.3).

3.5 Analysis of protein expression

As described in Section 2.5, sample protein expression was assessed by SDS-PAGE and western blot analysis. This is a technique that can be used as both a qualitative and quantitative comparison of UPR protein expression throughout both BC and FBC.

3.5.1 Batch

First, the samples from BC were used in the comparison of UPR protein expression. Due to time constraints, the genes of interest that were examined were BiP and Xbp1 alongside the housekeeping gene ERK2.

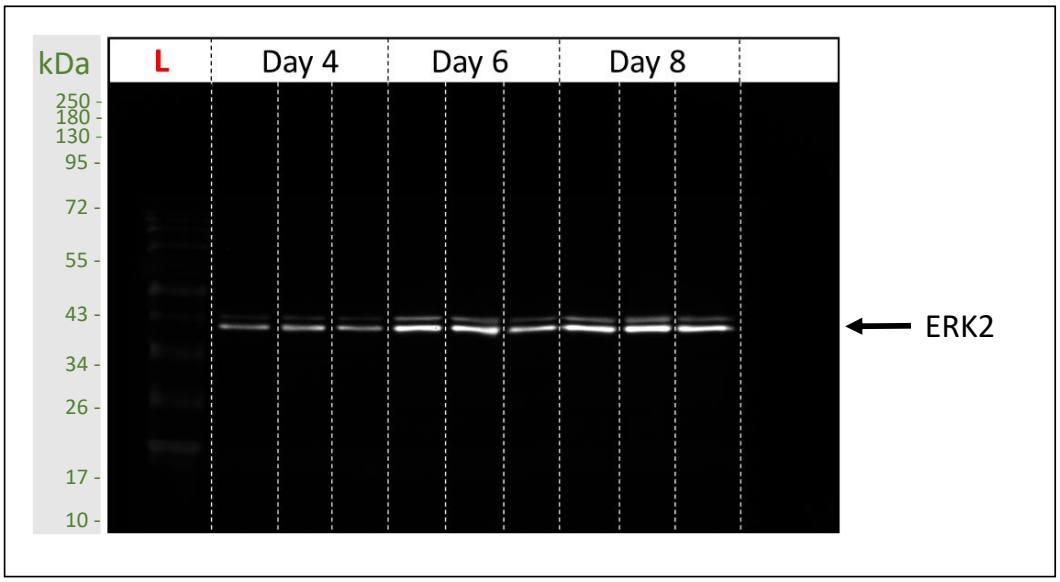

Figure 3.16. *Image of the western blot analysis of batch culture (BC) for the housekeeping gene ERK2 in the CHO-S IgG1 cell line.*

The complete method is as described in Section 2.5, with the western blot analysis being detailed in Section 2.5.3. The image was taken using the ChemiDoc MP Imaging System (Bio-Rad).

The lane containing the colour pre-stained protein standard 10-250kDA (NEB) is marked with a red 'L' and the green numbering to the left-hand side of the image is the molecular weights denoted by the standard. The remaining lanes of the gel contain the samples. The lanes labelled 'Day 4' contain day 4 BC sample replicates A/B/C. The lanes labelled 'Day 6' contain day 6 BC sample replicates A/B/C. The lanes labelled 'Day 8' contain day 8 BC sample replicates A/B/C.

Figure 3.16 depicts the western blot for BC sample days 4, 6 and 8 for the housekeeping gene ERK2. As described in Section 3.4, running a housekeeping gene is necessary as a positive control. The ERK signalling cascade regulates processes such as proliferation, differentiation, and migration within the cell, with ERK1 and ERK2 being effector kinases (Buscà *et al.*, 2018).

Due to the core role ERK2 has within the cell and its routine use in the laboratory to standardise protein loading on gels, it would be expected to be abundant and produce a strong definitive band in each of the samples. Such result can be seen in Figure 3.16. Unfortunately, due to the makeup of the gel and a suspected breach in the end lane containing the ladder sample, a clear ladder is not visible in this image so it is not possible to determine band weight and therefore kDa. Looking at the results from the western blot analysis from a paper looking at the modification of expression of UPR-/ERAD- related genes by temperature down-shift and the enhanced production of chimeric fusion protein in CHO cells, the bp of ERK2 is expected to be between 48-35kDa at around 42kDa (Torres *et al.*, 2021). The full ladders in BC can be seen in Figures 3.17 and 3.18. The western blot analysis of the BC samples in ERK2 produce bright defined bands for each of the samples. The bands from the day 4 samples are noticeably weaker than the samples from days 6 and 8. This may be a result of poorer quality cell samples taken from day 4 as a result of a lower VCD in culture at this time (See Figure 3.1). Western blot analysis can be used to quantify the abundance of a specified protein in a sample by measuring the signal intensity of the band produced in the western using software such as Image J.

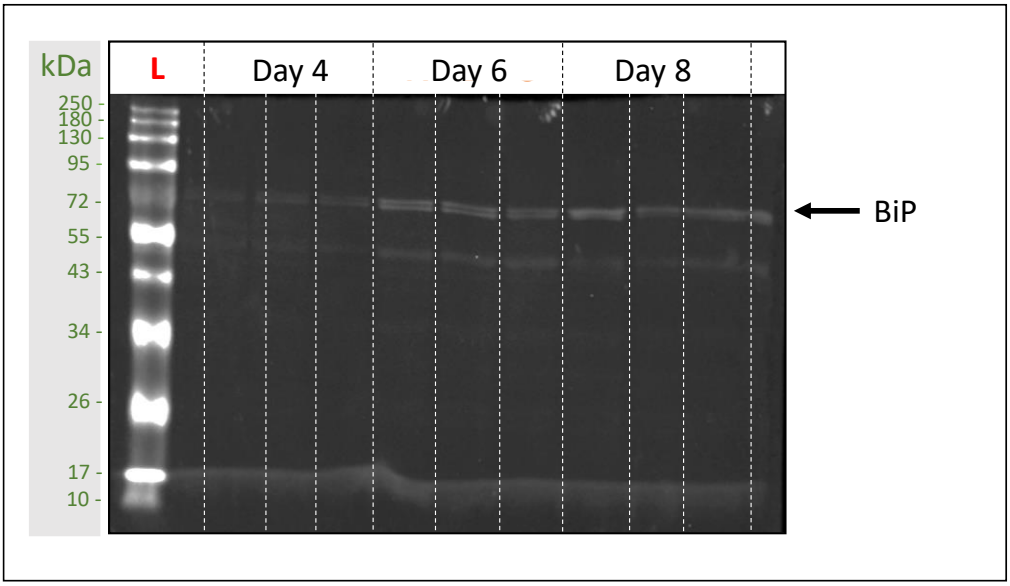

Figure 3.17. *Image of the western blot analysis of batch culture (BC) for the unfolded protein response (UPR) -related gene BiP in the CHO-S IgG1 cell line.*

The complete method is as described in Section 2.5, with the western blot analysis being detailed in Section 2.5.3. The image was taken using the ChemiDoc MP Imaging System (Bio-Rad).

The lane containing the colour pre-stained protein standard 10-250kDA (NEB) is marked with a red 'L' and the green numbering to the left-hand side of the image is the molecular weights denoted by the standard. The remaining lanes of the gel contain the samples. The lanes labelled 'Day 4' contain day 4 BC sample replicates A/B/C. The lanes labelled 'Day 6' contain day 6 BC sample replicates A/B/C. The lanes labelled 'Day 8' contain day 8 BC sample replicates A/B/C.

Figure 3.17 is showing the results of the western blot analysis for the expression of BiP in the BC samples days 4, 6 and 8. The ladder that was missing from Figure 3.16 is clearly visible in Figure 3.17, although the bands are more drawn out with the gel in comparison to the ladders used to mark the RT-PCR results seen in Section 3.4. Despite this, the ladder can be used to determine a band for each of the samples at 78kDa. This is in keeping with other studies such as the paper looking at the Endogenous BiP reporter system for simultaneous identification of ER stress and antibody production in CHO cells by Kyeong and Lee (2022), where the western

blot for BiP produced a band at 78kDa. The constant drawn out band at the bottom of the image is the tracker dye front can be disregarded as a result in the image.

As seen in Figure 3.16, the signals from the day 4 results are much less intense than seen in days 6 and 8. This is also the case for Figure 3.17, which is to be expected as if there is less of the housekeeping ERK2 protein in the sample it would suggest that there would be less of other proteins in the sample in total. Overall, the bands produced for BiP in Figure 3.17 are much less intense than seen for the bands produced for ERK2 seen in Figure 3.16. As ERK2 is the housekeeping gene used to produce an intense signal for comparison, it was expected for the signal produced by BiP to be less intense, but the overall band is weaker than anticipated. The primary and secondary antibodies used in this experiment are detailed in Section 2.1.4.

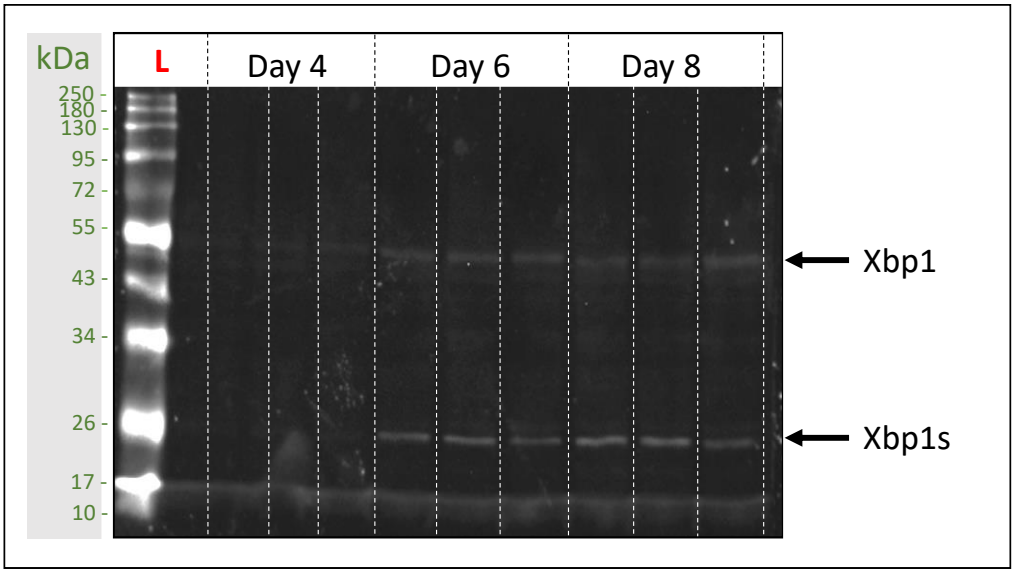

Figure 3.18. *Image of the western blot analysis of batch culture (BC) for the unfolded protein response (UPR) -related gene Xbp1 in the CHO-S IgG1 cell line.*

The complete method is as described in Section 2.5, with the western blot analysis being detailed in Section 2.5.3. The image was taken using the ChemiDoc MP Imaging System (Bio-Rad).

The lane containing the colour pre-stained protein standard 10-250kDA (NEB) is marked with a red 'L' and the green numbering to the left-hand side of the image is the molecular weights denoted by the standard. The remaining lanes of the gel contain the samples. The lanes labelled 'Day 4' contain day 4 BC sample replicates A/B/C. The lanes labelled 'Day 6' contain day 6 BC sample replicates A/B/C. The lanes labelled 'Day 8' contain day 8 BC sample replicates A/B/C.

Figure 3.18 depicts the image taken of the western blot of Xbp1 for days 4, 6 and 8 of BC. As seen in Figure 3.17, the dye front is slightly visible at the bottom of the image but can be disregarded. In Figure 3.18, two faint sets of bands can be seen across the samples at 50 kDa and 28kDa using the seen on the left-hand side of the image ladder as a reference. A paper by Ku *et al.*, (2010) investigating the regulation of Xbp1 signalling during transient and stable recombinant protein production in CHO cells also shows bands at these intervals. The paper states that the 50kDa band is the unspliced Xbp1 and the band (Ku *et al.*, 2010). The band at

28kDa could be the spliced Xbp1 (Xbp1s) that Ku et al., states is visible at 33kDa, which is close to the 28kDa but inconclusive. As with both Figures 3.16 and 3.17, in 3.18 the day 4 samples produce little to no reading after the western blot analysis. As with all the blots conducted in this set of experiments, the antibodies used are detailed in Section 2.1.4.

The intention of conducting the western blot on the BC samples for ERK2, BiP and Xbp1 was to see if there was a difference in the amount of protein between the days in which samples were taken throughout culture. Western blot data is semi-quantitative as the data provides a relative comparison of protein levels rather than an absolute quantity (Mahmood and Yang, 2012). Western blot data is only semi-quantitative rather than quantitative, as the signal detected is not linear across the concentration range of samples, as well as the fact that there is variation in loading and transfer rates between samples in separate blots (Mahmood and Yang, 2012). However, due to a lack of definition within the bands, the bands could not be subjected scanning and subsequent semi-quantification. As the same samples were used for all proteins, the difference in day 4 samples are likely due to less protein being present in the samples overall rather than a specific difference between BiP and ERK2 expression between days 4 and 6. This is because the same difference is seen in the ERK2 western in Figure 3.16, which should have a consistently high expression throughout BC.

3.5.2 Fed-batch

After the samples from BC were used in the comparison of UPR protein expression, FBC samples were used in the same analysis. Like the BC analysis, the genes examined were BiP, Xbp1 and the housekeeping gene ERK2.

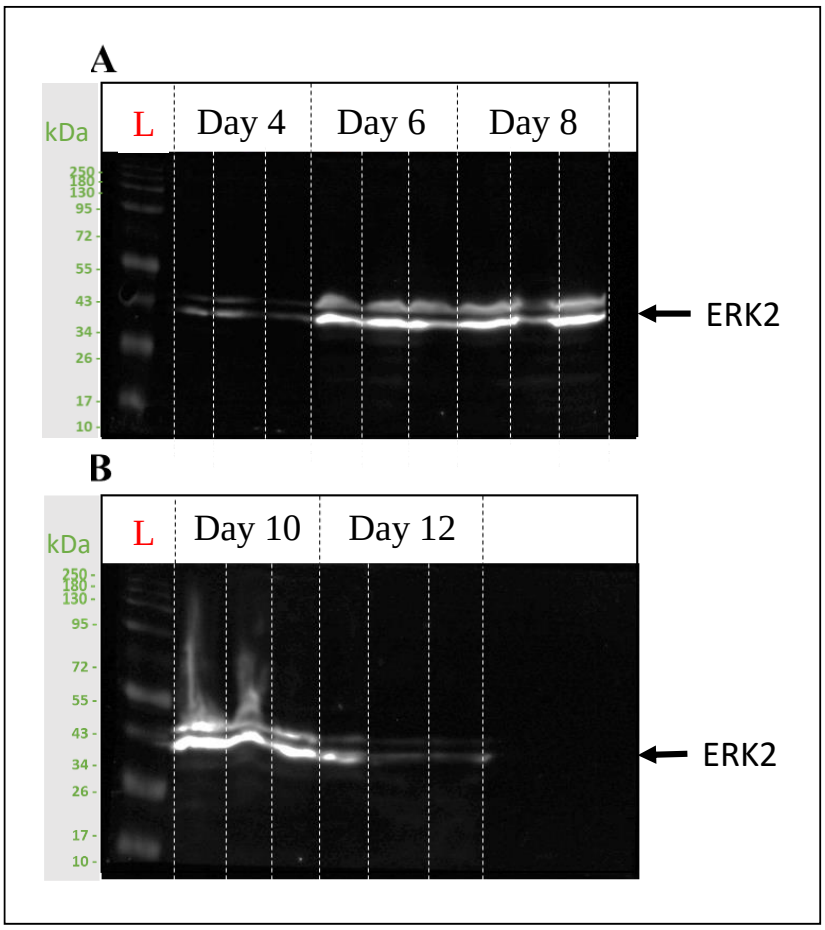

Figure 3.19. *Image of the western blot analysis of fed-batch culture (FBC) for the unfolded protein response (UPR) -related gene ERK2 in the CHO-S IgG1 cell line.*

The complete method is as described in Section 2.5, with the western blot analysis being detailed in Section 2.5.3. The image was taken using the ChemiDoc MP Imaging System (Bio-Rad).

The lane containing the colour pre-stained protein standard 10-250kDA (NEB) is marked with a red 'L' and the green numbering to the left-hand side of the image is the molecular weights denoted by the standard. The remaining lanes of the gel contain the samples. The lanes labelled 'Day 4' contain day 4 FBC sample replicates A/B/C. The lanes labelled 'Day 6' contain day 6 FBC sample replicates A/B/C. The lanes labelled 'Day 8' contain day 8 FBC sample replicates A/B/C. The lanes labelled 'Day 10' contain day 10 FBC sample replicates A/B/C. The lanes labelled 'Day 12' contain day 12 FBC sample replicates A/B/C.

Figure 3.19 contains images taken from western blot analysis for ERK2 for FBC samples taken from days 4, 6, 8, 10 and 12 of culture. As can be seen in image A, the day 4 samples

appear to produce and incredibly faint reading. This was also seen in day 4 of Figures 3.16, 3.17 and 3.18 for the BC western blot analysis in Section 3.5.1. The method described in 2.5.1 detailing the protein extraction of the intracellular proteins.

The signal intensity for ERK2 at 42kDa is strong in both BC and FBC of IgG1 CHO-S cells, see Figure 3.16. Although, samples in Figure 3.19 are spread down the gel, rather than producing the definitive bands seen in BC of the same ERK2 protein (Figure 3.16). This makes the image difficult to analyse using software such as Image J. In the image a shadow band is visible behind the band at 44 kDa.

In image B of Figure 3.19, the day 12 sample bands are notably weaker than the bands seen for day 10 in image B and days 6 and 8 in image A. As shown in Figure 3.1, at this timepoint in

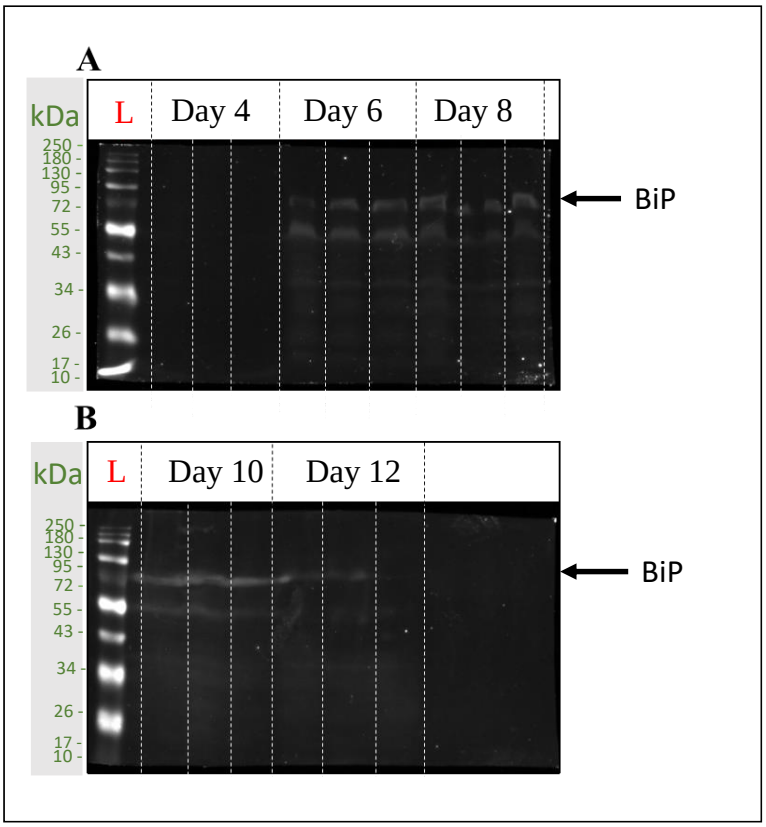

Figure 3.20. *Image of the western blot analysis of fed-batch culture (FBC) for the unfolded protein response (UPR) -related gene BiP in the CHO-S IgG1 cell line.*

The complete method is as described in Section 2.5, with the western blot analysis being detailed in Section 2.5.3. The image was taken using the ChemiDoc MP Imaging System (Bio-Rad).

The lane containing the colour pre-stained protein standard 10-250kDA (NEB) is marked with a red 'L' and the green numbering to the left-hand side of the image is the molecular weights denoted by the standard. The remaining lanes of the gel contain the samples. The lanes labelled 'Day 4' contain day 4 FBC sample replicates A/B/C. The lanes labelled 'Day 6' contain day 6 FBC sample replicates A/B/C. The lanes labelled 'Day 8' contain day 8 FBC sample replicates A/B/C. The lanes labelled 'Day 10' contain day 10 FBC sample replicates A/B/C. The lanes labelled 'Day 12' contain day 12 FBC sample replicates A/B/C.

FBC, the VCD and percentage viability of the culture are both zero, so there are no viable cells to make an abstract from.

Figure 3.20 shows the western blot analysis results for BiP in samples taken from FBC. Like Figure 3.19, of analysis of ERK2 in samples taken from FBC, there are weak bands seen in in the pink lanes of image B containing the day 12 samples and no bands seen in the blue lanes containing the day 4 samples.

Unlike Figure 3.19, the bands for samples from days 6 and 8 in Figure 3.20 are spread across the gel, instead of presenting definitive bands. As expected as seen in previous publications, the strongest band can be seen at 78kDa as also seen in Figure 3.17 for the analysis of BiP in BC samples Aside from this band other faint bands can be seen across the gel for the day 6 and 8 samples.

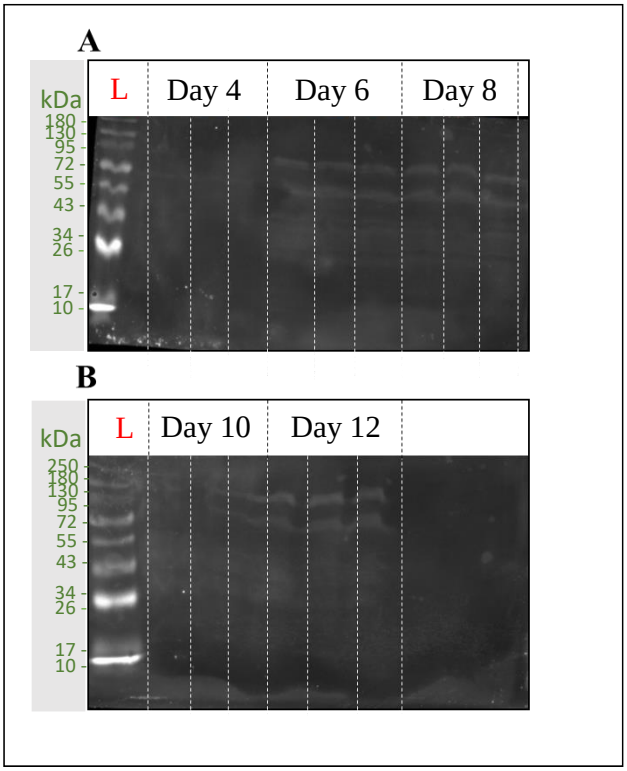

Figure 3.21. *Image of the western blot analysis of fed-batch culture (FBC) for the unfolded protein response (UPR) -related gene Xbp1 in the CHO-S IgG1 cell line.*

The complete method is as described in Section 2.5, with the western blot analysis being detailed in Section 2.5.3. The image was taken using the ChemiDoc MP Imaging System (Bio-Rad).

The lane containing the colour pre-stained protein standard 10-250kDA (NEB) is marked with a red 'L' and the green numbering to the left-hand side of the image is the molecular weights denoted by the standard. The remaining lanes of the gel contain the samples. The lanes labelled 'Day 4' contain day 4 FBC sample replicates A/B/C. The lanes labelled 'Day 6' contain day 6 FBC sample replicates A/B/C. The lanes labelled 'Day 8' contain day 8 FBC sample replicates A/B/C. The lanes labelled 'Day 10' contain day 10 FBC sample replicates A/B/C. The lanes labelled 'Day 12' contain day 12 FBC sample replicates A/B/C.

Figure 3.21 shows the image taken from the western blot analysis of FBC samples for the protein Xbp1. Much like Figure 3.20, there is not a clear definitive band for the Xbp1 protein. As seen in Figure 3.18 for the quantification of Xbp1, a band should be visible at 50kDa. Although some evidence of the blot occurring can be seen in the slight presence of bands, particularly in the lanes of days 6, 8 and 12, these bands are extremely faint and are spread across the gel, instead of presenting definitive bands.

Chapter 4: Discussion

As previously conferred in Chapter 1, the development of products in the biopharmaceutical industry is largely dependent on the use of expression systems, with CHO cell lines being used to produce 89% of the individual mAbs expressed by mammalian systems (Walsh & Walsh, 2022). Since the advent of recombinant technology in the 1980s, in order to increase the yield, product quality and scale of biopharmaceutical production in expression systems, research into culture process and cell line engineering has been conducted. As previously stated in Section 1.9, the aim of this report is to contribute to a better understanding of the molecular biology of the recombinant CHO-S IgG1 cell line in order to generate information that could potentially contribute to the improvement of the manufacturing capacity of the biopharmaceutical industry. In order to meet the overall project aim, four objectives were proposed as summarised in Figure 4.1. These were: (1) to study the growth and IgG1 production of the recombinant CHO-S cell line in BC and FBC, to assess the effect of the addition of feed to these parameters, (2) to develop methods to assess the expression of a set of UPR-relevant proteins, using RT-PCR, qRT-PCR and Western blotting techniques, (3) to examine the expression of these UPR-relevant proteins in BC and FBC and (4) to assess the relationship between the expression of the UPR-relevant proteins, the specific productivity of the cell line and the overall IgG1 yield in response to BC and FBC conditions. Here, the extent to which these objectives were accomplished and the how the overall aim was affected will be examined.

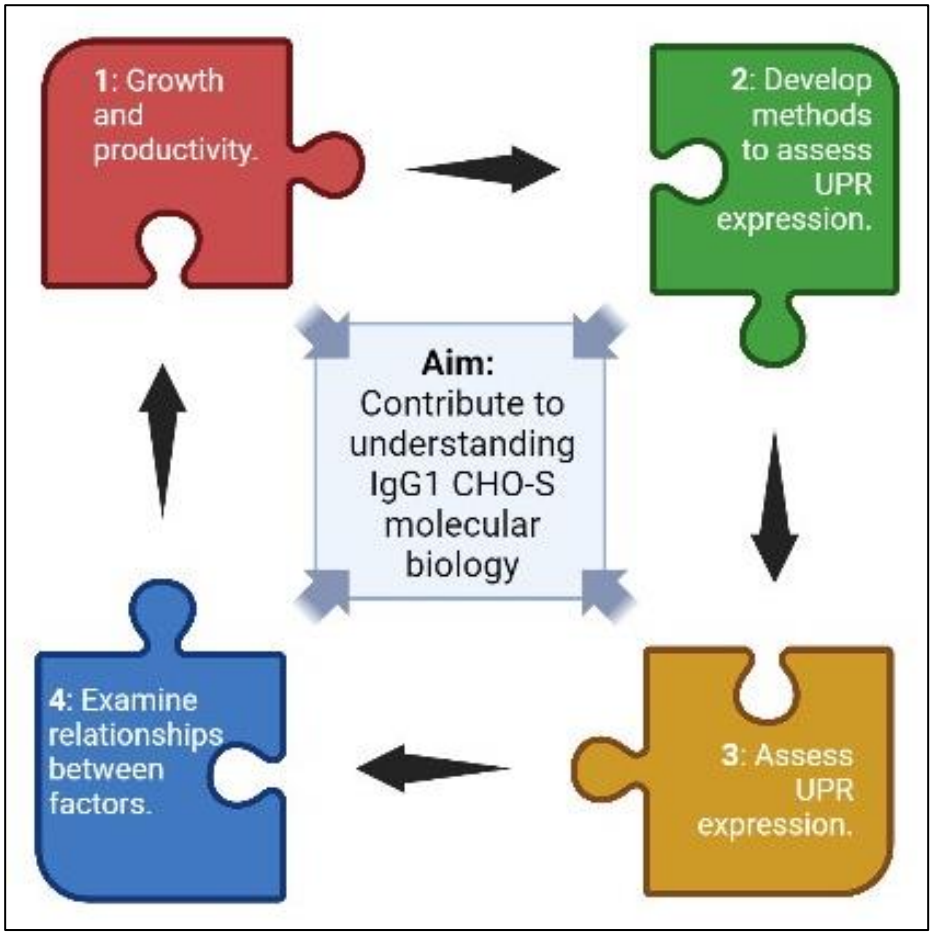

Figure 4.1. *A Schematic overview of the overall report.*

The aims and overall objectives are condensed to represent how they fit together within the report. Created with BioRender.com.

4.1 Cell line growth and productivity

Studying the growth and IgG1 production of the recombinant CHO-S cell line in BC is important for understanding the archetypal phenotype of the cell line. Incidentally, growth and productivity are key aspects of an expression system. Using the BC growth and productivity data as standard, the effect of the addition of feed on these parameters can then be assessed by conducting a FBC for comparison. Knowing the impact of the feeding regime on cell growth and productivity helps understand the molecular biology of the expression system, as the cell line is exposed to and affected by the supplementation, denoting what is required by cellular

metabolism and what is detrimental. Ensuring the cell line is exposed to the correct balance of nutrients can be used to optimise growth and productivity.

As described in Section 3.1, BC and FBC of the IgG1 CHO-S cell line were successfully conducted so that growth patterns and characteristics could be established. As shown in Figure 3.1, in comparison to the results of the BC, the addition of feed in this manner did result in the extension of culture period by 48 hours, and increased peak cell density by almost two-fold. The VCD of a culture is an important parameter for the use as an expression system, as the more living cells there are in the culture the more there are to work with. As discussed in Section 3.1.1, the growth profile of this IgG1 CHO-S cell line of the BC conducted in this report is similar to that of the published data of the same cell line in BC of Torres and Dickson (2022), which supports the credibility of the results. The incidence that cultures were conducted in triplicate increased the reliability of the results by accounting towards experimental variability. Furthermore, this increase in peak cell density and culture duration as a result of the addition of feed has been seen in the surrounding literature, including that of Braasch *et al.*, (2021), which saw a just over two-fold increase between control BC and FBC as a result of feed addition. The differences in the growth profile of the two cultures resulted in a significant difference in specific growth rate and cell doubling time between BC and FBC in both the 48-96 and 96-144 culture period intervals. This was most likely a result of the difference caused by the extension in culture duration.

The productivity of the CHO-S cell line in the same BC and FBC was examined, and the outcome assessed in Section 3.2. In tandem with cell growth, the productivity of a cell line is the foundation of its function as an expression system. As shown in Figures 3.4 and 3.5, the difference in IgG1 titres between BC and FBC was significant, with FBC resulting in a much higher antibody titre. This is conducive with the surrounding literature, such as Reinhart *et al.*,

(2015) that provides supporting evidence that the addition of complimentary feed to the culture of CHO expression systems increased the overall antibody titre, which, as previously conferred in Section 1.4.1, is a fundamental reason for FBC being the most used cultivation method for CHO cell lines to produce mAbs in industrial practice (Schellenberg *et al.*, 2022). As shown in Figure 3.6, although the specific productivity of cells in FBC was slightly greater than in BC, the difference was not significant. The difference in titre resulting in a far greater antibody yield is therefore a result of the increase in the VCD, prolonged cell survival and greater percentage viability in FBC than by direct impact on the ability of individual cells to produce recombinant proteins. While there are instances of the specific productivity being significantly greater in FBC compared to BC, such as the study conducted by Sellick *et al.*, (2015), typically the addition of feed increases overall antibody titre by increasing the overall VCD rather than impacting the specific productivity of the cell line, supporting the results of this study as previously discussed in Sections 1.4.2 and 3.2.2 (Reinhart *et al.*, 2019; Braasch *et al.*, 2021). Further investigation could be conducted into factors that affect specific productivity other than the survival and longevity of CHO cell lines, although a proposed explanation for occurrence of an increased is some FBC and not others is the use of inadequate basal media for the cell line.

Overall, examination of the growth and productivity of the IgG1 CHO-S cell line under BC and FBC went a long way towards satisfying the first objective of the study, and produced results that were supported by the findings of the surrounding literature. However, there are further experiments that would add to the overall objective of understanding the molecular biology of the IgG1 CHO-S cell line, such as the investigation into the difference in the concentration of metabolites between the culture conditions. Although the VCD, the overall antibody titre and the specific productivity of the cell lines are important parameters and can

be used as a key performance indicator of the cell culture, metabolic analysis is important for assessing how factors such as the addition of feed impact cell health.

4.1.1 Metabolite analysis

As a result, in order further the objective and the overall aim of the project, enzymatic assays were conducted on the metabolites glucose, lactate and ammonia. As discussed in Section 1.4 and referred to in Section 3.3, metabolites have roles in various cellular functions and the study of them, metabolomics, is closely connected to cell phenotype (Xu *et al.*, 2023). These metabolites were chosen based on their impact on cellular metabolism in culture. Glucose is the primary carbon source in cellular metabolism. As seen in Figure 3.7, the glucose decreases throughout culture in both BC and FBC, at roughly the same rate, but is depleted 48 hours earlier in BC. Lactate is produced as glucose is metabolised but is also a secondary carbon source so is consumed later in culture. As can be seen in Figure 3.8, lactate is consumed in FBC earlier and to a greater extent than BC. This may appear unexpected as glucose supplementation in the form of the feed addition on alternate days from Day 2 till the end of culture means that glucose is available as a carbon source throughout culture. However, other studies have seen a similar lactate switch with the earlier consumption of lactate in FBC than in BC, as feed addition was interpreted to promote greater efficiency within the TCA cycle (Sellick *et al.*, 2011). Figure 3.8 shows the build-up of ammonia within BC and FBC. Ammonia is a toxic by-product of cellular metabolism and can be detrimental to cell growth and viability. As discussed in Section 1.4.2, ammonia concentrations above 5mM have been shown to negatively impact cell proliferation (Yang and Butler, 2000; Xu *et al.*, 2023). The ammonia concentrations in both BC and FBC at the start of culture were ~6mM and ~7mM respectively and continued to rise steadily throughout the duration of both cultures, with no obvious impact on cell growth or productivity.

The use of metabolomics, similar to that of Sellick *et al.*, (2015), where GC-MS analysis is used to identify difference in metabolites in the media could also be used to optimise the medium the expression system is seeded in and the feeding regime to analyse what is being consumed or produced throughput the duration of the culture and tailor these features accordingly. As relayed in Section 3.3.2, a shortcoming of this report is a lack of conclusive results generated from methodologies in Section 2.4.2 that arose due to the time limitations of the project. Future work would include the generation of useable data from the methods described, although the practice of developing such methods and the undertaking of trial runs provides an outline for work that would contribute to this objective and the overall aim.

Aside from directly comparing the growth and productivity data in BC and FBC conducted in Complete Medium (Section 2.2.1), the basal medium was CD CHO. As previously mentioned in Section 1.4.2, studies such as those of Pan *et al* (2017) have looked at the differing effects of media and feed combinations on the growth and productivity of CHO cell lines. This report compliments those studies by experimenting with a different medium/cell line combination. As detailed in Section 1.2.1.1, the IgG1 CHO-S cell line, was developed in a study conducted by Torres and Dickson, (2021), however, the comparison of BC and FBC in this cell line have not been the key focus of published papers. The objective to study the growth and productivity of BC and FBC could be extended by examining these parameters in different media and feed combinations, which would contribute to the overall aim of understanding the molecular biology of the IgG1 CHO-S cell line and provide information how to optimise these parameters.

As industry focus is placed on product yield and quality, more research could be conducted to identify feed regimes that not only extend culture duration and overall cell density, but also optimise cell specific productivity for increased antibody production without compromising product quality. Pan *et al* (2017), identified feeding regimes in other cell lines that have extended culture period and increased peak cell density in other CHO lines, to greater effect

than the feeding regime used in this report. Experimenting with timing intervals and feed composition in the conduct of multiple further FBC to compare the effect on growth and productivity to see what regime is must beneficial would be one method in which the process could be optimised. This process could be compounded by the use of metabolomics that could be used to identify specific targets that are differentially expressed in fed and non-fed conditions.

To further contribute to the overall aim, this initial objective could be extended to include the study of growth and productivity of this cell line in perfusion culture. As described in Section 1.4.1, alongside FBC perfusion culture is a key culture technique in the manufacture of biopharmaceuticals in industry (Bielser *et al.*, 2018). Therefore, conducting a perfusion culture of the IgG1 CHO-S cell line to study the growth and productivity would further contribute to the aim of understanding the molecular biology in a capacity that would be applicable to industry development.

4.2 Development of methods to assess UPR-related gene expression

The second objective of this report was to develop methods to assess the expression of a set of UPR-relevant proteins, using RT-PCR, qRT-PCR and western-blotting techniques. This objective is conducive to the overall aim of generating information that provides a better understanding of the molecular biology of the recombinant CHO-S IgG1 cell line to potentially contribute to the improvement of the manufacture capacity, as methodologies are repeatable and can be used experimentally to produce reliable results. As previously described in Section 1.7.2, the UPR-relevant target genes chosen for analysis in this report were BiP, GRP94, Xbp1s and CHOP. As stated, the monitoring of the changes in expression of these target genes was decided upon as the surrounding literature (Section 1.8) has identified these proteins to have key roles within the UPR including studies specifically regarding CHO cell lines, most notably Torres *et al.*, (2021) which identified them as being significantly upregulated in

response to treatment with the pharmacological agent tunicamycin, in the same CHO-S IgG1 cell line. As described in Section 1.6, the UPR has been identified as a bottleneck in the protein secretion by expression system. A key success in this objective was the design of effective primers (Table 2.1) for these target genes. As stated in Section 2.5, RT-PCR and qRT-PCR was conducted. In order to conduct these experiments, primers were designed as described in ection 2.1.3. These primers were used for RT-PCR of each of the target UPR-related proteins, BiP, GRP94, Xbp1s and CHOP throughout the duration of BC and FBC, as evidenced in Section 3.4.1. The use of these primers produced clear and interpretable gels, that provided evidence that the cDNA in the samples were of high enough quality for use in qRT-PCR, in which the difference in expression of the samples could be analysed. As described in Section 1.8.2, work conducted by Torres et al. (2021), on the effect of temperature on the expression of UPR-/ERAD- related genes and the impact on recombinant protein production in a CHO cell line, identified that each of the four genes were significantly upregulated after treatment with tunicamycin, a UPR-inducing pharmacological agent. Tunicamycin treatment was used as a control (Section 2.2.5.1) for UPR activation following the results of this study and cDNA generated from these samples resulted in positive expression using primers for the target genes. Therefore, the expression of these genes throughout both culture durations is indicative of the UPR being triggered by the expression of the IgG1 recombinant protein.

4.3 Assessment of UPR-related gene expression

The third objective of this report was to examine the expression of these UPR-relevant proteins in BC and FBC. This objective built upon the methodologies developed in the previous objective, and contributes to the overall aim directly by determining the difference in the levels of expression of the UPR-related proteins and assesses whether expression is affected by the timing of cellular culture and/or by the presence of feed. The UPR is indicative of ER stress and is interlinked with cellular processes such as autophagy and apoptosis, that result in cell

death and/or degradation that subsequently may limit recombinant protein production by the expression system, as detailed in Section 1.6. Knowing the impact of culture duration, in the presence and absence of feed, enables a rationalisation towards the engineering of cells and their processes. RT-PCR analysis provided qualitative evidence that enabled the identification of mRNA specific to the genes that were expressed and detectable, as shown in Section 3.4.1. However, the expression of the GOIs in RT-PCR was not quantitative, therefore qRT-PCR was conducted. The qRT-PCR (Section 3.4.2) for BC using day 4 expression levels as a baseline for comparison to days 6 and 8 saw no significant difference in expression across the target genes, although the difference was greatest between the two days in BiP and CHOP. This was also seen in FBC, where expression levels at day 4 were again used as a baseline for comparison and then the fold change between days 6, 8, 10 and 11 was calculated. In this instance, CHOP mRNA showed a significant difference in expression between the days, while the others did nit not, although there was indication of difference in BiP expression. The fold change in expression levels was then directly compared between BC and FBC for days 4, 6 and 8, using BC levels as the baseline for foldchange comparison. The most notable difference was that of the significance of the difference in Xbp1s. As previously referred to in Sections 1.4.3, 1.8.3 and 3.4, an earlier study explored differences in the expression of proteins in BC and FBC of a CHO cell line was conducted by Wong *et al.*, (2006) investigated proteins involved in apoptotic pathways. As a different set of pathways were being examined, the focus of the study was different to this report, however as previously described in sections 1.5 and 1.7, the UPR is implicated in certain aspects of the apoptotic pathway. The CHO IFN-γ cell line was also had a low specific productivity similar to that of this report, and BiP was shown not to be differentially expressed and proteins involved in the activation of CHOP were shown to be downregulated (Wong *et al.*, 2006).

Following RT-PCR and qRT-PCR, western-blot analysis was then conducted for two of the respective genes, BiP and Xbp1. A more comprehensive study would have included GRP94 and CHOP, so that all four of the genes of interest were included in the analysis, but due to the time constraints of the project, only BiP and Xbp1 were analysed. The choice of BiP and Xbp1 was made based on their roles in the UPR and from the surrounding literature (Torres *et al.*, 2021; Torres and Dickson, 2022). However, from the results of the qPCR, CHOP was the gene that produced significant differences in expression between timepoints throughout culture duration, indicating it may be of greatest interest to analyse this in comparison to the other genes. As previously discussed, CHOP is a downstream target of the transcription factor Xbp1s in the UPR. Aside from this, the results attained from the western blot analysis of BiP and Xbp1 did not produce clear data sets that categorically stated whether there was any difference in expression levels. An advantage of western blot analysis, is that typically the light intensity of the band produced as signal the of gene expression can be measured so that the expression level can be quantified using computer software programmes such as ImageJ. In the absence of clear definitive bands this was not possible in this report. A positive from the analysis though is that a signal was produced, meaning the antibodies used and the method devised did prove to be viable. As mentioned in Section 1.7.2, time constraints targets limited the number of UPR-related genes that could be investigated. Had there been more time available in the projects, targets in other arms of the UPR pathway would be considered, including pro-survival targets in the PERK signalling pathways.

4.4 Examination of relationships between factors

The fourth and final objective of this report was to assess the relationship between the expression of the UPR-relevant proteins, the specific productivity of the cell line and the overall IgG1 yield in response to BC and FBC conditions. Compared to the other objectives, it is difficult to give a conclusive verdict on whether this objective was met. It is clear from the first

objective that the addition of feed impacted on growth and productivity profile of the cell line, but the results from the third objective to examine the expression of UPR-relevant proteins indicated there was little change between BC and FBC, with any discrepancies between expression in the two cultures being a result of an increase in the duration of FBC. It is not possible to deduce a relationship between these factors specifically as there are many other contributing factors involved. As previously discussed, in some other studies such as that of Sellick *et al.*, (2015), the addition of feed has been shown to increase the specific productivity of cells in culture (Alhuthali *et al.*, 2021). This increase in specific productivity could have potentially increased the load on the protein-folding machinery, leading to ER stress and subsequent activation of the UPR. Therefore, the logic of this study was to investigate whether a progressive induction of ER stress and the specific productivity increases effected the expression of proteins involved in various stages of the UPR. This would complement the data that influenced the choice of the target genes BiP, GRP94, Xbp1 and CHOP based on work conducted by Torres *et al.* (2021), the same IgG1 CHO-S cell line, in which the UPR is induced by treatment with the pharmacological agent tunicamycin. However, like other studies on CHO cell lines such as that of Reinhart *et al.*, (2019) and Braasch *et al.*, (2021), in this report there was not a significant difference in the specific productivity between BC and FBC. In the absence of change in specific productivity between cultures, from the data in this report it is not possible to say whether the lack of change in UPR-related expression is a result of the lack of change in the specific productivity or because expression is not affected. The relationship between specific productivity and overall yield was not a factor in this report. However, in the study conducted by Sellick *et al.*, (2015) in which there was a significant difference between the specific productivity in BC and FBC, it is stated that although the increased specific productivity supported greater accumulation, the prolonged growth/stationary phase that resulted from feed addition was a ‘major facet’ to increased product accumulation.

From this, a clear attempt has been made to contribute to a better understanding of the molecular biology of the recombinant CHO-S IgG1 cell line in order to generate information that could potentially contribute to the improvement of the manufacturing capacity of the biopharmaceutical industry, which was the aim of this project. The growth and productivity of the IgG1 CHO-S line was studied, methods for assessing the expression of UPR-related proteins were developed, which was followed by a limited assessment of the expression of these target proteins in BC and FBC, the relationship between the expression of the UPR-relevant proteins, the specific productivity of the cell line and the overall IgG1 yield was considered but due to inadequate data no conclusions were drawn. Shortcomings of the report included the lack of interpretable data in the western-blot analysis and the lack of a clear relationship between the specific productivity of the cell line and the expression of the UPR-relevant proteins that was driven by the absence of a significant change in the specific productivity between BC and FBC.

4.5 Future work

The overall aim of the project is to better understand the molecular biology of a specific CHO expression system with the intention that this data could be used to increase the manufacture capacity of the cell line. Although the investigations have been specific to the IgG1 CHO-S cell line, it would be of interest to evaluate whether these methods are generally applicable to different recombinant CHO cell lines. The heterogeneity of CHO as an expression system has resulted in multiple sublines, with differing specific productivity capabilities. This would be achieved by conducting the same experiments, such as BC and FBC, metabolite analysis, PCR and western-blot analysis in multiple cell lines and comparing the results. This approach would be similar to that see in studies such as Reinhart *et al.*, (2015) and Pan *et al.*, (2017) in which multiple media and feed combinations were used to assess their impact on CHO cell line antibody production. It would also be of interest to see if the same experiments had different

effects on the specific productivity in different cell lines. This could relate to further work using the same cell line that has been transfected with alternative proteins, particularly those with differing difficultly levels of expression. As touched on in Section 1.1.2.1, the IgG1 antibody is relatively easy to express. However, there are difficult to express antibodies such as those produced by cell lines used by Torres *et al.*, (2021). Engineering the CHO-S line to become recombinant for a difficult to express protein such as hEPO-Fc, would make for an interesting comparison to see if the UPR-related proteins are differentially expressed, as this would suggest that the difficulty of expression level impacts ER stress (Torres *et al.*, 2021). Another aspect to consider is that there are many proteins involved in the UPR pathway. As previously mentioned, it would be of interest to look at proteins involved in other arms of the signalling pathways, such as ATF4, or pro-survival proteins, or those more closely related to the autophagy and apoptosis pathways, such as BCL-2. Following a similar sort of logic, the cell line could be engineered to overexpress these UPR-related proteins and examined to assess the effect this has on cell growth and productivity, to optimise the cell as an expression system (Torres and Dickson, 2021). Alternatively, the cell line could be engineered to express proteins involved in the secretory pathways of cells that have a greater secretory ability, such as the transcription factor pERp1 from human plasma cells (Torres and Dickson, 2021). This would be a new line of experiments but would contribute to the overall aim of this project.

4.6 Concluding remarks

In conclusion work has been conducted to contribute to the understanding of CHO as an expression system using a novel combination of medium, cell line, feed, and analysis of expression targets. Potential targets for both process engineering and cell line engineering have been highlighted by investigating the impact of feed addition to cell culture and examining UPR-related protein expression. BC and FBC of the cell line generated results that were comparable to the surrounding literature and the design of primers for RT-PCR and qRT-PCR

has shown an outcome that directs future work. The identification of antibodies that have produced signals for ERK2, BiP and Xbp1 in western-blot analysis maybe useful for the conduction of future blots. It is not possible to draw a conclusive statement regarding the relationship between the specific productivity, the UPR expression and the antibody titre, but it has been highlighted as a key area of interest which may assist in future work.

Overall, this report has gone some way into generating data as part of a contribution to a better understanding of the molecular biology of the recombinant CHO-S IgG1 cell line, that could potentially contribute to the improvement of the manufacture capacity of the biopharmaceutical industry.

Bibliography

Alhuthali, S. et al. (2021) Osmolality Effects on CHO Cell Growth, Cell Volume, Antibody Productivity and Glycosylation. International Journal of Molecular Sciences, 22(7), 3290.

Almanza, A. et al. (2019) Endoplasmic reticulum stress signalling – from basic mechanisms to clinical applications. The FEBS Journal, 286(2), 241–278.

al-Rubeai, M. et al. (1990) Electron microscopy of hybridoma cells with special regard to monoclonal antibody production. Cytotechnology, 4(1), 13–28.

Andersen, D.C. & Krummen, L. (2002) Recombinant protein expression for therapeutic applications. *Current Opinion in Biotechnology*, 13(2), 117–123.

Balchin, D. et al. (2016) In vivo aspects of protein folding and quality control. *Science*, 353(6294), aac4354. American Association for the Advancement of Science.

Becker, E. et al. (2008) An XBP-1 dependent bottle-neck in production of IgG subtype antibodies in chemically defined serum-free Chinese hamster ovary (CHO) fed-batch processes. Journal of Biotechnology, 135(2), 217–223.

Bielser, J.-M. et al. (2018) Perfusion mammalian cell culture for recombinant protein manufacturing – A critical review. *Biotechnology Advances*, 36(4), 1328–1340.

Braasch, K. et al. (2021) Autophagy-inducing peptide increases CHO cell monoclonal antibody production in batch and fed-batch cultures. Biotechnology and Bioengineering, 118(5), 1876–1883.

Buscà, R. et al. (2018) ERK1 and ERK2. In: Choi, S. (ed.) *Encyclopedia of Signaling Molecules*. [Online]. Cham: Springer International Publishing. Available at: doi:10.1007/978-3-319-67199-4_470 [Accessed: 10 April 2023].

Bustamante-Córdova, L. et al. (2018) Recombinant Antibodies in Veterinary Medicine: An Update. *Frontiers in Veterinary Science*, 5, 175.

Calmels, C. et al. (2019) Application of a genome-scale model in tandem with enzyme assays for identification of metabolic signatures of high and low CHO cell producers. *Metabolic Engineering Communications*, 9, e00097.

Chakrabarti, A. et al. (2011) A review of the mammalian unfolded protein response. Biotechnology and Bioengineering, 108(12), 2777–2793.

Chen, Q. et al. (2018) The independence of and associations among apoptosis, autophagy, and necrosis. *Signal Transduction and Targeted Therapy*, 3(1), 1–11. Nature Publishing Group.

Chou, K.-C. & Elrod, D.W. (1999) Prediction of membrane protein types and subcellular locations. Proteins: Structure, Function, and Bioinformatics, 34(1), 137–153.

Chusainow, J. et al. (2009) A study of monoclonal antibody-producing CHO cell lines: What makes a stable high producer? *Biotechnology and Bioengineering*, 102(4), 1182–1196.

Coats, M.T. et al. (2020) mRNA Transfection into CHO-Cells Reveals Production Bottlenecks. Biotechnology Journal, 15(2), 1900198.

Covic, A. & Kuhlmann, M.K. (2007) Biosimilars: recent developments. *International Urology and Nephrology*, 39(1), 261–266.

Cui, J. et al. (2021) Regulated cell death: discovery, features and implications for neurodegenerative diseases. Cell Communication and Signaling, 19(1), 120.

Dhara, V.G. et al. (2018) Recombinant Antibody Production in CHO and NS0 Cells: Differences and Similarities. *BioDrugs*, 32(6), 571–584.

Dumont, J. et al. (2016) Human cell lines for biopharmaceutical manufacturing: history, status, and future perspectives. Critical Reviews in Biotechnology, 36(6), 1110–1122.

Ecker, D.M. et al. (2015) The therapeutic monoclonal antibody market. *mAbs*, 7(1), 9–14. Taylor & Francis.

Eletto, D. et al. (2010) GRP94 in ER quality control and stress responses. Seminars in Cell & Developmental Biology, 21(5), 479–485.

Erickson, L.E. (2009) Bioreactors. In: Schaechter, M. (ed.) *Encyclopedia of Microbiology (Third Edition)*. [Online]. Oxford: Academic Press. Available at: doi:10.1016/B978-012373944-5.00136-X [Accessed: 9 June 2023].

Estes, S. & Melville, M. (2014) Mammalian Cell Line Developments in Speed and Efficiency. In: Zhou, W. & Kantardjieff, A. Mammalian Cell Cultures for Biologics Manufacturing Advances in Biochemical Engineering/Biotechnology, 139, 11-33.

Evie, I.M. et al. (2017) Metabolite Profiling of Mammalian Cell Culture Processes to Evaluate Cellular Viability. In: Gilbert, D.F. & Friedrich, O. (eds.) *Cell Viability Assays: Methods and Protocols* Methods in Molecular Biology. [Online]. New York, NY: Springer. Available at: doi:10.1007/978-1-4939-6960-9_12 [Accessed: 06 February 2023].

Fan, Y.-J. & Zong, W.-X. (2013) The cellular decision between apoptosis and autophagy. *Chinese Journal of Cancer*, 32(3), 121–129.

Farfan-Portet, M.-I. et al. (2014) Are biosimilars the next tool to guarantee cost-containment for pharmaceutical expenditures? The European Journal of Health Economics, 15(3), 223–228.

Feng, Y. et al. (2014) The machinery of macroautophagy. *Cell Research*, 24(1), 24–41. Nature Publishing Group.

Gifre, L. et al. (2017) Trends in recombinant protein use in animal production. *Microbial Cell Factories*, 16(1), 40.

Gils, A. et al. (2017) Biopharmaceuticals: Reference Products and Biosimilars to Treat Inflammatory Diseases. *Therapeutic Drug Monitoring*, 39(4), 308–315.

Gottesman, M.M. (1987) [1] Chinese hamster ovary cells. In: Academic Press Methods in Enzymology. [Online]. Academic Press. Available at: doi:10.1016/S0076-6879(87)51004-7 [Accessed: 2 October 2022].

Groenendyk, J. & Michalak, M. (2004) Calcium Buffering Proteins: ER Luminal Proteins. In: Lennarz, W.J. & Lane, M.D. (eds.) Encyclopedia of Biological Chemistry. [Online]. New York: Elsevier. Available at: doi:10.1016/B0-12-443710-9/00060-0 [Accessed: 3 May 2023].

Guideline on Similar Biological Medicinal Products. 2014. Available at: http://www.ema.europa.eu/docs/en_GB/document_library/Scientific_guideline/2014/10/WC500176768.pdf. [Accessed 08 October, 2022].

Hacker, D.L. & Wurm, F.M. (2017) Recombinant DNA Technology for Production of Protein Therapeutics in Cultured Mammalian Cells. In: Elsevier *Reference Module in Life Sciences*. [Online]. Elsevier. Available at: doi:10.1016/B978-0-12-809633-8.09079-8 [Accessed: 15 March 2023].

Hanack, K. et al. (2016) Antibodies and Selection of Monoclonal Antibodies. In: Böldicke, T. (eds) *Protein Targeting Compounds: Prediction, Selection and Activity of Specific Inhibitors* Advances in Experimental Medicine and Biology, vol 917 (11-22). [Online]. Cham: Springer International Publishing. Available at: doi:10.1007/978-3-319-32805-8_2 [Accessed: 16 March 2023].

Hartl, F.U. et al. (2011) Molecular chaperones in protein folding and proteostasis. Nature, 475(7356), 324–332. Nature Publishing Group.

He, Y. et al. (2018) Emerging Roles for XBP1, a sUPeR Transcription Factor. Gene Expression, 15(1), 13–25.

Hetz, C. et al. (2015) Proteostasis control by the unfolded protein response. Nature Cell Biology, 17(7), 829–838. Nature Publishing Group.

Hoppe, T. & Cohen, E. (2020) Organismal Protein Homeostasis Mechanisms. *Genetics*, 215(4), 889–901.

Hu, H. et al. (2019) The C/EBP Homologous Protein (CHOP) Transcription Factor Functions in Endoplasmic Reticulum Stress-Induced Apoptosis and Microbial Infection. Frontiers in Immunology, 9, 3083.

Huang, Y.-M. et al. (2010) Maximizing productivity of CHO cell-based fed-batch culture using chemically defined media conditions and typical manufacturing equipment. *Biotechnology Progress*, 26(5), 1400–1410.

Hwang, S.O. & Lee, G.M. (2008) Nutrient deprivation induces autophagy as well as apoptosis in Chinese hamster ovary cell culture. Biotechnology and Bioengineering, 99(3), 678–685.

Jahn, T.R. & Radford, S.E. (2005) The Yin and Yang of protein folding. The FEBS Journal, 272(23), 5962–5970.

Jaishankar, J. & Srivastava, P. (2017) Molecular Basis of Stationary Phase Survival and Applications. *Frontiers in Microbiology*, 8. [Accessed: 24 April 2023].

Jayapal KP, Wlaschin KF, Yap MGS, Hu WS. Recombinant protein therapeutics from CHO cells—20 years and counting. *Chem Eng Prog.* 2007; 103:40–47.

Junjappa, R.P. et al. (2018) IRE1α Implications in Endoplasmic Reticulum Stress-Mediated Development and Pathogenesis of Autoimmune Diseases. Frontiers in Immunology, 9. [Accessed: 1 May 2023].

Kaufman, R.J. et al. (1985) Coamplification and coexpression of human tissue-type plasminogen activator and murine dihydrofolate reductase sequences in Chinese hamster ovary cells. *Molecular and cellular biology*, 5(7), 1750–1759. Scopus.

Kerr, J.F.R. et al. (1972) Apoptosis: A Basic Biological Phenomenon with Wideranging Implications in Tissue Kinetics. *British Journal of Cancer*, 26(4), 239–257. Nature Publishing Group.

Kesik-Brodacka, M. (2018) Progress in biopharmaceutical development. Biotechnology and Applied Biochemistry, 65(3), 306–322.

Khan, I. et al. (2021) A decade of cell death studies: Breathing new life into necroptosis. Pharmacology & Therapeutics, 220, 107717.

Kim, I. et al. (2008) Cell death and endoplasmic reticulum stress: disease relevance and therapeutic opportunities. Nature Reviews Drug Discovery, 7(12), 1013–1030. Nature Publishing Group.

Kim, J.Y. et al. (2012) CHO cells in biotechnology for production of recombinant proteins: current state and further potential. *Applied Microbiology and Biotechnology*, 93(3), 917–930.

Kim, N.S. & Lee, G.M. (2002) Response of recombinant Chinese hamster ovary cells to hyperosmotic pressure: effect of Bcl-2 overexpression. Journal of Biotechnology, 95(3), 237–248.

Kober, L. et al. (2013) Optimized signal peptides for the development of high expressing CHO cell lines. Biotechnology and Bioengineering, 110(4), 1164–1173.

Korrapati, M.C. (2014) Puromycin. In: Wexler, P. *Encyclopedia of Toxicology (Third Edition)*, 1141-1142. [Online]. Oxford: Academic Press. Available at: doi:10.1016/B978-0-12-386454-3.00349-3 [Accessed: 22 April 2023].

Krampe, B. & Al-Rubeai, M. (2010) Cell death in mammalian cell culture: molecular mechanisms and cell line engineering strategies. Cytotechnology, 62(3), 175–188.

Kroemer, G. et al. (2009) Classification of cell death: recommendations of the Nomenclature Committee on Cell Death 2009. *Cell Death & Differentiation*, 16(1), 3–11. Nature Publishing Group.

Ku, S.C.Y. et al. (2010) Regulation of XBP-1 signaling during transient and stable recombinant protein production in CHO cells. *Biotechnology Progress*, 26(2), 517–526.

Kunert, R. & Reinhart, D. (2016) Advances in recombinant antibody manufacturing. *Applied Microbiology and Biotechnology*, 100, 3451–3461.

Kyeong, M. & Lee, J.S. (2022) Endogenous BiP reporter system for simultaneous identification of ER stress and antibody production in Chinese hamster ovary cells. *Metabolic Engineering*, 72, 35–45.

Lanza, A.M. et al. (2013) Evaluating the influence of selection markers on obtaining selected pools and stable cell lines in human cells. *Biotechnology Journal*, 8(7), 811–821.

Le Fourn, V. et al. (2014) CHO cell engineering to prevent polypeptide aggregation and improve therapeutic protein secretion. Metabolic Engineering, 21, 91–102.

Lewis, N.E. et al. (2013) Genomic landscapes of Chinese hamster ovary cell lines as revealed by the Cricetulus griseus draft genome. Nature Biotechnology, 31(8), 759–765. Nature Publishing Group.

Mahmood, T. & Yang, P.-C. (2012) Western Blot: Technique, Theory, and Trouble Shooting. *North American Journal of Medical Sciences*, 4(9), 429–434.

Majors, B.S. et al. (2009) Mcl-1 overexpression leads to higher viabilities and increased production of humanized monoclonal antibody in Chinese hamster ovary cells. Biotechnology Progress, 25(4), 1161–1168.

Mammalian Protein Expression | Lonza. Available at: https://bioscience.lonza.com/lonza_bs/GB/en/mammalian-protein-expression [Accessed: 9 June 2023].

Mehrara, E. et al. (2007) Specific Growth Rate versus Doubling Time for Quantitative Characterization of Tumor Growth Rate. *Cancer Research*, 67(8), 3970–3975.

Meusser, B. et al. (2005) ERAD: the long road to destruction. *Nature Cell Biology*, 7(8), 766–772. Nature Publishing Group.

Mitra, S. & Tomar, P.C. (2021) Hybridoma technology; advancements, clinical significance, and future aspects. *Journal of Genetic Engineering & Biotechnology*, 19, 159.

Nishitoh, H. (2012) CHOP is a multifunctional transcription factor in the ER stress response. The Journal of Biochemistry, 151(3), 217–219.

Oliveira, C. & Domingues, L. (2018) Guidelines to reach high-quality purified recombinant proteins. Applied Microbiology and Biotechnology, 102(1), 81–92.

Osbourn, J.K. (2007) 1.10 - Biological Macromolecules. In: Taylor, J.B. & Triggle, D.J. (eds.) Comprehensive Medicinal Chemistry II. [Online]. Oxford: Elsevier. Available at: doi:10.1016/B0-08-045044-X/00013-4 [Accessed: 12 May 2023].

Oslowski, C.M. & Urano, F. (2011) Measuring ER stress and the unfolded protein response using mammalian tissue culture system. *Methods in enzymology*, 490, 71–92.

Oyadomari, S. & Mori, M. (2004) Roles of CHOP/GADD153 in endoplasmic reticulum stress. Cell Death & Differentiation, 11(4), 381–389. Nature Publishing Group.

Pan, X. et al. (2017) Metabolic characterization of a CHO cell size increase phase in fed-batch cultures. *Applied Microbiology and Biotechnology*, 101(22), 8101–8113.
Pan, X. et al. (2017) Selection of chemically defined media for CHO cell fed-batch culture processes. *Cytotechnology*, 69(1), 39–56.

Petricciani, J. & Sheets, R. (2008) An overview of animal cell substrates for biological products. *Biologicals*, 36(6), 359–362.
Pobre, K.F.R. et al. (2019) The endoplasmic reticulum (ER) chaperone BiP is a master regulator of ER functions: Getting by with a little help from ERdj friends. Journal of Biological Chemistry, 294(6), 2098–2108. Elsevier.
Prashad, K. & Mehra, S. (2015) Dynamics of unfolded protein response in recombinant CHO cells. *Cytotechnology*, 67(2), 237–254.
Puck, T.T. (1994) Living history biography. *American Journal of Medical Genetics*, 53(3), 274–284.
Puck, T.T. et al. (1964) Life Cycle Analysis of Mammalian Cells: II. Cells from the Chinese Hamster Ovary Grown in Suspension Culture. Biophysical Journal, 4(6), 441–450.

Rader, R.A. (2008) (Re)defining biopharmaceutical. Nature Biotechnology, 26(7), 743–751. Nature Publishing Group.

Rasmussen, A.S.B. et al. (2021) Definition, categorization, and environmental risk assessment of biopharmaceuticals. Science of The Total Environment, 789, 147884.

Reinhart, D. et al. (2015) Benchmarking of commercially available CHO cell culture media for antibody production. *Applied Microbiology and Biotechnology*, 99(11), 4645–4657.
Reinhart, D. et al. (2015) Influence of cell culture media and feed supplements on cell metabolism and quality of IgG produced in CHO-K1, CHO-S, and CHO-DG44. *BMC Proceedings*, 9(9), P36.

Reinhart, D. et al. (2019) Bioprocessing of Recombinant CHO-K1, CHO-DG44, and CHO-S: CHO Expression Hosts Favor Either mAb Production or Biomass Synthesis. *Biotechnology Journal*, 14(3), 1700686.
Rita Costa, A. et al. (2010) Guidelines to cell engineering for monoclonal antibody production. *European Journal of Pharmaceutics and Biopharmaceutics*, 74(2), 127–138.

Rutkowski, D.T. & Kaufman, R.J. (2004) A trip to the ER: coping with stress. Trends in Cell Biology, 14(1), 20–28.

Schröder, M. & Friedl, P. (1997) Overexpression of recombinant human antithrombin III in Chinese hamster ovary cells results in malformation and decreased secretion of recombinant protein. Biotechnology and Bioengineering, 53(6), 547–559.

Schröder, M. (2006) The unfolded protein response. Molecular Biotechnology, 34(2), 279–290.

Schröder, M. et al. (2002) Induction of protein aggregation in an early secretory compartment by elevation of expression level. Biotechnology and Bioengineering, 78(2), 131–140.

Sellick, C.A. et al. (2011) Metabolite profiling of recombinant CHO cells: Designing tailored feeding regimes that enhance recombinant antibody production. *Biotechnology and Bioengineering*, 108(12), 3025–3031.

Sellick, C.A. et al. (2015) Metabolite profiling of CHO cells: Molecular reflections of bioprocessing effectiveness. Biotechnology Journal, 10(9), 1434–1445.

Stolfa, G. et al. (2018) CHO-Omics Review: The Impact of Current and Emerging Technologies on Chinese Hamster Ovary Based Bioproduction. Biotechnology Journal, 13(3), 1700227.

Strober, W. (2015) Trypan Blue Exclusion Test of Cell Viability. *Current Protocols in Immunology*, 111(1), A3.B.1-A3.B.3.

Szegezdi, E. et al. (2006) Mediators of endoplasmic reticulum stress-induced apoptosis. EMBO Reports, 7(9), 880–885.

Thompson, L.H. & Baker, R.M. (1973) Chapter 7: Isolation of Mutants of Cultured Mammalian Cells. In: Prescott, D.M. (ed.) Methods in Cell Biology. [Online]. Academic Press. Available at: doi:10.1016/S0091-679X(08)60052-7 [Accessed: 8 October 2022].

Thuerauf, D.J. et al. (2004) Opposing roles for ATF6alpha and ATF6beta in endoplasmic reticulum stress response gene induction. The Journal of Biological Chemistry, 279(20), 21078–21084.

Tigges, M. & Fussenegger, M. (2006) Xbp1-based engineering of secretory capacity enhances the productivity of Chinese hamster ovary cells. *Metabolic Engineering*, 8(3), 264–272.

Torday, J.S. (2015) Homeostasis as the Mechanism of Evolution. *Biology*, 4(3), 573–590.

Torres, M. & Dickson, A.J. (2021) Overexpression of transcription factor BLIMP1/prdm1 leads to growth inhibition and enhanced secretory capacity in Chinese hamster ovary cells. *Metabolic Engineering*, 67, 237–249.

Torres, M. & Dickson, A.J. (2022) Reprogramming of Chinese hamster ovary cells towards enhanced protein secretion. Metabolic Engineering, 69, 249–261.

Torres, M. et al. (2018) Process and metabolic engineering perspectives of lactate production in mammalian cell cultures. *Current Opinion in Chemical Engineering*, 22, 184–190.

Torres, M. et al. (2021) Metabolic profiling of Chinese hamster ovary cell cultures at different working volumes and agitation speeds using spin tube reactors. *Biotechnology Progress*, 37(2), e3099.

Torres, M. et al. (2021) Temperature Down-Shift Modifies Expression of UPR-/ERAD-Related Genes and Enhances Production of a Chimeric Fusion Protein in CHO Cells. Biotechnology Journal, 16(2), 2000081.

Torres, M. et al. (2022) The secretory pathway – the key for unlocking the potential of Chinese hamster ovary cell factories for manufacturing therapeutic proteins. Critical Reviews in Biotechnology, 0(0), 1–18. Taylor & Francis.

Torres, M. et al. (2023) Long term culture promotes changes to growth, gene expression, and metabolism in CHO cells that are independent of production stability. *Biotechnology and Bioengineering*, 1-14.

Ubeda, M. et al. (1996) Stress-induced binding of the transcriptional factor CHOP to a novel DNA control element. Molecular and Cellular Biology, 16(4), 1479–1489. American Society for Microbiology.

Vembar, S.S. & Brodsky, J.L. (2008) One step at a time: endoplasmic reticulum-associated degradation. *Nature Reviews Molecular Cell Biology*, 9(12), 944–957. Nature Publishing Group.

Walsh, G. & Walsh, E. (2022) Biopharmaceutical benchmarks 2022. *Nature Biotechnology*, 40(12), 1722–1760. Nature Publishing Group.

Walsh, G. (2018) Biopharmaceutical benchmarks 2018. Nature Biotechnology, 36(12), 1136–1145. Nature Publishing Group.

Wiseman, R.L. et al. (2007) An Adaptable Standard for Protein Export from the Endoplasmic Reticulum. *Cell*, 131(4), 809–821.

Wong, D.C.F. et al. (2006) Transcriptional profiling of apoptotic pathways in batch and fed-batch CHO cell cultures. *Biotechnology and Bioengineering*, 94(2), 373–382.

Wu, J. & Kaufman, R.J. (2006) From acute ER stress to physiological roles of the Unfolded Protein Response. *Cell Death & Differentiation*, 13(3), 374–384. Nature Publishing Group.

Wurm, F.M. (2004) Production of recombinant protein therapeutics in cultivated mammalian cells. *Nature Biotechnology*, 22(11), 1393–1398. Nature Publishing Group.

Wurm, F.M. (2013) CHO Quasispecies—Implications for Manufacturing Processes. Processes, 1(3), 296–311. Multidisciplinary Digital Publishing Institute.

Xu, N. et al. (2017) Comparative Proteomic Analysis of Three Chinese Hamster Ovary (CHO) Host Cells. Biochemical Engineering Journal, 124, 122–129.

Xu, W.-J. et al. (2023) Progress in fed-batch culture for recombinant protein production in CHO cells. *Applied Microbiology and Biotechnology*, 107(4), 1063–1075.

Yang, M. & Butler, M. (2000) Effects of ammonia on CHO cell growth, erythropoietin production, and glycosylation. *Biotechnology and Bioengineering*, 68(4), 370–380.

Zalai, D. et al. (2016) A control strategy to investigate the relationship between specific productivity and high-mannose glycoforms in CHO cells. Applied Microbiology and Biotechnology, 100(16), 7011–7024.

Zhao, M.-H. et al. (2016) GlutaMAX prolongs the shelf life of the culture medium for porcine parthenotes. *Theriogenology*, 85(3), 368–375.

Zhao, W. et al. (2022) Chapter 1 - Cell structure and physiology. In: Schnoor, M. et al. (eds.) *Cell Movement in Health and Disease*. [Online]. Academic Press. Available at: doi:10.1016/B978-0-323-90195-6.00007-3 [Accessed: 26 April 2023].

Zhou, Y. et al. (2018) Debottlenecking protein secretion and reducing protein aggregation in the cellular host. Current Opinion in Biotechnology, 53, 151–157.

Zhu, G. & Lee, A.S. (2015) Role of the Unfolded Protein Response, GRP78 and GRP94 in Organ Homeostasis. Journal of cellular physiology, 230(7), 1413–1420.

Zustiak, M.P. et al. (2008) Feast or famine: autophagy control and engineering in eukaryotic cell culture. Current Opinion in Biotechnology, 19(5), 518–526.